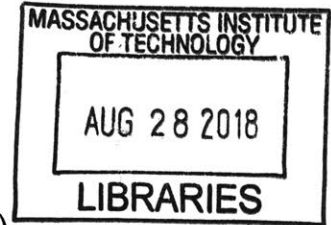# A Novel DNA Damage Quantification Platform Enables High Throughput Screening for Genes that Impact DNA Double Strand Breaks

by

Ian Jun Jie Tay

B.Eng., Imperial College London (2010)

Submitted to the Department of Biological Engineering
in partial fulfillment of the requirements for the degree of

Doctor of Philosophy

at the

MASSACHUSETTS INSTITUTE OF TECHNOLOGY

June 2018

© Ian Jun Jie Tay, MMXVIII. All rights reserved.

The author hereby grants to MIT permission to reproduce and distribute publicly paper and electronic copies of this thesis document in whole or in part in any medium now known or hereafter created.

Author . . . . Signature redacted . . . .
Department of Biological Engineering
May 21, 2018

Certified by. . . . . Signature redacted . . . .
Bevin P. Engelward
Professor of Biological Engineering
Thesis Supervisor

Certified by. . . . . Signature redacted . . . .
Scott R. Floyd
Associate Professor of Radiation Oncology, Duke University School of Medicine
Thesis Supervisor

Accepted by . . . . Signature redacted . . . .
Forest M. White
Chair, Biological Engineering Graduate Committee

This doctoral thesis has been examined by a committee of the Department of Biological Engineering as follows:

Professor Peter C. Dedon
Committee Chair

Professor Bevin P. Engelward
Thesis Supervisor

Associate Professor Scott R. Floyd
Duke University School of Medicine
Thesis Co-Supervisor

Professor Leona D. Samson

Acknowledgements

First, I would like to thank my advisors, Professors Bevin Engelward and Scott Floyd for guiding me during my thesis work, and for their excellent mentorship throughout all these years. It was such a great honor to be a student in their laboratories. I have learnt to think critically, and to write about and present my work effectively under their tutorage. They also taught me to constantly think about alternative solutions to solve problems and to always be positive in the face of adversity. Through their network of collaborators, I had the opportunity to work with other scientists outside of our research group and form collaborations that increased the quality of my work. I am forever grateful for this experience that they have given me.

I would also like to thank my thesis committee, Professors Peter Dedon and Leona Samson, for their constant support and encouragement. They have always raised insightful questions during discussions of my work, which encouraged me to perform careful and critical interpretations of the results I achieved. Also, it was Prof. Dedon's suggestion to view apoptotic comets in my screen as an additional source of data that encouraged me to reanalyze my dataset for both DNA damage and apoptosis. Reanalysis of my dataset contributed to the discovery of a novel candidate DNA repair gene, and forms the basis of Chapter 4 in this thesis.

I am extremely grateful for the wonderful companionship of my colleagues in both the Floyd and Engelward labs. From the Floyd lab, I would like to thank Dr. Fred Lam for teaching me many of the techniques that were used in my work. Special thanks also go to Ms. Amanda Maffa and Ms. Elena Balkanska-Sinclair for their work in organizing the Floyd lab and making it a conducive place to do science. From the Engelward lab, I would especially like to thank Dr. Jing Ge for teaching me the CometChip technique. Thank you to Dr. Orsolya Kiraly, Dr. Michelle Jackson, Dr. Jing Ge, Dr. Marcus Parish and Patrizia Mazzucatto for the warm reception when I first joined the lab as a fresh graduate student. Also, thank you to Dr. Le Ngo, Dr. Jenny Kay, Christy Chao and

Joshua Corrigan for scientific discussions that helped me in my work and random chit chatting to make the lab a more lively place!

I am also grateful to the Biological Engineering Department at MIT, for the accepting me as a prospective graduate student back in 2011, and henceforth giving me the opportunity to be part of the this wonderful MIT BE community. I have met many talented individuals during my stay at MIT, and would like to especially thank the following people: Mr. Andrew Ryan at the MIT Central Machine Shop for his expertise in fabricating the HTS CometChip apparatus, Dr. Jaime Cheah and Christian Soule at the Koch Institute High Throughput Screening Core Facility for their expertise in high throughput screening, and Dr. Charles Whittaker and Dr. Duanduan Ma at the MIT BioMicro Center for their expertise in bioinformatics analysis.

I would also like to thank my friends and course mates, especially Dr. Eric Ma, Dr. Chen Gu and Souparno Ghosh, whom I had frequently met up with throughout the thesis years for science, sports and food.

Finally, I would like to express my love and gratitude to my family. To my parents, who have always encouraged me to try new experiences and to do my best. To my loving wife, Lia, for the steadfast companionship right from the start of this journey! It is incredible that we uprooted and settled into MIT 7 years ago, and soon we will be doing the reverse journey back home. Also to my two children, Aaron and Robin, who never fail to remind me that there is more in life than work for my thesis. Both of you are little scientists in your own right, experimenting with and exploring the world around you, and inspiring me to do the same!

A Novel DNA Damage Quantification Platform Enables High Throughput Screening For Genes that Impact DNA Double Strand Breaks

by

Ian Jun Jie Tay

Submitted to the Department of Biological Engineering on
May 18th 2018 in partial fulfillment of the requirements for
the degree of
Doctor of Philosophy

Abstract

DNA is the blueprint of life, and the high fidelity transmission of genetic information from parent cells to progeny is essential for an organism's viability. However, our genomes are constantly being damaged by reactive molecules generated from cellular metabolic processes or introduced from the environment. The resulting DNA damage can alter the information encoded in DNA, and can interfere with the accurate transmission of genetic information when cells divide. The accumulation of cells with highly damaged or altered DNA within an organism can cause diseases, such as growth defects, aging and cancer. Fortunately, cells possess the capability to repair damaged DNA. Since DNA repair mechanisms can reverse the deleterious effects of DNA damage, they are important in disease prevention, and in particular play an important role in preventing cancer.

DNA repair factors are also important targets for cancer therapies. Tumor cells frequently harbor defects in DNA repair, rendering them vulnerable to DNA damage. Many cancer therapies exploit this vulnerability by treatment with DNA damaging agents. However, tumor cells can have differential DNA repair capacities based on the expression levels of various DNA repair genes. Thus, some cancer cells are variable in their response to chemotherapy and radiation. It is well established that inhibiting DNA repair can increase the efficacy of treatment. Therefore, it is critical to develop a better understanding of the network of genes that regulate DNA repair mechanisms both to understand susceptibility to cancer, and also in order to improve the outcomes of cancer therapy.

DNA repair is a complex process that requires the coordination of many proteins to respond to specific classes of DNA damage. Many of the major proteins that directly participate in DNA repair pathways are well characterized. However, recent research has indicated that the core DNA repair factors make up only a small fraction of the proteins that respond to DNA damage, suggesting that a large number of novel DNA repair factors have yet to be discovered and characterized.

In this work, we leveraged the CometChip, a high-throughput DNA damage quantification assay, to screen thousands of genes for their ability to modulate DNA repair, by knocking them down with shRNAs. We first designed hardware for the CometChip to make it compatible with high-throughput robotics so as to reduce the amount of manual labor needed to execute our screen. We then exploited the ability of

our assay to measure DNA damage at an unparalleled rate to screen an shRNA library targeting 2564 oncology-associated genes. We performed gene network analysis on the top candidate genes and found LATS2 to be a novel DNA repair factor. Further investigation revealed that LATS2 is a modulator of the homologous recombination repair pathway. In addition, we merged our screen data with that from an assay that queries proteins for their ability to bind to DNA double strand breaks. Our results showed that we were able to identify known DNA repair factors via the intersection of the two datasets, and we pinpointed at least one other novel DNA repair gene for further investigation.

Taken together, this work represents an advancement in the ability to discover novel DNA repair factors by large-scale parallel measurement of physical DNA damage in cells. Our technology enables high-throughput screening for DNA damage and repair factors faster than ever before, allowing for extensive studies of DNA damage and opening doors to the discovery of new genes and molecules that affect DNA repair.

Thesis Supervisor: Bevin P. Engelward
Title: Professor of Biological Engineering

Thesis Supervisor: Scott R. Floyd
Title: Associate Professor of Radiation Oncology

Contents

List of Figures

List of Tables

List of Abbreviations

•OH	Hydroxyl radical
γIR	Gamma ionizing radiation
γH2AX	Histone 2A variant X phosphorylated at serine 139
53BP1	p53 binding protein 1
6-4 PPs	6–4 photoproducts
8-oxoG	8 oxo guanine
AFB1	Aflatoxin B1
ASTRO	American Society of Radiation Oncology
ATM	Ataxia Telangiectasia Mutated
ATR	Ataxia and Rad3-related
ATRIP	ATR interacting protein
BER	Base excision repair
BFP	Blue Fluorescent Protein
BRCA1	Breast And Ovarian Cancer Susceptibility Protein 1
BRCA2	Breast And Ovarian Cancer Susceptibility Protein 2
CBX1	Chromobox 1
CHK2	Checkpoint kinase 2
CHO	Chinese hamster ovary
COV	Coefficient of variation
CPDs	Cyclobutane pyrimidine dimers
CRISPR	Clustered Regularly Interspaced Short Palindromic Repeats
DDR	DNA Damage Response
DNA	Deoxyribonucleic acid
DNA-PKcs	DNA-dependent Protein Kinase catalytic subunit
DSB	Double strand break
EXO1	Exonuclease 1
FM-HCR	Fluorescence-based multiplex flow-cytometric HCR
GFP	Green Fluorescent Protein
H2AX	Histone 2A variant X
HCR	Host cell reactivation
HR	Homologous recombination
HTS	High throughput screening
IPA	Ingenuity Pathway Analysis
IR	Ionizing radiation
kDa	Kilo daltons
LATS2	Large Tumor Suppressor Kinase 2

Lig4	Ligase 4
MDC1	Mediator Of DNA Damage Checkpoint 1
MGMT	MethylGuanine DNA Methyl Transferase
MMR	Mismatch repair
MRE11	Meiotic Recombination 11 Homolog 1
MRN	MRE11-Rad50-NBN
NBN	Nibrin
NER	Nucleotide excision repair
NHEJ	Non homologous end joining
OGG1	8-Oxoguanine DNA Glycosylase
PAHs	Polycyclic aromatic hydrocarbons
PARP-1	Poly ADP Ribose Polymerase-1
PDMS	Polydimethylsiloxane
PI3KK	Phosphatidylinositol 3-kinase-related kinase
PNKP	Polynucleotide Kinase 3'-Phosphatase
PRKDC	Protein Kinase, DNA-Activated, Catalytic Polypeptide
RFC5	Replication Factor Complex subunit 5
RNAi	Ribonucleic acid interference
RoMa	Robotic Manipulator
ROS	Reactive oxygen species
RPA	Replication Protein A
SAM	S-adenosylmethionine
SCID	Severe combined immunodeficiency
SFN	Stratifin
shRNA	short hairpin RiboNucleic Acid
siRNA	small interfering ribonucleic acid
SSB	Single strand break
ssDNA	single stranded DNA
TOPBP1	Topoisomerase binding protein 1
TMZ	Temozolomide
TRC	The RNAi Consortium
UV	Ultraviolet
VDJ	Variable-diversity-joining
XLF	XRCC4-Like Factor
XP	Xeroderma pigmentosum
XRCC	X-ray cross complementing

Chapter 1

Introduction

1.1   DNA Damage

The genomes of our cells are constantly exposed to DNA damaging agents[1]. These agents are ubiquitously present in the form of highly reactive molecules, which are generated from the cell's metabolic processes or from the environment. These highly reactive molecules react with the cell's DNA, resulting in DNA damage. There are many forms of DNA damage, including oxidized and alkylated bases, bulky lesions, DNA crosslinks, single strand breaks (SSBs) and double strand breaks (DSBs). These lesions can interfere with critical cellular processes, such as transcription and replication, and can lead to permanent changes in a cell's genome. The accumulation of cells with highly damaged or altered DNA within an organism can cause diseases, such as growth defects, aging and cancer[2]. While DNA damage is generally considered harmful in a healthy organism, it is intentionally inflicted on tumor cells in many cancer therapies to exploit their vulnerability to DNA damaging agents[3]. In the following subsections, the role of DNA damage in disease, as well as its role in cancer therapy, are described below.

1.1.1 Types of DNA Damage

One of the most well studied forms of DNA damage is oxidative damage[4]. Oxidative damage mainly arises from reactive oxygen species (ROS) produced by cellular energy metabolism, as well as exposure of cells to ionizing radiation. Examples of ROS include the hydroxyl radical ($\bullet$OH), which can extract hydrogen atoms or add across double bonds in DNA bases[5], therefore changing their structure. The end products of the reaction between ROS and DNA bases include pyrimidine glycols, formaminopyrimidines, and hydroxypurines[6]. These modified bases often have different base pairing characteristics as their parent bases, and therefore can lead to changes in the genetic code.

DNA bases can also be damaged by alkylating agents. Cells produce S-adenosylmethionine (SAM)[7], which is used as a methyl group donor in many cellular processes, including the conversion of cytosine to 5-methyl cytosine as an epigenetic mark on DNA. However, SAM can also alkylate other sites on the DNA bases, forming 3-methyl adenine and 7-methyl guanine[8]. 7-methyl guanine is thought to be a relative benign damaged base, but 3-methyl adenine can cause stalling during DNA replication by blocking the passage of DNA polymerases[9]. Other sources of alkylation damage on DNA include methyl chloride found in the environment[10], tobacco smoke[11] and chemotherapeutic agents[12].

Another group of lesions that arises from modifications in DNA bases are the bulky lesions. This class of DNA damage is distinguished from base oxidation and alkylation by its ability to distort the DNA double helix. Distortions of the DNA double

helix inhibit the activity of DNA polymerases, resulting in replication stalling. The most well studied bulky lesions are the cyclobutane pyrimidine dimers (CPDs) and 6–4 photoproducts (6-4 PPs), which are both produced by the interaction of ultraviolet (UV) light with DNA[13-16]. Other common sources of bulky lesions in DNA include polycyclic aromatic hydrocarbons (PAHs) found in tobacco smoke and burnt food.

DNA mispairs can be caused by errors made by DNA polymerases during DNA replication. The canonical Watson-Crick base pairing dictates that adenine bases should pair with thymine and cytosine with guanine and vice versa. Despite the high fidelity of replicative DNA polymerases[17], errors resulting in mismatched bases can still occur during DNA replication. Mismatched bases can also occur in places of the genome where there are repetitive sequences in DNA[18,19]. Repetitive sequences can cause DNA polymerases to backtrack or skip bases, resulting in insertion and deletion loops in one of the DNA strands. Mismatched bases, if left unfixed, will lead to changes in the genetic code during the next replication cycle, since the information encoded by one of the DNA strands is different from the opposite strand.

When the sugar phosphate backbone of the DNA is damaged, it can lead to breakages known as strand breaks. A single strand break (SSB) occurs when one of the deoxyribose phosphate backbones is broken, but the broken ends are still tethered together by the complementary strand. Two SSBs opposite each other or in close proximity will result in a double strand break (DSB). DNA DSBs are extremely deleterious to the cell, because they activate cell cycle checkpoints and apoptotic pathways leading to cell death. The most well studied agent that causes DNA DSBs is ionizing radiation (IR). Natural sources of IR include cosmic radiation, radon and

potassium-40[20], while the most significant exposure to man-made IR occurs during radiotherapy treatment for cancer patients. In radiotherapy treatment, patients often receive high-energy photons in the form of x- or γ-rays aimed at the tumor. Fractionated doses of 1.8 - 2 Gy of radiation are often administered per setting, up to a total of 60 Gy[21].

1.1.2 Environmental Causes of DNA Damage

DNA damage can be harmful to cells and it can eventually lead to diseases such as cancer via conversion of DNA damage to mutations in the genome[22]. If a mutation occurs in a gene that is required for the maintenance of genomic stability, the cell will acquire a mutator phenotype, leading to an increase in rate of mutations. The probability of acquiring additional mutations in the genes that are involved in keeping cell growth and cell division in check will drastically increase, leading to uncontrolled cell division and cancer[3]. In this subsection, two examples of human activities that increase DNA damage burden on cells are described, including the process by which they lead to cancer.

It is estimated that about 50% of all cancer deaths in the U.S. result from smoking tobacco[23]. About 75% of the cancer deaths attributable to smoking were caused by lung, bronchus and trachea cancers. This is not surprising, since the lung, bronchus and trachea are directly exposed to the highest concentrations of tobacco smoke during smoking. The first studies linking smoking and lung cancer were conducted in the 1950s, and to date, more than 60 chemical entities in tobacco smoke

have been classified to be carcinogenic[24]. These chemicals include PAHs, heterocyclic compounds, N-nitrosoamines and many others. Further research has shown that PAHs can also cause guanine to thymine mutations in cells and this type of mutation is a signature of tobacco smoking induced DNA damage[25]. The guanine to thymine mutations is caused by the presence of oxidative DNA damage in those cells[26,27], specifically 8-oxo-guanine (8-oxoG), which is highly mutagenic[28]. When a guanine base on DNA is oxidized and turns into 8-oxoG, the damaged base can base pair with adenine instead of the correct cytosine base during replication. In the next replication cycle, a thymine will be base paired opposite of the adenine base, leading to a G->T transversion. OGG1 is an enzyme that initiates the DNA repair pathway to remove 8-oxoG, and studies have found that there is a higher risk of lung cancer for smokers who had low activity levels of OGG1[29]. This finding highlights the impact of 8-oxoG mutations on developing lung cancer, and the role of OGG1 initiated DNA repair in preventing it.

Aflatoxin is a class of molecules synthesized by the *Aspergillus flavus* and *Aspergillus parasiticus* fungi. Aflatoxin B1 (AFB1) in particular, is the most potent liver carcinogen known[30]. Human exposure to AFB1 is mainly caused by contamination of food by the fungi[31]. When AFB1 is ingested, it passes through the gastrointestinal tract and is transported to the liver to be metabolized. Biotransformation of AFB1 to AFB1-epoxide is carried out by the CYP3A4 enzyme in liver cells[32]. AFB1-epoxide can attack guanine bases in DNA, resulting in the formation of a bulky adduct[33,34]. This lesion causes a signature guanine to thymine mutation[35,36]. Mutations in key tumor suppressors such as p53 in the affected liver cells is thought to eventually lead to liver cancer.

1.1.3 Role of DNA Damage in Cancer Therapy

DNA damage inflicted by chemotherapeutic agents and radiotherapy are important for treating cancer. Cancer cells multiply rapidly and uncontrollably, and often do so despite the presence of damage in their genomes. This property of cancer cells causes them to be particularly vulnerable to genotoxic agents, since extensive DNA damage often leads to cell death. In this subsection, two commonly used cancer therapy strategies that rely on the induction of DNA damage for their efficacy are described.

Alkylating agents[12] are a common class of chemotherapeutic agents[37,38] used to treat a variety of cancers, such as gliomas, melanomas and lymphomas. They can be classified into two groups of agents (monofunctional or bifunctional), based on the number of number of covalent bonds (one or two respectively) that they can make with DNA bases. Commonly used monofunctional agents include Dacarbazine, Lomustine and Temozolomide while bifunctional agents include Cyclophosphamide and Melphalan. The major sites on DNA bases that are targeted by these agents are: N7 and O^6 positions on guanine, as well as N3 position on adenine. Genotoxic effects of these alkylating agents are primarily attributed to the N3 and O^6 modifications on adenine and guanine respectively. Alkylation on the N3 position of adenine blocks the passage of replicative polymerases during DNA replication[39], leading to stalling and collapse of the replication fork that encountered the lesion. On the other hand, alkylation on the O^6 position of guanine frequently results in the addition of a thymine base in the

newly synthesized strand during DNA replication. This is a mismatched base pair that can activate downstream cellular processes that may eventually lead to cell death[40].

Radiotherapy is also commonly used to treat tumors. According to the American Society of Radiation Oncology (ASTRO), more than 60% of cancer patients will receive radiation therapy as part of their treatment. Radiotherapy is frequently administered in the form of x-rays or γ-ionizing radiation (γIR) aimed at the tumor, and their mechanism of action is the induction of DNA damage in the targeted cells. On average, each gray (Gy) of γIR induces 600 to 1000 SSBs and 16 to 40 DSBs in DNA per cell, as well as leading to a wide variety of other damaged DNA bases[41]. These damages are primarily caused by the hydrolysis of water molecules near the DNA molecule when they are hit by γIR photons[41,42]. Highly reactive ROS species are produced, which then attack the nearby DNA, causing oxidized bases and strand breaks. Clusters of hydrolysis events occur when γIR photons travel through water, therefore DNA damage induced by γIR is also often clustered together[43]. When SSBs are formed in close proximity, they will lead to DSBs. DNA DSBs have been shown to be the major cause of lethality when cells are exposed to γIR [44,45].

1.2   DNA Repair

DNA damage exerts deleterious effects on cells, but fortunately, healthy cells possess the capability to repair DNA damage. Given the potential impact of DNA damage, it follows that loss of function of DNA repair genes can promote cancer. Damaged DNA is repaired via the coordination of many DNA repair factors, known as

DNA repair pathways. There are five major DNA repair pathways[46] in human cells namely the Base Excision Repair (BER), Nucleotide Excision Repair (NER), Mismatch Repair (MMR), Non Homologous End Joining (NHEJ) and Homologous Recombination (HR) pathways. Each of these pathways responds to specific types of DNA damage. The BER pathway repairs damaged bases, primarily caused by oxidation and alkylation of the purine and pyrimidine moieties in DNA[47-50]. The NER pathway recognizes lesions on damaged bases, which are large enough to obstruct transcription or results in significant distortions within the DNA double helix structure[51-53]. The MMR pathway corrects base pairs which are not paired according to the Adenine – Thymine and Cytosine – Guanine configuration and also removes insertion-deletion loops within DNA[54-56]. The NHEJ and HR repair pathways respond to DNA DSBs and is discussed in detail in the following subsections.

1.2.1 Non Homologous End Joining

NHEJ is one of the cell's DNA DSB repair pathways. Essentially, the pathway consists of steps that bring broken ends of DNA strands together, and re-ligate them to form a continuous DNA strand[57] (Fig. 1-1). The Ku complex, which is an initiating member of this repair pathway, was first discovered as a nuclear autoantigen complex[58]. Subsequent characterization of the Ku protein complex revealed that it was made up of two nuclear-localized, DNA binding proteins with molecular weights of approximately 70 kDa (Ku70) and 80 kDa (Ku80) in a 1:1 ratio. A few years later, the genes that encode for these proteins were being studied in CHO hybrid cells generated

by fusing X-ray sensitive mutant cells with each other[59]. The genes discovered that were mutated in the mutant cells were given the XRCC label, which is an acronym for 'X-ray cross complementing'. Apart from X-ray sensitivity, cells mutated for *XRCC7* were also found to be defective in VDJ recombination[60], suggesting that the mutated genes participate in the repair of DNA double strand breaks, which are generated when cells were exposed to X-rays or undergoing VDJ recombination. In 1994, it was discovered that Ku80 was the protein product of the *XRCC5* gene[61]. Subsequently, the *XRCC6* and *XRCC7* (also known as *PRKDC*) genes were found to be coding for Ku70 and DNAPKcs proteins respectively.

In the NHEJ repair pathway, the Ku70 and Ku80 heterodimer binds to DNA DSBs. The heterodimer forms a ring-like structure and protects the DNA ends from being excessively degraded[62-63]. The DNA DSB bound Ku complex is able to recruit DNAPKcs[64], which together forms the DNAPK holoenzyme. After the DNAPK complex binds to DNA DSBs, the DNAPKcs subunit auto-phosphorylates and trans-phosphorylate other proteins. This leads to the recruitment of the second major complex in this pathway, which consists of XLF, XRCC4 and Ligase 4[65]. XRCC4 and XLF4 are structural proteins, which help to bridge and align the broken DNA strands, while Ligase 4 joins the broken ends. Together, the proteins in the two complexes mentioned above form the core factors required for NHEJ. There are also other proteins involved in this repair pathway, and they function mostly to process and modify damaged bases at the break. These proteins are also critical for the efficient repair of DSBs by the NHEJ pathway, since DNA damage often create DNA ends that are not directly compatible for re-ligation. The modified DNA ends are restored by proteins including Artemis, which is

an endonuclease that can cleave DNA hairpin loops; PNKP, which creates DNA ends that are compatible for ligation by restoring a 5' phosphate and a 3' hydroxyl group and polymerases μ and λ which extends DNA strands to fill gaps at overhangs. Due to the requirement of DNA end processing before re-ligation, NHEJ is often associated with mutations, insertions and deletions at the site of the DSB.

The NHEJ repair pathway is a critical DNA DSB repair pathway in most mammalian cells. The pathway is active throughout the cell cycle[66,67], but it is especially important in the G_0/G_1 phases, as it is the only major repair pathway capable of repairing DNA DSBs in the G_0/G_1 phases. Cells that are deficient in NHEJ are often hypersensitive to agents that induce DNA DSBs, such as γIR [68-70]. Mutations in NHEJ genes also frequently cause severe combined immunodeficiency (SCID)[71]. This is due NHEJ's role in repairing DNA DSBs created during VDJ recombination in immune cells. The increased sensitivity of NHEJ deficient cells to DNA DSB inducing agents and reduced immune function of individuals with NHEJ gene mutations highlights NHEJ's universal role in repairing DNA DSBs, whether they are caused by external agents, or created by the cell itself.

1.2.2 Homologous Recombination

Apart from the NHEJ repair pathway, cells also utilize HR to repair DNA DSBs[72] (Fig. 1-2). The HR pathway is most active when cells are in the $S/G_2/M$ phases of the cell cycle. The pathway is initiated by the MRE11-Rad50-NBN (MRN) complex, which senses and binds to DNA DSBs. 5' end resection at the DNA DSB is initiated by MRN,

and continued by EXO1 to form kilobases of single stranded DNA (ssDNA) 3'

overhangs. The overhangs are first bound by RPA, before they are exchanged for

Rad51 by the BRCA2 protein[73]. The ssDNA-Rad51 nucleoprotein filament invades the

sister chromatid and identifies sequences that are homologous to the DNA near the site

of damage. Genetic information is generally donated by the sister chromatid, which is

used as a template to extend the broken DNA strands. The nucleoprotein filament

complex with its sister chromatid is then resolved by one of several mechanisms. In the

simplest mechanism, one of the 3' overhangs is sufficiently extended until it overlaps

with the sequences on the other unextended 3' overhang. The extended 3' overhang is

then detached from the sister chromatin and anneals with the unextended 3' overhang.

Gaps between the annealed strands are filled using the opposite strands as template

and religated to restore the DNA[74].

Since HR is a critical repair pathway for DNA DSBs, cells that are deficient for

HR exhibit increased sensitivity to agents that induce DNA DSBs, such as γIR.

Additionally, HR deficient cells are also more sensitive to agents that produce persistent

base damage or DNA single stranded breaks (SSBs), because the damage can be

converted into DSBs during DNA replication. This observation led to the development of

Poly ADP Ribose Polymerase-1 (PARP-1) inhibitors to target HR deficient breast and

ovarian tumor cells[75,76]. PARP-1 is an enzyme that binds to DNA SSBs and increases

the repair efficiency of these breaks[77]. When PARP-1 inhibitors are introduced into cells,

DNA SSBs remain unrepaired, and will lead to DSBs when the replication fork unwinds

the DNA double helix. HR deficient cells cannot repair the resulting DSBs efficiently,

and persistent DSBs will trigger cell death via apoptosis. The usage of PARP-1 in the

treatment of HR deficient cancers is therefore an example of how DNA DSB repair deficiencies in tumor cells are exploited for therapy.

1.2.3 DNA Damage Response

When DNA DSBs are induced in cells, vast networks of genes are activated and respond to the damage. The genes that respond to DNA DSBs include the NHEJ and HR repair factors, but recent research has provided evidence that these core DNA repair factors only make up a small fraction of the proteins that respond to DNA DSBs. The vast majority of the other proteins are involved in signal transduction, cell cycle arrest, and modulating the activity other repair factors. Collectively, the activity of these proteins is termed DNA Damage Response (DDR)[78,79]. At the core of the DDR signaling pathway is the triad of Phosphatidylinositol 3-kinase-related kinases (PI3KKs) - Ataxia Telangiectasia Mutated (ATM), Ataxia and Rad3-related (ATR) and DNA-dependent Protein Kinase catalytic subunit (DNA-PKcs). All three kinases have been shown to be activated in the presence of DNA DSBs[80-82]. ATM, ATR and DNAPKcs are recruited to DNA DSBs via the Mre-11 – Rad50 – NBN (MRN) complex[83], the ATRIP protein[84] and the Ku70/Ku80 heterodimer[64] respectively. These kinases are serine/threonine kinases and one of their most well studied substrates is the histone H2AX protein.

H2AX is a histone variant that is found in a subset of histone octamer complexes in chromatin[85]. It is targeted for phosphorylation at serine 139 residue when nearby DNA is damaged, forming γH2AX (Fig.1-3A). This event occurs within minutes of inducing the DSB, and spreads up to a few mega base pairs from the site of damage,

forming domains called γH2AX foci. Many downstream repair factors are recruited to γH2AX foci. These proteins include 53BP1[86], TOPBP1[87], BRCA1[88], MDC1[89] and NBN[90], among others. All of the proteins listed have (BRCA1 C-Terminus) BRCT domains within their protein structure, which allows them to bind to phosphorylated proteins, such as γH2AX[91]. The effect of γH2AX foci formation at a DSB is to concentrate repair factors at the damage site, for efficient repair[92].

Apart from phosphorylating H2AX, the PI3KKs initiate a phosphorylation cascade that involves more than 700 proteins[93]. Prominent phosphorylated proteins include the PI3KKs themselves (they autophosphorylate upon activation) as well as known DNA DSB repair factors, such as BRCA1, BRCA2, MRE11, NBN and PNKP. Other phosphorylated targets include CHK2, MDC1 and p53, which activate cell cycle checkpoints and halting the cell cycle in order to allow time for cells to repair the damage or activate apoptosis. Networks of genes that did not have direct implications for DNA DSB repair were also found to be phosphorylated, suggesting that they might play a role in DNA DSB repair.

1.3   Assays for Measuring DNA DSBs

Many assays have been developed to study DNA DSB induction and repair, in order to understand their importance in modulating cells' response to various lines of therapy. Researchers have used these assays in combination with other technologies, such as RNAi knockdown to discover new factors that influence the levels of DNA DSBs in cells. In the subsections below, commonly used assays to study DNA DSBs are

described, including the γH2AX assay, the host cell reactivation (HCR) assay and the comet assay. In addition, recent technological advances in the comet assay, named the CometChip, is also described.

1.3.1 γH2AX Immunofluorescence Assay

When a DNA DSB is introduced in a cell, a signaling cascade is activated within minutes. The most prominent signaling event that occurs is the phosphorylation of the histone variant H2AX at serine 139 to form γH2AX. γH2AX is formed at both ends of the DSB, and can spread up to several megabase pairs away from the break. These large γH2AX domains are called γH2AX foci. γH2AX foci can be probed using immunofluorescence techniques to study DNA DSBs (Fig. 1-3B). Several studies have shown that the number of γH2AX foci correlates with the dosage of γ-IR applied to cells, down to as low as 1 mGy[85]. This shows that γH2AX is a very sensitive assay for measuring DNA DSBs.

The γH2AX immunofluorescence assay is a typical immunocytochemistry assay[94]. Cells are first treated with DNA damaging agents on glass coverslips or glass bottom tissue culture plates and incubated for various amounts of time, before they are fixed. After washing and membrane permeabilization steps, anti- γH2AX antibodies are added, which binds specifically to the γH2AX foci. These antibodies can be fluorescently tagged, or secondarily probed by additional antibodies. Visualization of γH2AX foci is achieved by using an epifluorescence microscope. The number of γH2AX foci per cell is counted and reported as a measure of DNA DSBs in those cells.

26

The γH2AX immunofluorescence assay is frequently used in screens to study DNA repair factors, due to the convenience of automated microscopes and the versatility of analyzing digital images. These assays can be conducted with the assistance of high throughput screening robotics for the steps that require liquid changes, such as the addition of antibodies for detection and washing steps. The completed assay can then be queued for imaging with modern automated microscopes and the images collected can be analyzed digitally around the clock, requiring little manual work. This makes the assays ideal for large-scale genome wide screening, where tens of thousands of genes are screened in a single experiment.

In an example of such a screen, Paulsen and coworkers conducted the first genome wide DNA damage response screen in human cells in 2009[95]. They measured changes in γH2AX levels caused by unrepaired spontaneous DNA damage after gene knockdown and reported the discovery of mRNA-processing factors in preventing DNA damage, as well as a possible role of DNA damage in Charcot-Marie-Tooth syndrome. In 2013, Floyd and coworkers studied the roles of genes that modulate γ-IR induced γH2AX levels, and identified BRD4 as a novel modulator of DNA damage response signaling[96].

Despite the widespread usage of the γH2AX immunofluorescence assay, the assay has several limitations when used to measure physical levels of DNA DSBs[97]. γH2AX is a signaling event after induction of DNA DSBs, and therefore can be affected by the activity of the signaling kinases, as well as the resolving phosphatases[98]. For example, inhibiting the ATM kinase prior to DSB formation will lead to lower extent of yH2AX foci formation[99]. Also, changes in yH2AX levels between treatment conditions

may not always reflect differences in DNA DSB repair. This is exemplified in the work performed by Floyd and coworkers, where they found that BRD4 depletion led to more intense yH2AX foci formation, but no changes in DNA DSB repair kinetics as compared to control cells[96]. These observations highlight the limitation of using yH2AX foci formation as a proxy for measuring DNA DSBs in cells.

1.3.2 Host Cell Reactivation Assay

The Host Cell Reactivation (HCR) assay relies on the ability of cells to repair inactivating lesions on an antibiotic selection[100] or fluorescent reporter gene[101,102], which is introduced into cells via plasmids. If the cell repairs the lesions, the reporter gene will be expressed, and the cell can then be detected using an appropriate technique (applying an antibiotic, or analyzing fluorescent levels). Conditions that affect cells' ability to repair the lesions will result in changes in the percentage of cells that are detectable by the technique.

Recently, Samson and coworkers developed an advancement in HCR technology, named fluorescence-based multiplex flow-cytometric HCR (FM-HCR)[103]. The FM-HCR technology allows researchers to query various combinations of DNA repair pathways (BER, NER, MMR, NHEJ, HR and direct reversal of O^6-methylGuanine) simultaneously, as opposed to one pathway per experiment in traditional HCR assays. The usage of flow cytometers in the FM-HCR assay allows researchers to assay millions of cells within minutes, vastly increasing the throughput of the assay.

To illustrate the utility of the FM-HCR assay, Samson and coworkers have used it to measure the activity of five DNA repair pathways in 27 cell lines simultaneously within a few hours, a feat that was estimated to take several weeks to complete using traditional HCR methods. A wide variation in DNA repair abilities among healthy individuals was discovered in these cell lines, which is consistent with previous observations of variations in DNA repair in healthy human populations. This result show the potential of FM-HCR as a tool to query a large number of samples for defects in DNA repair, as well as to discover novel DNA repair factors.

1.3.3 Comet Assay

The comet assay (also known as the single cell gel electrophoresis assay) is a well-established assay that is used to measure DNA damage in cells[104-107]. The technique, first described by Ostling and Johanson in 1984[100], is based on the principle that damaged DNA (which has lost superhelical tension or is fragmented) has increased electrophoretic mobility in an agarose gel, as compared to intact DNA. Under an electric field, damaged DNA will migrate further than intact DNA, with the length of migration directly correlating with the extent of damage. This property of damaged DNA allows us to deduce the levels of all DNA damage that resulted in losses of superhelical tension regardless of the type of DNA damaging agent used, making the comet assay a versatile tool to study a wide variety of DNA damaging agents[108-111]. Singh and co-workers developed the steps required to perform the assay and showed that it could be used to detect x-ray induced DNA damage[108].

To perform the comet assay, cells that have been exposed to a DNA damaging agent are first mixed with molten low melting point agarose to form a single cell suspension and this suspension is pipetted onto glass slides (Fig. 1-4). The agarose is allowed to gelate, and the cells are then exposed to a lysis buffer, which dissolves membranes and inactivates all cellular activities, resulting in a 'nucleoid' of DNA trapped within agarose. The DNA is then subjected to electrophoresis. There are two versions of the electrophoresis step. In the one version, DNA is electrophoresed in a high pH buffer (alkaline comet assay), which unwinds the DNA double helix. SSBs in DNA will result in free DNA ends, which can readily migrate into agarose when an electric field is applied. The alkaline comet assay is primarily used to measure SSBs as well as abasic and alkali labile sites on DNA. The other version of the comet assay is performed using a buffer with neutral pH. At a neutral pH, the DNA double helix does not unwind, and therefore only DNA DSBs are assayed[112]. After electrophoresis, the DNA is stained and the extent of migration by DNA outside of the 'nucleoid' along the axis of electrophoresis can be measured by fluorescent microscopy. Images obtained from this assay typically show circular areas of staining originating from the nucleoid of cells, as well as tails exiting from the nucleoids, reflective of DNA damage. The more damage each cell had in its DNA prior to lysis, the more intense and longer the tail will be. The images of cells with damaged DNA reassemble a comet, which lends the assay its name.

Despite the fact that the principle underlying the comet assay is well grounded, the assay has not been used as a discovery tool to screen for DNA repair factors. The traditional comet assay is plagued by two major drawbacks that prevent its usage in large scale screening experiments. The first problem is that the assay is tedious to

execute. Each sample has to be plated on a separate glass slide and each comet has to be imaged and analyzed individually. A typical researcher can prepare up to 20 comet assay glass slides a day, and may take a few hours to acquire images from the glass slides. Given the slow rate of data acquisition with the traditional comet assay, it will be physically impossible to perform large scale screening experiments whereby tens of thousands of genes are tested, within a reasonable amount of time.

The traditional comet assay also suffers from high variability between identically prepared samples[113-115]. This problem limits the usefulness of the assay in a large scale screening experiment, even if the slow rate of data acquisition was compensated for. The high variability in the assay stems from various steps in its protocol. Since each sample has a lengthy preparation time, and has to be plated separately, there will be a significant time lag between the firstly and lastly prepared samples in each experiment. This time lag can cause changes in cells or reagents, which will eventually lead to fluctuations in the data. Human bias introduced during image acquisition and analysis steps also contribute to variability in the data produced by the assay.

1.3.4 CometChip

The CometChip was developed by Engelward and coworkers to address the limitations of the comet assay[116-118]. The technology exploits a micropatterned cell array on agarose to maximize the number of useful comets per unit area of agarose. The minimum number of required comets per sample (~100 comets) on a 75 mm by 25 mm glass slide could now be obtained from a 3 mm wide circular area on the CometChip,

representing a 200 fold increase in space efficiency. The area of space needed to obtain the required number of comets for each sample is now reduced to the area of a single macrowell on a standard 96-well tissue culture plate.

To directly exploit the space savings of the CometChip, custom-made stamps were created to span the area of a standard tissue culture plate (approx. 110 mm by 75 mm) and arrayed with cell-sized micro-posts (Fig. 1-5). These stamps can be applied to molten agarose to create a 110 mm by 75 mm agarose slab with an array of cell-sized microwells on its surface. The stamp is removed when the agarose solidifies and cells can be plated into the microwells by adding a cell suspension over it. Cells will settle down and enter the microwells via gravity. Rinsing the CometChip can wash away excess cells that did not enter the microwells and cells within the microwells will be encapsulated by applying a thin layer of molten low melting point agarose. The agarose can be placed on a glass plate for support and partitioned into 96 macrowells by clamping a bottomless 96-well plate onto the agarose. Alternatively, hardware for creating macrowells is available through Trevigen[119]. Each 96-well macrowell has approximately 300 microwells at its base, and can be treated with DNA damaging agents and analyzed for levels of DNA damage using the same protocol as the standard comet assay. In doing so, each glass slide can now be analyzed as a single macrowell in a 96 well plate.

The CometChip addresses the key limitations of the comet assay. First, since the CometChip can be 96-well plate-compatible, dozens of samples can now be prepared in parallel, increasing the rate at which the comet assay can be performed. Using a 12-channel pipette allows 12 samples to be loaded onto the CometChip in seconds as

compared to several minutes when using glass slides in the traditional comet assay. Furthermore, since the CometChip has microwells that can trap cells and enable the researcher to wash away excess cells, it eliminates the laborious step of needing to determine cell densities prior to plating cells on glass slides (as long as there are more than 10,000 cells per sample). This represents significant time savings in the preparation of the assay.

Additional time savings by the CometChip are achieved during the imaging and analysis steps. Since the CometChip is able to accommodate up to 96 samples in a single agarose slab, all of the samples can now be imaged in one sitting, without the need to change glass slides between samples. The amount of time spent to switch between glass slides and relocate the focal plane for every sample is not trivial (estimated to be between 30 seconds to a minute per sample), and adds significant fatigue to the researcher. Furthermore, the high density of cell-filled microwells in the CometChip allows the researcher to capture more than 100 comets with only four images, as compared to taking dozens of randomly dispersed comets in the traditional assay. The comets are regularly arranged and can be easily identified by software in a single step, instead of manually selecting comets for analysis for the traditional assay. With all these improvements, we estimated that the rate of performing the comet assay is improved by at least 1000 fold with the CometChip.

Apart from allowing researchers to more efficiently perform the comet assay, the CometChip also increases the consistency of data obtained from the assay[117,120]. Sample-to-sample variations are reduced simply by accommodating 96 samples and treatment conditions within the same slab of agarose. Regular arraying of comets in the

CometChip allows the usage of software to analyze images automatically, removing a source of variability from human bias. Together, these improvements increase the speed of analysis by orders of magnitude, while at the same time providing increased consistency, and thus increased sensitivity.

1.4   Discovering Novel DNA Repair Factors

Historically, many DNA repair factors were discovered by studying the diseases that were caused by deficiencies in the repair factors. Examples of such discoveries include NER repair factors by studying xeroderma pigmentosum (XP)[121] and BRCA genes by studying hereditary breast cancer[122]. Other strategies that were used to discover DNA repair genes include exposing model organisms such as *S. cerevisiae*, to known DNA damaging agents in large scale screening experiments[123]. The genes discovered were then cross referenced with the human genome, to find DNA repair gene homologs in human cells. Recently, the development of genome wide RNAi gene editing libraries, as well as high throughput analytical tools such as mass spectrometry and automated imaging systems, has led to an increase in screening activities performed on human cells. It has become clear from recent studies that we have only characterized a small fraction of genes that participate in DNA repair, and many novel DNA repair factors are yet to be discovered. Therefore, expanding our understanding of DNA repair genes will lead to advancements in the prevention of diseases resulting from DNA damage and new targets for cancer treatment[124-128].

1.5   Overview of the Thesis

The work presented in this thesis is driven by the hypothesis that we can identify novel DNA repair factors by harnessing the unparalleled ability of the CometChip to measure physical DNA damage. The immense throughput and reliability improvements of the CometChip as compared to its predecessor, the traditional comet assay, prime it for its usage in complex, high throughput screening experiments that can query DNA damage and repair.

In Chapter 2, we described the design of the hardware for the CometChip to make it compatible with high-throughput robotics. The usage of high-throughput robotics is a prerequisite in order for us to be able to successfully screen thousands of conditions within a reasonable amount of time and without suffering significant fatigue. The existing CometChip required large binder clips during its assembly. These clips disrupted the rectangular profile of the assay plates, and interfered with the ability of standard robotic arms to pick up and manipulate the assay. Furthermore, the inconsistency of placing the CometChip within an assay plate resulted in the incompatibility of the assay with high throughput automated imaging platforms. We overcome the key limitations of the CometChip hardware by creating High Throughput Screening CometChip (HTS CometChip) and showed that it is compatible with high throughput robotics. We tested the variability of the HTS CometChip, and showed that it preserves the improvements made by the CometChip. We evaluated the utility of the HTS CometChip to detect DNA DSBs in a pair of human glioblastoma cell lines that defer in their ability to repair DSBs. We treated the cell lines with various doses of γ-IR

and incubated the cells for various amounts of time to allow them to repair the damage. We also tested the utility of the HTS CometChip to detect DNA DSB repair defects in cells that were treated with shRNA reagents that target DNA DSB repair genes. Our results showed that the HTS CometChip is effective in detecting DNA DSB repair defects in the fraction of the time and labor required by the traditional comet assay, fulfilling the conditions for its usage in large scale high throughput screens.

Having developed the HTS CometChip that enables us to measure DNA damage faster than ever before, we surveyed a library of lentiviral shRNAs targeting 2564 genes for their ability to modulate DNA DSB levels described in Chapter 3. We rank ordered the results from our screen by levels of DNA DSBs four hours after exposure to γ-IR and performed bioinformatics analysis on the top 100 genes. We isolated LATS2 as a novel DNA DSB modulator and showed that LATS2 deficient cells had a DNA DSB repair defect. In addition, we also discovered that LATS2 deficient cells were more susceptible to apoptosis when placed in the HTS CometChip agarose for an extended period of time, showing that the screen can also reveal genes that impact susceptibility to apoptosis.

In Chapter 4, we refined our image analysis strategy, in order to focus on genes that impact DNA DSB repair. Since the shapes of comets from apoptotic cells were distinctively different from comets from viable cells, we designed image segregation software that could exclude apoptotic comets from our analysis. We overlapped our refined HTS CometChip dataset with an orthogonal dataset obtained by screening for proteins that bind to DSBs and remarkably found known DNA DSB repair factors among our top 10 hits. The most exciting result was that we were able to identify candidate

genes that have not been directly shown to participate in DNA DSB repair, but are known to associate with other DNA repair factors. Deficiencies in the expression of these genes have also been shown to increase sensitivity of cells to DNA damaging agents. These findings show that our strategy of combining datasets was effective in identifying novel DNA DSB repair factors for further investigation.

References

1.   Hoeijmakers, J. H. J. (2009). DNA damage, aging, and cancer. *The New England Journal of Medicine, 361*(15), 1475–1485.

2.   Shimizu, I., Yoshida, Y., Suda, M., & Minamino, T. (2014). DNA damage response and metabolic disease. *Cell Metabolism, 20*(6), 967–977.

3.   Hanahan, D., & Weinberg, R. A. (2011). Hallmarks of cancer: the next generation. *Cell, 144*(5), 646–674.

4.   Cooke, M. S., Evans, M. D., Dizdaroglu, M., & Lunec, J. (2003). Oxidative DNA damage: mechanisms, mutation, and disease. *FASEB Journal : Official Publication of the Federation of American Societies for Experimental Biology, 17*(10), 1195–1214.

5.   Breen, A. P., & Murphy, J. A. (1995). Reactions of oxyl radicals with DNA. *Free Radical Biology & Medicine, 18*(6), 1033–1077.

6.   Bjelland, S., & Seeberg, E. (2003). Mutagenicity, toxicity and repair of DNA base damage induced by oxidation. *Mutation Research, 531*(1-2), 37–80.

7.   Lutz, W. K. (1990). Endogenous genotoxic agents and processes as a basis of spontaneous carcinogenesis. *Mutation Research, 238*(3), 287–295.

8.   Rydberg, B., & Lindahl, T. (1982). Nonenzymatic methylation of DNA by the intracellular methyl group donor S-adenosyl-L-methionine is a potentially mutagenic reaction. *The EMBO Journal, 1*(2), 211–216.

9.   Engelward, B. P., Allan, J. M., Dreslin, A. J., Kelly, J. D., Wu, M. M., Gold, B., & Samson, L. D. (1998). A chemical and genetic approach together define the biological consequences of 3-methyladenine lesions in the mammalian genome. *The Journal of Biological Chemistry, 273*(9), 5412–5418.

10.   Ballschmiter, K. (2003). Pattern and sources of naturally produced organohalogens in the marine environment: biogenic formation of organohalogens. *Chemosphere, 52*(2), 313–324.

11.   Hecht, S. S. (2006). Cigarette smoking: cancer risks, carcinogens, and mechanisms. *Langenbeck's Archives of Surgery, 391*(6), 603–613.

12.   Fu, D., Calvo, J. A., & Samson, L. D. (2012). Balancing repair and tolerance of DNA damage caused by alkylating agents. *Nature Reviews. Cancer, 12*(2), 104–120.

13.   Setlow, R. B. (1966). Cyclobutane-type pyrimidine dimers in polynucleotides. *Science (New York, N.Y.), 153*(3734), 379–386.

14.   Brash, D. E. (1988). UV mutagenic photoproducts in Escherichia coli and human cells: a molecular genetics perspective on human skin cancer. *Photochemistry and Photobiology, 48*(1), 59–66.

15.   Mitchell, D. L., & Nairn, R. S. (1989). The biology of the (6-4) photoproduct. *Photochemistry and Photobiology, 49*(6), 805–819.

16.   Rycyna, R. E., & Alderfer, J. L. (1985). UV irradiation of nucleic acids: formation, purification and solution conformational analysis of the "6-4 lesion" of dTpdT. *Nucleic Acids Research, 13*(16), 5949–5963.

17.   Kunkel, T. A. (2004). DNA replication fidelity. *The Journal of Biological Chemistry, 279*(17), 16895–16898.

18.   Tran, H. T., Keen, J. D., Kricker, M., Resnick, M. A., & Gordenin, D. A. (1997). Hypermutability of homonucleotide runs in mismatch repair and DNA polymerase proofreading yeast mutants. *Molecular and Cellular Biology, 17*(5), 2859–2865.

19.   Karran, P. (1996). Microsatellite instability and DNA mismatch repair in human cancer. *Seminars in Cancer Biology, 7*(1), 15–24.

20.   National Research Council (US) Committee on Health Effects of Exposure to Low Levels of Ionizing Radiations (BEIR VII). (1998). Health Effects of Exposure to Low Levels of Ionizing Radiations: Time for Reassessment?

21.   The Royal College of Radiologists, Clinical Oncology. (2016). Radiotherapy Dose Fractionation, 2nd Edition. https://www.rcr.ac.uk/publication/radiotherapy-dose-fractionation-second-edition Accessed April 2018

22.   Loeb, L. A., Loeb, K. R., & Anderson, J. P. (2003). Multiple mutations and cancer. *Proceedings of the National Academy of Sciences of the United States of America, 100*(3), 776–781.

23.   Siegel, R. L., Jacobs, E. J., Newton, C. C., Feskanich, D., Freedman, N. D., Prentice, R. L., & Jemal, A. (2015). Deaths Due to Cigarette Smoking for 12 Smoking-Related Cancers in the United States. *JAMA Internal Medicine, 175*(9), 1574–1576.

24.   Hecht, S. S. (1999). DNA adduct formation from tobacco-specific N-nitrosamines. *Mutation Research, 424*(1-2), 127–142.

25.   Hainaut, P., & Pfeifer, G. P. (2001). Patterns of p53 G-->T transversions in lung cancers reflect the primary mutagenic signature of DNA-damage by tobacco smoke. *Carcinogenesis, 22*(3), 367–374.

26.   Asami, S., Manabe, H., Miyake, J., Tsurudome, Y., Hirano, T., Yamaguchi, R., et al. (1997). Cigarette smoking induces an increase in oxidative DNA damage, 8-hydroxydeoxyguanosine, in a central site of the human lung. *Carcinogenesis, 18*(9), 1763–1766.

27.   Asami, S., Hirano, T., Yamaguchi, R., Tomioka, Y., Itoh, H., & Kasai, H. (1996). Increase of a type of oxidative DNA damage, 8-hydroxyguanine, and its repair activity in human leukocytes by cigarette smoking. *Cancer Research, 56*(11), 2546–2549.

28.   Grollman, A. P., & Moriya, M. (1993). Mutagenesis by 8-oxoguanine: an enemy within. *Trends in Genetics : TIG, 9*(7), 246–249.

29.   Paz-Elizur, T., Krupsky, M., Blumenstein, S., Elinger, D., Schechtman, E., & Livneh, Z. (2003). DNA repair activity for oxidative damage and risk of lung cancer. *Journal of the National Cancer Institute, 95*(17), 1312–1319.

30.   Kensler, T. W., Roebuck, B. D., Wogan, G. N., & Groopman, J. D. (2011). Aflatoxin: a 50-year odyssey of mechanistic and translational toxicology. *Toxicological Sciences : an Official Journal of the Society of Toxicology, 120 Suppl 1*(Supplement 1), S28–48.

31.   Liu, Y., Chang, C.-C. H., Marsh, G. M., & Wu, F. (2012). Population attributable risk of aflatoxin-related liver cancer: systematic review and meta-analysis. *European Journal of Cancer (Oxford, England : 1990), 48*(14), 2125–2136.

32.   Dohnal, V., Wu, Q., & Kuča, K. (2014). Metabolism of aflatoxins: key enzymes and interindividual as well as interspecies differences. *Archives of Toxicology, 88*(9), 1635–1644.

33. Smela, M. E., Currier, S. S., Bailey, E. A., & Essigmann, J. M. (2001). The chemistry and biology of aflatoxin B(1): from mutational spectrometry to carcinogenesis. *Carcinogenesis, 22*(4), 535–545.

34. Bedard, L. L., & Massey, T. E. (2006). Aflatoxin B1-induced DNA damage and its repair. *Cancer Letters, 241*(2), 174–183.

35. Bailey, E. A., Iyer, R. S., Stone, M. P., Harris, T. M., & Essigmann, J. M. (1996). Mutational properties of the primary aflatoxin B1-DNA adduct. *Proceedings of the National Academy of Sciences of the United States of America, 93*(4), 1535–1539.

36. Chawanthayatham, S., Valentine, C. C., Fedeles, B. I., Fox, E. J., Loeb, L. A., Levine, S. S., et al. (2017). Mutational spectra of aflatoxin B1in vivo establish biomarkers of exposure for human hepatocellular carcinoma. *Proceedings of the National Academy of Sciences of the United States of America, 114*(15), E3101–E3109.

37. Ferguson, L. R., & Pearson, A. E. (1996). The clinical use of mutagenic anticancer drugs. *Mutation Research, 355*(1-2), 1–12.

38. Lawley, P. D., & Phillips, D. H. (1996). DNA adducts from chemotherapeutic agents. *Mutation Research, 355*(1-2), 13–40.

39. Settles, S., Wang, R.-W., Fronza, G., & Gold, B. (2010). Effect of n3-methyladenine and an isosteric stable analogue on DNA polymerization. *Journal of Nucleic Acids, 2010*(7), 1–14.

40. Noonan, E. M., Shah, D., Yaffe, M. B., Lauffenburger, D. A., & Samson, L. D. (2012). O6-Methylguanine DNA lesions induce an intra-S-phase arrest from which cells exit into apoptosis governed by early and late multi-pathway signaling network activation. *Integrative Biology : Quantitative Biosciences From Nano to Macro, 4*(10), 1237–1255.

41. Ward, J. F. (1990). The yield of DNA double-strand breaks produced intracellularly by ionizing radiation: a review. *International Journal of Radiation Biology, 57*(6), 1141–1150.

42. Riley, P. A. (1994). Free radicals in biology: oxidative stress and the effects of ionizing radiation. *International Journal of Radiation Biology, 65*(1), 27–33.

43. Hutchinson, F. (1985). Chemical changes induced in DNA by ionizing radiation. *Progress in Nucleic Acid Research and Molecular Biology, 32*, 115–154.

44. Olive, P. L. (1998). The role of DNA single- and double-strand breaks in cell killing by ionizing radiation. *Radiation Research, 150*(5 Suppl), S42–51.

45. Iliakis, G. (1991). The role of DNA double strand breaks in ionizing radiation-induced killing of eukaryotic cells. *BioEssays : News and Reviews in Molecular, Cellular and Developmental Biology, 13*(12), 641–648.

46. Wood, R. D., Mitchell, M., Sgouros, J., & Lindahl, T. (2001). Human DNA repair genes. *Science (New York, N.Y.), 291*(5507), 1284–1289.

47. Almeida, K. H., & Sobol, R. W. (2007). A unified view of base excision repair: lesion-dependent protein complexes regulated by post-translational modification. *DNA Repair, 6*(6), 695–711.

48. Wallace, S. S. (2014). Base excision repair: a critical player in many games. *DNA Repair, 19*, 14–26.

49.   Tell, G., & Demple, B. (2015). Base excision DNA repair and cancer. *Oncotarget*, *6*(2), 584–585.

50.   Krokan, H. E., Standal, R., & Slupphaug, G. (1997). DNA glycosylases in the base excision repair of DNA. *The Biochemical Journal*, *325 (Pt 1)*(Pt 1), 1–16.

51.   Kisker, C., Kuper, J., & Van Houten, B. (2013). Prokaryotic nucleotide excision repair. *Cold Spring Harbor Perspectives in Biology*, *5*(3), a012591–a012591.

52.   de Boer, J., & Hoeijmakers, J. H. (2000). Nucleotide excision repair and human syndromes. *Carcinogenesis*, *21*(3), 453–460.

53.   Schärer, O. D. (2013). Nucleotide excision repair in eukaryotes. *Cold Spring Harbor Perspectives in Biology*, *5*(10), a012609–a012609.

54.   Iyer, R. R., Pluciennik, A., Burdett, V., & Modrich, P. L. (2006). DNA mismatch repair: functions and mechanisms. *Chemical Reviews*, *106*(2), 302–323.

55.   Kunkel, T. A., & Erie, D. A. (2015). Eukaryotic Mismatch Repair in Relation to DNA Replication. *Annual Review of Genetics*, *49*(1), 291–313.

56.   Jiricny, J. (2013). Postreplicative mismatch repair. *Cold Spring Harbor Perspectives in Biology*, *5*(4), a012633–a012633.

57.   Lieber, M. R., Ma, Y., Pannicke, U., & Schwarz, K. (2003). Mechanism and regulation of human non-homologous DNA end-joining. *Nature Reviews. Molecular Cell Biology*, *4*(9), 712–720.

58.   Mimori, T., Akizuki, M., Yamagata, H., Inada, S., Yoshida, S., & Homma, M. (1981). Characterization of a high molecular weight acidic nuclear protein recognized by autoantibodies in sera from patients with polymyositis-scleroderma overlap. *The Journal of Clinical Investigation*, *68*(3), 611–620.

59.   Jeggo, P. A. (1990). Studies on mammalian mutants defective in rejoining double-strand breaks in DNA. *Mutation Research*, *239*(1), 1–16.

60.   Taccioli, G. E., Cheng, H. L., Varghese, A. J., Whitmore, G., & Alt, F. W. (1994). A DNA repair defect in Chinese hamster ovary cells affects V(D)J recombination similarly to the murine scid mutation. *The Journal of Biological Chemistry*, *269*(10), 7439–7442.

61.   Taccioli, G. E., Gottlieb, T. M., Blunt, T., Priestley, A., Demengeot, J., Mizuta, R., et al. (1994). Ku80: product of the XRCC5 gene and its role in DNA repair and V(D)J recombination. *Science (New York, N.Y.)*, *265*(5177), 1442–1445.

62.   Spagnolo, L., Rivera-Calzada, A., Pearl, L. H., & Llorca, O. (2006). Three-dimensional structure of the human DNA-PKcs/Ku70/Ku80 complex assembled on DNA and its implications for DNA DSB repair. *Molecular Cell*, *22*(4), 511–519.

63.   Walker, J. R., Corpina, R. A., & Goldberg, J. (2001). Structure of the Ku heterodimer bound to DNA and its implications for double-strand break repair. *Nature*, *412*(6847), 607–614.

64.   Hammel, M., Yu, Y., Mahaney, B. L., Cai, B., Ye, R., Phipps, B. M., et al. (2010). Ku and DNA-dependent protein kinase dynamic conformations and assembly regulate DNA binding and the initial non-homologous end joining complex. *The Journal of Biological Chemistry*, *285*(2), 1414–1423.

65. Aceytuno, R. D., Piett, C. G., Havali-Shahriari, Z., Edwards, R. A., Rey, M., Ye, R., et al. (2017). Structural and functional characterization of the PNKP-XRCC4-LigIV DNA repair complex. *Nucleic Acids Research*, *45*(10), 6238–6251.

66. Rothkamm, K., Krüger, I., Thompson, L. H., & Löbrich, M. (2003). Pathways of DNA double-strand break repair during the mammalian cell cycle. *Molecular and Cellular Biology*, *23*(16), 5706–5715.

67. Mao, Z., Bozzella, M., Seluanov, A., & Gorbunova, V. (2008). DNA repair by nonhomologous end joining and homologous recombination during cell cycle in human cells. *Cell Cycle*, *7*(18), 2902–2906.

68. Nussenzweig, A., Sokol, K., Burgman, P., Li, L., & Li, G. C. (1997). Hypersensitivity of Ku80-deficient cell lines and mice to DNA damage: the effects of ionizing radiation on growth, survival, and development. *Proceedings of the National Academy of Sciences of the United States of America*, *94*(25), 13588–13593.

69. Adachi, N., Ishino, T., Ishii, Y., Takeda, S., & Koyama, H. (2001). DNA ligase IV-deficient cells are more resistant to ionizing radiation in the absence of Ku70: Implications for DNA double-strand break repair. *Proceedings of the National Academy of Sciences of the United States of America*, *98*(21), 12109–12113.

70. Riballo, E., Critchlow, S. E., Teo, S. H., Doherty, A. J., Priestley, A., Broughton, B., et al. (1999). Identification of a defect in DNA ligase IV in a radiosensitive leukaemia patient. *Current Biology : CB*, *9*(13), 699–702.

71. Nicolas, N., Moshous, D., Cavazzana-Calvo, M., Papadopoulo, D., de Chasseval, R., Le Deist, F., et al. (1998). A human severe combined immunodeficiency (SCID) condition with increased sensitivity to ionizing radiations and impaired V(D)J rearrangements defines a new DNA recombination/repair deficiency. *The Journal of Experimental Medicine*, *188*(4), 627–634.

72. West, S. C. (2003). Molecular views of recombination proteins and their control. *Nature Reviews. Molecular Cell Biology*, *4*(6), 435–445.

73. Esashi, F., Galkin, V. E., Yu, X., Egelman, E. H., & West, S. C. (2007). Stabilization of RAD51 nucleoprotein filaments by the C-terminal region of BRCA2. *Nature Structural & Molecular Biology*, *14*(6), 468–474.

74. McIlwraith, M. J., McIlwraith, M. J., Vaisman, A., Liu, Y., Fanning, E., Woodgate, R., & West, S. C. (2005). Human DNA polymerase eta promotes DNA synthesis from strand invasion intermediates of homologous recombination. *Molecular Cell*, *20*(5), 783–792.

75. Drew, Y. (2015). The development of PARP inhibitors in ovarian cancer: from bench to bedside. *British Journal of Cancer*, *113 Suppl 1*(S1), S3–9.

76. Bryant, H. E., Schultz, N., Thomas, H. D., Parker, K. M., Flower, D., Lopez, E., et al. (2005). Specific killing of BRCA2-deficient tumours with inhibitors of poly(ADP-ribose) polymerase. *Nature*, *434*(7035), 913–917.

77. Eustermann, S., Videler, H., Yang, J.-C., Cole, P. T., Gruszka, D., Veprintsev, D., & Neuhaus, D. (2011). The DNA-binding domain of human PARP-1 interacts with DNA single-strand breaks as a monomer through its second zinc finger. *Journal of Molecular Biology*, *407*(1), 149–170.

78.   Jackson, S. P., & Bartek, J. (2009). The DNA-damage response in human biology and disease. *Nature*, *461*(7267), 1071–1078.

79.   Zhou, B. B., & Elledge, S. J. (2000). The DNA damage response: putting checkpoints in perspective. *Nature*, *408*(6811), 433–439.

80.   Myers, J. S., & Cortez, D. (2006). Rapid activation of ATR by ionizing radiation requires ATM and Mre11. *The Journal of Biological Chemistry*, *281*(14), 9346–9350.

81.   Lee, J.-H., & Paull, T. T. (2007). Activation and regulation of ATM kinase activity in response to DNA double-strand breaks. *Oncogene*, *26*(56), 7741–7748.

82.   Stiff, T., O'Driscoll, M., Rief, N., Iwabuchi, K., Löbrich, M., & Jeggo, P. A. (2004). ATM and DNA-PK function redundantly to phosphorylate H2AX after exposure to ionizing radiation. *Cancer Research*, *64*(7), 2390–2396.

83.   Williams, R. S., Moncalian, G., Williams, J. S., Yamada, Y., Limbo, O., Shin, D. S., et al. (2008). Mre11 dimers coordinate DNA end bridging and nuclease processing in double-strand-break repair. *Cell*, *135*(1), 97–109.

84.   Unsal-Kaçmaz, K., & Sancar, A. (2004). Quaternary structure of ATR and effects of ATRIP and replication protein A on its DNA binding and kinase activities. *Molecular and Cellular Biology*, *24*(3), 1292–1300.

85.   Dickey, J. S., Redon, C. E., Nakamura, A. J., Baird, B. J., Sedelnikova, O. A., & Bonner, W. M. (2009). H2AX: functional roles and potential applications. *Chromosoma*, *118*(6), 683–692.

86.   Fernandez-Capetillo, O., Chen, H. T., Celeste, A., Ward, I., Romanienko, P. J., Morales, J. C., et al. (2002). DNA damage-induced G2-M checkpoint activation by histone H2AX and 53BP1. *Nature Cell Biology*, *4*(12), 993–997.

87.   Morishima, K.-I., Sakamoto, S., Kobayashi, J., Izumi, H., Suda, T., Matsumoto, Y., et al. (2007). TopBP1 associates with NBS1 and is involved in homologous recombination repair. *Biochemical and Biophysical Research Communications*, *362*(4), 872–879.

88.   Krum, S. A., la Rosa Dalugdugan, E. de, Miranda-Carboni, G. A., & Lane, T. F. (2010). BRCA1 Forms a Functional Complex with γ-H2AX as a Late Response to Genotoxic Stress. *Journal of Nucleic Acids*, *2010*(51), 1–9.

89.   Goldberg, M., Stucki, M., Falck, J., D'Amours, D., Rahman, D., Pappin, D., et al. (2003). MDC1 is required for the intra-S-phase DNA damage checkpoint. *Nature*, *421*(6926), 952–956.

90.   Furuta, T., Takemura, H., Liao, Z.-Y., Aune, G. J., Redon, C., Sedelnikova, O. A., et al. (2003). Phosphorylation of histone H2AX and activation of Mre11, Rad50, and Nbs1 in response to replication-dependent DNA double-strand breaks induced by mammalian DNA topoisomerase I cleavage complexes. *The Journal of Biological Chemistry*, *278*(22), 20303–20312.

91.   Yu, X., Chini, C. C. S., He, M., Mer, G., & Chen, J. (2003). The BRCT domain is a phospho-protein binding domain. *Science (New York, N.Y.)*, *302*(5645), 639–642.

92.   Paull, T. T., Rogakou, E. P., Yamazaki, V., Kirchgessner, C. U., Gellert, M., & Bonner, W. M. (2000). A critical role for histone H2AX in recruitment of repair factors to nuclear foci after DNA damage. *Current Biology : CB*, *10*(15), 886–895.

93.	Matsuoka, S., Ballif, B. A., Smogorzewska, A., McDonald, E. R., Hurov, K. E., Luo, J., et al. (2007). ATM and ATR substrate analysis reveals extensive protein networks responsive to DNA damage. *Science (New York, N.Y.)*, *316*(5828), 1160–1166.

94.	Nakamura, A., Sedelnikova, O. A., Redon, C., Pilch, D. R., Sinogeeva, N. I., Shroff, R., et al. (2006). Techniques for gamma-H2AX detection. *Methods in Enzymology*, *409*, 236–250.

95.	Paulsen, R. D., Soni, D. V., Wollman, R., Hahn, A. T., Yee, M.-C., Guan, A., et al. (2009). A Genome-wide siRNA Screen Reveals Diverse Cellular Processes and Pathways that Mediate Genome Stability. *Molecular Cell*, *35*(2), 228–239.

96.	Floyd, S. R., Pacold, M. E., Huang, Q., Clarke, S. M., Lam, F. C., Cannell, I. G., et al. (2013). The bromodomain protein Brd4 insulates chromatin from DNA damage signalling. *Nature*, *498*(7453), 246–250.

97.	Löbrich, M., Shibata, A., Beucher, A., Fisher, A., Ensminger, M., Goodarzi, A. A., et al. (2010). gammaH2AX foci analysis for monitoring DNA double-strand break repair: strengths, limitations and optimization. *Cell Cycle*, *9*(4), 662–669.

98.	Chowdhury, D., Keogh, M.-C., Ishii, H., Peterson, C. L., Buratowski, S., & Lieberman, J. (2005). gamma-H2AX dephosphorylation by protein phosphatase 2A facilitates DNA double-strand break repair. *Molecular Cell*, *20*(5), 801–809.

99.	Wang, Hongyan, Wang, M., Wang, H., Böcker, W., & Iliakis, G. (2005). Complex H2AX phosphorylation patterns by multiple kinases including ATM and DNA-PK in human cells exposed to ionizing radiation and treated with kinase inhibitors. *Journal of Cellular Physiology*, *202*(2), 492–502.

100.	Qiao, Y., Spitz, M. R., Shen, H., Guo, Z., Shete, S., Hedayati, M., et al. (2002). Modulation of repair of ultraviolet damage in the host-cell reactivation assay by polymorphic XPC and XPD/ERCC2 genotypes. *Carcinogenesis*, *23*(2), 295–299.

101.	Mendez, P., Taron, M., Moran, T., Fernandez, M. A., Requena, G., & Rosell, R. (2011). A modified host-cell reactivation assay to quantify DNA repair capacity in cryopreserved peripheral lymphocytes. *DNA Repair*, *10*(6), 603–610.

102.	Burger, K., Matt, K., Kieser, N., Gebhard, D., & Bergemann, J. (2010). A modified fluorimetric host cell reactivation assay to determine the repair capacity of primary keratinocytes, melanocytes and fibroblasts. *BMC Biotechnology*, *10*(1), 46.

103.	Nagel, Z. D., Margulies, C. M., Chaim, I. A., McRee, S. K., Mazzucato, P., Ahmad, A., et al. (2014). Multiplexed DNA repair assays for multiple lesions and multiple doses via transcription inhibition and transcriptional mutagenesis. *Proceedings of the National Academy of Sciences of the United States of America*, *111*(18), E1823–32.

104.	Ostling, O., & Johanson, K. J. (1984). Microelectrophoretic study of radiation-induced DNA damages in individual mammalian cells. *Biochemical and Biophysical Research Communications*, *123*(1), 291–298.

105.	Collins, A. R. (2004). The comet assay for DNA damage and repair: principles, applications, and limitations. *Molecular Biotechnology*, *26*(3), 249–261.

106.	Olive, P. L., & Banáth, J. P. (2006). The comet assay: a method to measure DNA damage in individual cells. *Nature Protocols*, *1*(1), 23–29.

107.	Singh, N. P., McCoy, M. T., Tice, R. R., & Schneider, E. L. (1988). A simple technique for quantitation of low levels of DNA damage in individual cells. *Experimental Cell Research*, *175*(1), 184–191.

108.	Azqueta, A., Langie, S. A. S., Slyskova, J., & Collins, A. R. (2013). Measurement of DNA base and nucleotide excision repair activities in mammalian cells and tissues using the comet assay--a methodological overview. *DNA Repair*, *12*(11), 1007–1010.

109.	Fortini, P., Raspaglio, G., Falchi, M., & Dogliotti, E. (1996). Analysis of DNA alkylation damage and repair in mammalian cells by the comet assay. *Mutagenesis*, *11*(2), 169–175.

110.	Speit, G., & Rothfuss, A. (2012). The comet assay: a sensitive genotoxicity test for the detection of DNA damage and repair. *Methods in Molecular Biology (Clifton, N.J.)*, *920*(Chapter 6), 79–90.

111.	Hartmann, A., Schumacher, M., Plappert-Helbig, U., Lowe, P., Suter, W., & Mueller, L. (2004). Use of the alkaline in vivo Comet assay for mechanistic genotoxicity investigations. *Mutagenesis*, *19*(1), 51–59.

112.	Olive, P. L., & Banáth, J. P. (1993). Detection of DNA double-strand breaks through the cell cycle after exposure to X-rays, bleomycin, etoposide and 125IdUrd. *International Journal of Radiation Biology*, *64*(4), 349–358.

113.	Lovell, D. P., & Omori, T. (2008). Statistical issues in the use of the comet assay. *Mutagenesis*, *23*(3), 171–182.

114.	Forchhammer, L., Johansson, C., Loft, S., Möller, L., Godschalk, R. W. L., Langie, S. A. S., et al. (2010). Variation in the measurement of DNA damage by comet assay measured by the ECVAG inter-laboratory validation trial. *Mutagenesis*, *25*(2), 113–123.

115.	Møller, P., Möller, L., Godschalk, R. W. L., & Jones, G. D. D. (2010). Assessment and reduction of comet assay variation in relation to DNA damage: studies from the European Comet Assay Validation Group. *Mutagenesis*, *25*(2), 109–111.

116.	Wood, D. K., Weingeist, D. M., Bhatia, S. N., & Engelward, B. P. (2010). Single cell trapping and DNA damage analysis using microwell arrays. *Proceedings of the National Academy of Sciences of the United States of America*, *107*(22), 10008–10013.

117.	Weingeist, D. M., Ge, J., Wood, D. K., Mutamba, J. T., Huang, Q., Rowland, E. A., et al. (2013). Single-cell microarray enables high-throughput evaluation of DNA double-strand breaks and DNA repair inhibitors. *Cell Cycle*, *12*(6), 907–915.

118.	Ge, J., Prasongtanakij, S., Wood, D. K., Weingeist, D. M., Fessler, J., Navasummrit, P., et al. (2014). CometChip: a high-throughput 96-well platform for measuring DNA damage in microarrayed human cells. *Journal of Visualized Experiments : JoVE*, (92), e50607–e50607.

119.	Sykora, P., Witt, K. L., Revanna, P., Smith-Roe, S. L., Dismukes, J., Lloyd, D. G., et al. (2018). Next generation high throughput DNA damage detection platform for genotoxic compound screening. *Scientific Reports*, *8*(1), 2771.

120.	Ge, J., Chow, D. N., Fessler, J. L., Weingeist, D. M., Wood, D. K., & Engelward, B. P. (2015). Micropatterned comet assay enables high throughput and sensitive DNA damage quantification. *Mutagenesis*, *30*(1), 11–19.

121. Lehmann, A. R. (2003). DNA repair-deficient diseases, xeroderma pigmentosum, Cockayne syndrome and trichothiodystrophy. *Biochimie, 85*(11), 1101–1111.

122. Hall, J. M., Lee, M. K., Newman, B., Morrow, J. E., Anderson, L. A., Huey, B., & King, M. C. (1990). Linkage of early-onset familial breast cancer to chromosome 17q21. *Science (New York, N.Y.), 250*(4988), 1684–1689.

123. Begley, T. J., Rosenbach, A. S., Ideker, T., & Samson, L. D. (2002). Damage recovery pathways in Saccharomyces cerevisiae revealed by genomic phenotyping and interactome mapping. *Molecular Cancer Research : MCR, 1*(2), 103–112.

124. Madhusudan, S., & Hickson, I. D. (2005). DNA repair inhibition: a selective tumour targeting strategy. *Trends in Molecular Medicine, 11*(11), 503–511.

125. Lord, C. J., & Ashworth, A. (2012). The DNA damage response and cancer therapy. *Nature, 481*(7381), 287–294.

126. Nickoloff, J. A., Jones, D., Lee, S.-H., Williamson, E. A., & Hromas, R. (2017). Drugging the Cancers Addicted to DNA Repair. *Journal of the National Cancer Institute, 109*(11), 85.

127. Helleday, T., Petermann, E., Lundin, C., Hodgson, B., & Sharma, R. A. (2008). DNA repair pathways as targets for cancer therapy. *Nature Reviews. Cancer, 8*(3), 193–204.

128. Curtin, N. (2007). Therapeutic potential of drugs to modulate DNA repair in cancer. *Expert Opinion on Therapeutic Targets, 11*(6), 783–799. http://doi.org/10.1517/14728222.11.6.783
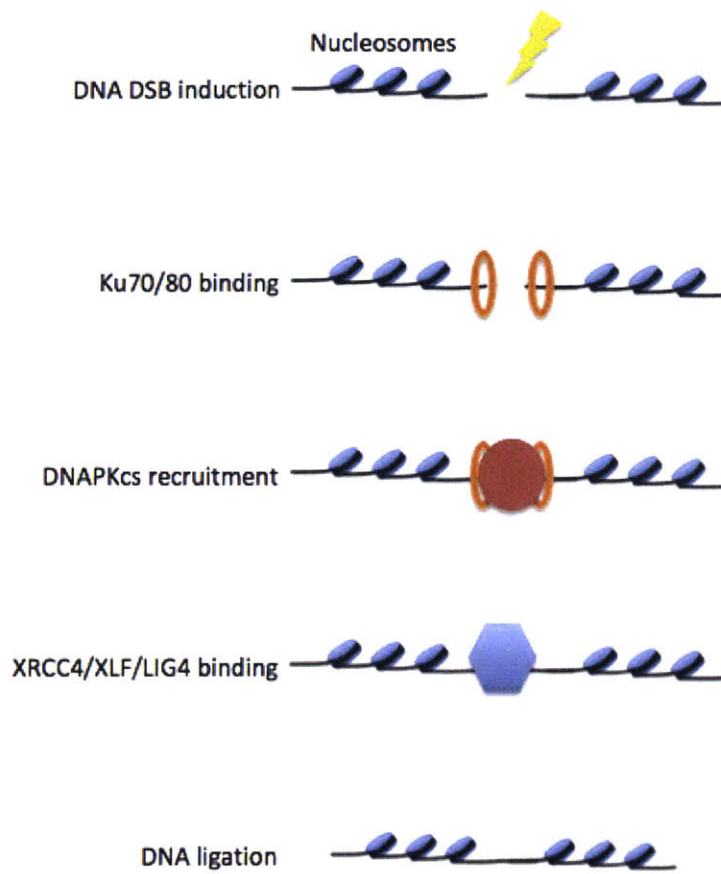
Figure 1-1.　Schematic of the NHEJ repair pathway.

Broken DNA strand

Unbroken sister chromatid

5' end resection by EXO1,
leaving 3' overhangs

Binding of Rad51 to form
nucleoprotein filament

Strand invasion
and repair synthesis

Annealing and extension

Ligation
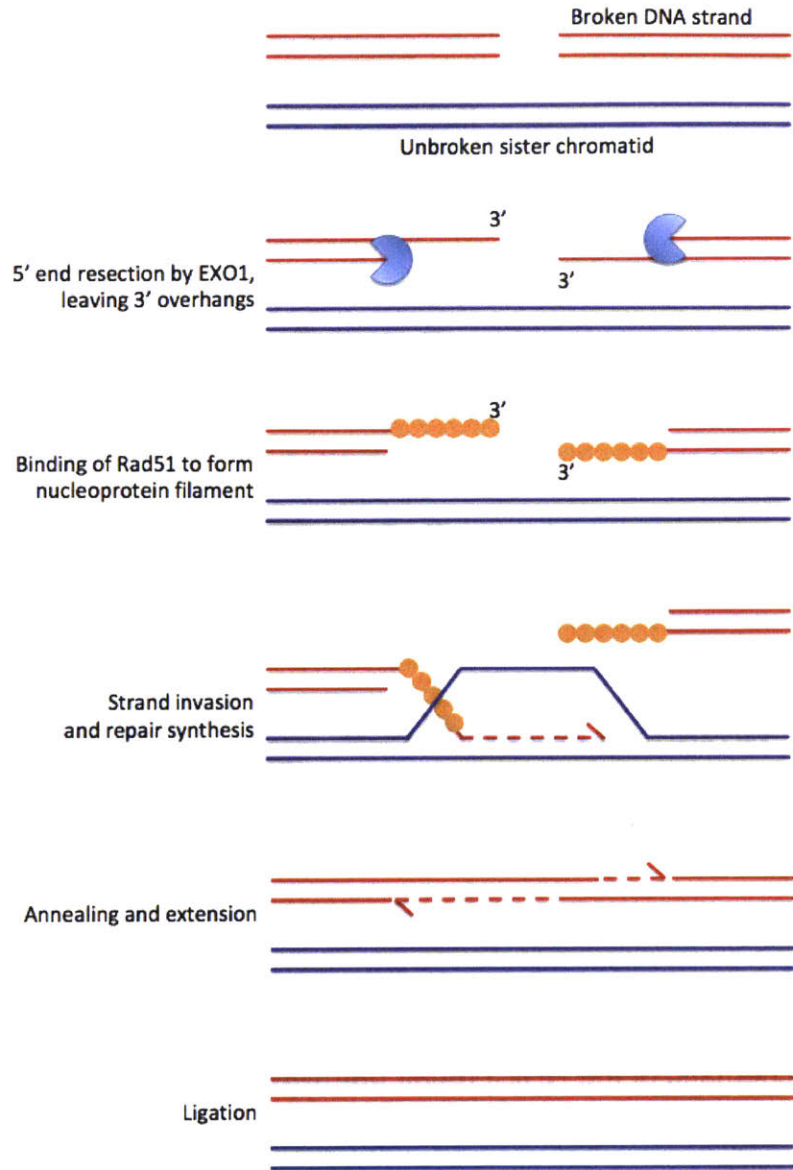
Figure 1-2. Schematic of the HR repair pathway.

A
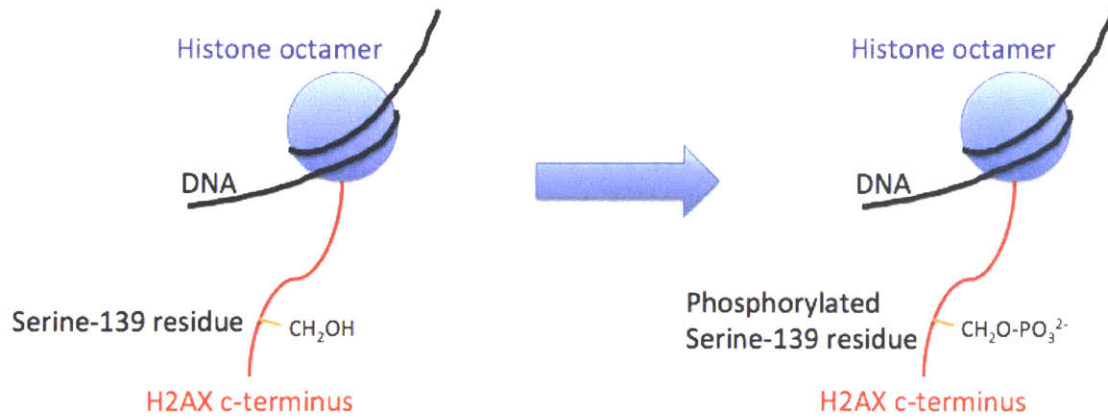
B
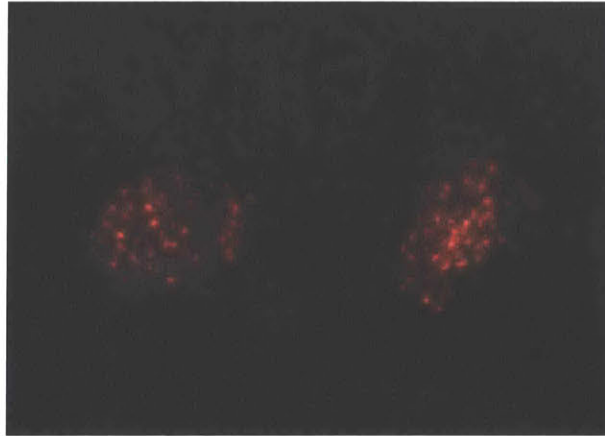
Figure 1-3. (A) Phosphorylation of H2AX at serine 139 to form γH2AX. (B) Example of an image obtained from γH2AX immunocytochemistry staining of cells 4 hours after they were treated with 10 Gy γ-IR. Bright spots indicate detection of γH2AX foci.
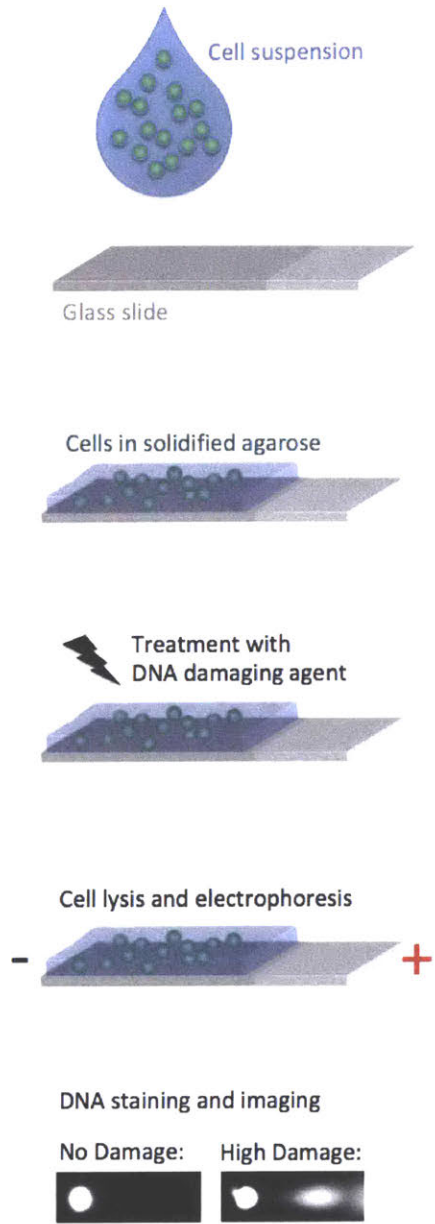
Figure 1-4. Steps for preparing the traditional comet assay.
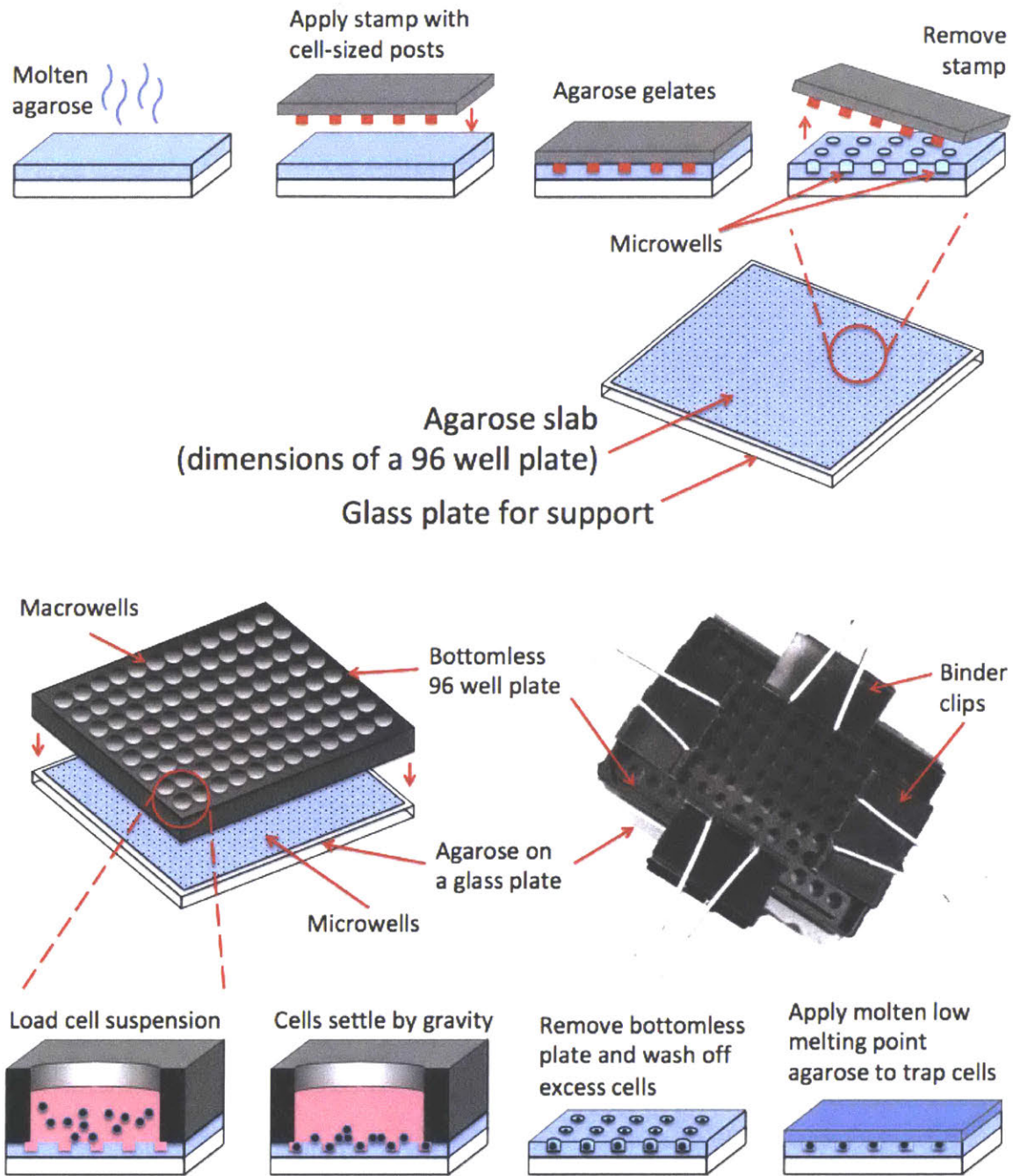
Figure 1-5.   Casting, assembling and loading the CometChip.

Chapter 2

Novel Apparatus for the CometChip Cell Microarray Enables Higher Throughput Screening for DNA Double Strand Breaks

2.1 Abstract

Radiotherapy and many cancer chemotherapy treatments rely on the induction of DNA damage for their efficacy, but cells can respond by repairing the damage, enabling resistance. The ability of therapeutics to damage DNA, as well as the ability of genes to modulate that damage, can be tested by using the comet assay. Here, we designed the High Throughput Screening CometChip (HTS CometChip), which enables the application of high throughput screening equipment to perform large-scale assessment of DNA damage using the comet assay. The apparatus consists of an aluminum base plate and a bottomless 96-well plate sandwiching an agarose slab, which is placed within a uni-well tray. The agarose slab has prepositioned mircowells, where cells can enter and later be assayed for their levels of DNA damage. Since the entire assay is contained within the uni-well tray, which has the dimensions of a standard multi-well plate, it can be manipulated by robotic arms and automatic liquid handling machines.

The result is the ability to perform the comet assay on 92 samples simultaneously within a 96 well format. Multiple assay pates can be analyzed sequentially with reduced manual labor and increased precision. Using the HTS CometChip, we examined the variability between identical samples loaded on the same assay and between assays, and we showed that HTS CometChip could produce more consistent results as compared to the traditional comet assay. We tested the HTS CometChip for its ability to detect DNA double stranded breaks (DSBs) by treating cells with ionizing radiation and assaying the levels of DNA damage over time. We also treated cells with a panel of RNAi reagents known to target DNA DSB repair genes and showed that depleting DNA DSB repair proteins resulted in detectable DNA DSB repair defects when the cells were exposed to ionizing radiation. Taken together, our results showed that HTS CometChip can produce data that is reliable and consistent, in a fraction of the time and manual labor required by the traditional comet assay.

2.2   Introduction

The genomes of our cells are constantly exposed to DNA damaging agents. Importantly, unrepaired DNA lesions can lead to mutations and cell death, causing many diseases, including cancer[1,2]. Given the potential impact of DNA damage, it follows that loss of function of DNA repair genes can promote cancer[3,4]. In addition, DNA repair genes also play a critical role in modulating the efficacy of cancer treatment, since many cancer therapy regimens exploit the vulnerability of tumor cells to DNA damage[5-7]. Therefore, discovering and studying genes that participate in DNA repair is

immensely beneficial both in terms of improving our understanding of cancer prevention as well as enabling more effective cancer treatment[8-12]. Here, we describe a novel advance in the throughput of DNA damage detection using a platform that is designed to be compatible with high throughput screening equipment. Our method is based on the neutral comet assay[13], a well-established approach for quantification of DNA double strand breaks (DSBs).

There are several established approaches for studying DNA damage[14,15] that could potentially be used to discover genes that participate in DNA repair. These include immunofluorescence based assays (e.g., γH2AX foci quantification[16-18]), plasmid based assays (e.g., the host cell reactivation assay[19-21]), radio-nucleotide incorporation based assays (e.g., unscheduled DNA synthesis assay[22,23]) and electrophoresis based assays, such as the comet assay[24-27]. Of these approaches, the comet assay is the only assay that directly measures physical chromosomal DNA damage, as opposed to measuring processes that are downstream of DNA damage. The comet assay can also be used to measure the effect of DNA damage or the impact of genes that modulate strand breaks, without a priori knowledge of their mechanism of action[28-31]. As such, the comet assay is particularly valuable as a tool for drug and gene discovery.

The comet assay (a.k.a., the single cell gel electrophoresis assay), is a well-established assay that is used to measure DNA damage in cells. The technique, first described by Ostling and Johanson[24] in 1984, is based on the principle that damaged DNA (which has lost superhelical tension or is fragmented) has increased electrophoretic mobility in an agarose gel, as compared to intact DNA. To perform the

comet assay, cells that have been exposed to a DNA damaging agent are first mixed with molten low melting point agarose to form a single cell suspension and this suspension is pipetted onto glass slides. The agarose is allowed to gelate, and the cells are then exposed to a lysis buffer, which dissolves membranes and inactivates all cellular activities, resulting in a 'nucleoid' of DNA trapped within agarose. The DNA is then subjected to electrophoresis. Under neutral conditions, the comet assay measures the frequency of DNA DSBs[13]. The DNA is stained and the extent of migration by DNA outside of the 'nucleoid' along the axis of electrophoresis can be measured by fluorescent microscopy. Images obtained from this assay typically show circular areas of staining originating from the nucleoid of cells, as well as tails exiting from the nucleoids, reflective of DNA damage. The more damage each cell had in its DNA prior to lysis, the more intense and longer the tail will be. The images of cells with damaged DNA reassemble a comet, which lends the assay its name.

Despite the fact that the principle underlying the comet assay is well grounded, the assay has not been used as a tool to screen for the effects of exposures or genes on DNA damage. For the traditional comet assay, each condition requires a single glass microscope slide. This approach quickly becomes cumbersome if a study requires testing of multiple variables in the same experiment. For example, a relatively simple experiment with the goal of measuring the level of DNA damage in cells exposed to 3 doses of ionizing radiation (γIR) over 4 time points will require at least 13 glass slides (including one for a non-treated control). More slides will be needed for replicates. As experiments scale up in size and complexity, the number of glass slides rapidly becomes unfeasible, due to the limited number of slides that the researcher can

effectively handle. Further, separate preparations of each sample also leads to significant variance among samples[32]. In addition to difficulties in handling a glass slide for each condition, the traditional comet assay also suffers from several other challenges. The randomness of the positions of the cells within the agarose necessitates optimization of cell densities for each sample preparation, in order to avoid overlapping and unanalyzable comets, while at the same time providing sufficient comets for analysis. Random positioning of cells within the agarose also leads to comets having different focal planes, which means that each comet needs to be imaged individually, which is extremely laborious.

To address these limitations of the comet assay, Engelward and co-workers developed the CometChip[33-35], which exploits a micropatterned cell array on agarose to maximize the number of useful comets per unit area of agarose. To accomplish this, microfabrication techniques are exploited to create custom-made stamps, each with an array of cell-sized micro-posts. These stamps can be applied to molten agarose to create an agarose slab with an array of cell-sized microwells (Fig. 2-1A). A cell suspension is then pipetted over the agarose microwell array, and cells will enter the microwells when they settle down via gravity. The CometChip is then rinsed, which washes away excess cells and cells within the microwells are encapsulated by applying a thin layer of molten low melting point agarose (Fig. 2-1B). The CometChip agarose slab can be made to be the size of a 96 well plate, and partitioned into multiple individual macrowells by clamping a bottomless well plate onto the agarose, which is supported by a glass plate. Alternatively, hardware for creating macrowells is available through Trevigen[36]. Each 96-well macrowell has ~300 microwells at its base, and can

be treated with DNA damaging agents and analyzed for levels of DNA damage using the same protocol as the standard comet assay. In doing so, each glass slide can now be analyzed as a single well in a 96 well plate.

The CometChip addresses the key limitations of the comet assay. First, since the CometChip can be 96-well plate-compatible, dozens of samples can now be prepared in parallel, increasing the rate at which the comet assay can be performed. The ability to perform experiments within a single agarose unit using the CometChip also helps to reduce sample-to-sample variations that will occur if multiple glass slides are used for the standard comet assay[34]. Imaging 96 assays on a single CometChip also eliminates the need to change glass slides between samples, saving time during the imaging process. Furthermore, since the CometChip has microwells that can trap cells and enable the researcher to wash away excess cells, it eliminates the laborious step of needing to determine cell densities prior to plating cells on glass slides (as long as there are more than 10,000 cells per sample). Unloaded excess cells that did not enter the microwells can be easily washed away during rinsing; therefore overlapping comets are rarely observed when the CometChip is used. The regular array also places cells at the same depth within the agarose, therefore researchers can now take single images of multiple 'in-focused' comets, rather than changing focal planes frequently, or rejecting 'out-of-focus' comets in the standard assay. A single image taken with a microscope using a 5X objective typically contains 25 well-spaced comets, representing significant time-savings as compared to taking 25 individual images for the traditional comet assay. Also, due to the fact that the comets are now regularly spaced, in-house written software can automatically select comets by comparing the distance between each

comet and its immediate neighbors. Together, these improvements increase the speed of analysis by orders of magnitude, while at the same time providing increased consistency, and thus increased sensitivity.

All of the advantages of the existing CometChip prime it for its usage in complex, high throughput screening experiments that might query DNA damage and repair. However, the CometChip was not yet amendable for high throughput screening, because the hardware dimensions did not match a typical multiwell plate, leading to incompatibility with high throughput screening equipment. Specifically, the original CometChip is assembled by clamping a microwell-arrayed agarose between a glass plate and a bottomless 96-well plate using 2-inch binder clips (Fig. 2-1B). This assembly had two issues that prevented it from being used with high throughput robotics and imaging. First, while the binder clips provide the clamping force necessary to seal the individual macrowells, they disrupt the form factor of a standard multiwell plate. Additionally, the clips are problematic because they extend beyond the boundaries of a regular multiwell plate, interfering with the ability of standard robotic arms to pick up and manipulate the platform. Second, the arbitrary placement of the bottomless 96-well plate on top of the microwell-arrayed agarose in the original CometChip assembly resulted in the random positioning of wells relative to the boundaries of the CometChip. This is incompatible with the high throughput robotics and automatic imaging systems because the machines assume consistency in the positioning of the wells. It is noteworthy that the commercially available CometChip® is also incompatible with high throughput screening technologies, due to unorthodox outer dimensions[36].

Here, we have overcome the key limitations of the CometChip hardware by creating a High Throughput Screening CometChip (HTS CometChip), which is compatible with high throughput robotics. We removed the binder clips and replaced them with an internal clamping mechanism. We also positioned the clamping mechanism such that the bottomless 96-well plate is in a fixed position relative to the outer dimensions of the apparatus. We prepared multiple HTS CometChips simultaneously and tested them for variability among plates. Together, these improvements make it possible to harness high throughput screening robotics and imaging tools to obtain data at an unprecedented rate, thus unlocking the assay's potential for large-scale drug and gene screening experiments.

2.3   Materials and Methods

Cell culture. M059K and M059J glioblastoma cells were cultured in 1:1 DMEM/F12 nutrient mix (Invitrogen) supplemented with 10% FBS (Atlanta Biologicals, Atlanta, GA), MEM Non-Essential Amino Acids (Invitrogen) and 100-units/ml penicillin-streptomycin (Invitrogen).

HTS CometChip apparatus fabrication. A 120 by 78 mm aluminum base plate was cut from a 3 mm thick aluminum sheet to fit tightly in a uni-well tray (VWR). Four aluminum posts (6 mm in diameter and 6.5 mm in height) were welded onto the base plate with their centers 28.5 mm and 7.5 mm from the short and long edges of the plate respectively. A 2 mm wide and 5 mm deep hole was drilled into each aluminum post

and threaded on surface. The outer edges of a bottomless 96-well plate (VWR) were sawed off, leaving a 110 by 74 mm grid of 96 wells. Wells A3, A10, H3 and H10 were plugged with tight fitting polystyrene cylinders with a 2 mm wide hole drilled at their centers. HTS CometChip was assembled by sandwiching the microwell arrayed agarose between the aluminum base plate and the bottomless well plate, such that the posts on the aluminum plate meet the pegs on the bottomless plate, and fastened together by screws.

Neutral CometChip. The CometChip was prepared as described previously. Briefly, 12ml of 1% molten agarose in PBS was poured over a GelBond flim (Lonza) placed on a uni-well tray (VWR) before applying a reusable PDMS stamp arrayed with microposts. When the agarose was solidified, the PDMS stamp was removed to reveal microwells for cell loading. After the CometChip was loaded with cells, excess cells were washed off with PBS and a thin layer of 1% molten low melting point agarose in PBS was applied. Cells were lysed at 43°C overnight after desired timepoints by submerging the CometChip into lysis buffer containing 2.5M NaCl, 100 mM Na$_2$EDTA, 10 mM Tris, 1% N-Lauroylsarcosine, pH 9.5 with 0.5% Triton X-100 and 10% DMSO. The CometChip was washed thrice with neutral electrophoresis buffer containing 90 mM Tris, 90 mM Boric Acid, 2 mM Na$_2$EDTA, pH 8.5. Electrophoresis was conducted using pre-chilled neutral electrophoresis buffer at 4°C for 1 hr at 0.6 V/cm and 6 mA.

High throughput screening robotics. Access to high throughput screening robotics and equipment was obtained via MIT's Koch Institute of Integrative Cancer Research,

Swanson Biotechnology Center, High Throughput Screening Core Facility. Robotic manipulation of the HTS CometChip was performed using a Tecan Evo 100 liquid handler, equipped with a 96-well MultiChannel Arm (MCA96) and a Robotic Manipulator (RoMa) arm. The Evo 100 is also integrated with a Liconic STX110 incubator with temperature, humidity, CO_2 control. Imaging of the HTS CometChip was performed using Thermo Scientific Cellomics® ArrayScan® VTI HCS Reader using a 5X objective.

Lentiviral shRNA knockdown. shRNA lentiviral reagents were obtained from the Genetic Perturbation Platform of the Broad Institute of MIT and Harvard. The list of shRNA IDs and their target sequences are shown in Supplementary Fig. 2-1. The shRNA lentiviral reagents were arrayed in a 96-well format: each well contains a unique virus encoding an individual shRNA. M059K cells were plated on 5 tissue culture 96-well plates per experiment at a density of 600 cells per well, transduced with lentiviruses with an average MOI of 8, 24 hours after cell plating and selected with 1.5 μg/ml puromycin 48 hours after transduction. Puromycin was applied for 72 hours and cells were allowed to recover in selection free media for 24 hours. All media changes were performed using a BioTek EL406 microplate washer under sterile conditions. Transfer of cells from tissue culture plates to HTS CometChips were performed using high throughput screening robotics equipment (see above). During the transfer, media was removed from the tissue culture plates before trypsin was added to dislodge the cells. Media was added to quench the trypsin and triturated to create single cell suspensions in each well. Cell suspensions from each tissue culture plate were transferred onto 1 HTS CometChip for a total of 5 HTS CometChips and allowed to incubate at 37°C for 20

minutes. Excess unloaded cells were washed off and a thin layer of low melting point agarose was applied to encapsulate cells trapped in microwells. The HTS CometChip assigned as non-treated control is lysed immediately while the 4 remaining HTS CometChips were submerged in media and treated with 100 Gy of γ-rays at 1 Gy/min using a ^{137}Cs source. Using neutral conditions that detect DNA DSBs, cells were allowed to repair DNA damage at 37°C for 0, 1, 2, or 4 hours in media before they were lysed. Tail length was then used as a measure of the frequency of DNA DSBs.

Treatment with ionizing radiation. Cells that were encapsulated in the HTS CometChip were exposed to 25, 50 or 100 Gy of γIR at a dose rate of about 100 Gy/min from a ^{60}Co source (GammaCell 220 Excel).

Western blotting. M059K cells were treated with lentiviral shRNA constructs targeting DNAPKcs or GFP, and whole cell lysates were harvested after successful transduction. Whole cell lysates were collected using RIPA buffer (Pierce) supplemented with HALT protease inhibitor (ThermoFisher Scientific) and frozen at -20°C. Lysates were thawed on ice and spun down at max speed for 15 minutes. Lysates were mixed with Laemmli sample buffer (BIO-RAD) according to manufacturer's instructions and incubated at 95°C for 5 minutes and then chilled on ice. Samples were loaded onto a 6% PAGE gel, and electrophoresed at 200V for about 90 minutes with TRIS-glycine-SDS running buffer (BIO-RAD). Proteins were transferred onto nitrocellulose membranes (BIO-RAD) at 100V for 2 hours in TRIS-glycine-methanol transfer buffer (BIO-RAD). Membranes were blocked in Odyssey blocking buffer (LI-COR) for 2 hours at room temperature with

gentle shaking. DNAPKcs and Ku80 were probed with primary antibodies (Cell Signaling Technologies cat#4602 and cat#2180) in blocking buffer overnight at 4°C with gentle shaking. Secondary antibodies (LI-COR) were applied to the membrane in blocking buffer for 2 hours at room temperature with gentle shaking. Bands were visualized using a LI-COR Odyssey scanner.

2.4   Results

High throughput screening robotic workstations typically employ a Robotic Manipulator (RoMa) arm to manipulate assays. The RoMa consists of two parallel grippers that converge to pick up an assay plate, or separate to release it. The interaction between assay plates and the RoMa requires the assay plate's exterior profile to match that of a typical multiwell assay plate. As described above, binder clips had been used to compress a bottomless 96-well plate against the thin layer of agarose supported by a glass plate. The clamping force ensured that there was no detectable leakage between the macrowells. The challenge was to be able to mimic the clamping force of the binder clips, while maintaining standard dimensions. Our approach was to create a set of internal fasteners that are within the boundaries of a typical multiwell plate.

Achieving an effective approach required iterations, described here. In our first iteration of the HTS CometChip, we designed the apparatus such that four internally threaded polystyrene posts were fused directly onto a standard uni-well tray at positions corresponding to wells A1, A12, H1 and H12 on a 96-well plate (Fig. 2-2A). These posts

were paired with hollow pegs (e.g., polystyrene cylinders), each with a 2 mm hole in their centers. These hollow pegs were then fused to the inner surface of the wells of a bottomless 96-well plate (Fig. 2-2A). The apparatus was then assembled by placing the CometChip agarose onto the uni-well tray. Holes in the agarose (suppored by gel bond) enable passage of the pegs through the agarose layer. The bottomless 96-well plate was then fastened to the apparatus at each corner of the plate (Fig. 2-2B). While somewhat effective, the posts frequently detached from the tray when the screws were applied to clamp the bottomless 96-well plate onto the apparatus. We overcame this limitation by changing the material of the base plate to steel. Thus, machined steel posts were welded onto a 1 mm thick steel plate that was cut to snugly fit within the uni-well tray (transperancy is not an issue, because the apparatus is disassembled prior to imaging). Thus, the uni-well tray base provides the requisite form factor for robotic handling. While compatible with HTS robotics, the point forces exerted at the corner wells by the screw systems caused a slight warping of the thin steel plate. This resulted in an inadequate sealing between the clamped bottomless 96-well plate and the microwell arrayed agarose, which lead to leakage of media between wells, particularly in the middle of the plate. This led us to our final iteration of the HTS CometChip apparatus where we replaced the 1 mm steel plate with a 3 mm aluminum plate (Fig. 2-3A). The increase in thickness of the base plate made it stiffer, such that it would not warp when the apparatus is assembled. The change in material from steel to aluminum reduced the weight of the apparatus, which reduced the chances that the plate would be dropped when handled by the RoMa robotic hander. We also shifted the posts form

wells A1, A12, H1 and H12 to more central wells A3, A10, H3 and H10, in order to more evenly distribute the forces across the entire 96-well plate.

In the final setup, for each HTS CometChip, a piece of GelBond flim with the agarose microwell overlay is cut to the size of the internal dimensions of a standard uni-well rectangular plate. The GelBond film is then punctured to create holes at the A3, A10, H3 and H10 positions and slotted into position over the aluminum plate (with the posts passing through the holes). The bottomless 96-well plate with its cylindrical plugs is then placed over the agarose and screws are inserted and tightened (Fig. 2-3A). The assembled apparatus is placed in a standard uni-well tray (Fig. 2-3B), which can be handled by high throughput screening robotics and liquid handling machines.

We performed several tests to ensure efficacy for high throughput screening. First, we tested the ability of the apparatus to consistently achieve effective sealing among the 96 macrowells. To do this, we assembled HTS CometChips and loaded alternate columns of wells with either PBS or PBS colored with dye for 20 minutes. We observed that there was no evidence of leakage between wells (e.g., we did not see evidence of dye in the PBS-only wells), indicating that we have achieved effective sealing between the agarose and the bottomless 96-well plate within the HTS CometChip.

We next tested the compatibility of the HTS CometChip with our robotic apparatus. We used a Tecan Evo 100 liquid handling deck enclosed within a Baker Hood (HEPA filtered) enclosure, and the liquid handling deck was connected to a Liconic automatic incubator via a shuttling tray. A script was developed to load cell culture media into the HTS CometChip while on the deck, followed by transfer to the

incubator. Through this process, we optimized several parameters in the robotic scripts, such as amount of force to apply on the apparatus by the robotic gripper, movement speed of the robotic gripper when it is handling the apparatus and the contact points between the apparatus and the robotic gripper. When the optimization process was completed, there was an acceptable residual failure rate of about once every 50 cycles.

To test the consistency of the results using the HTS-CometChip, we loaded all 92-wells of three HTS CometChips with cells and exposed the embedded cells to 50 Gy of γIR, followed immediately with lysis conditions. We performed the neutral comet assay using standard conditions for DSB detection[13] and found that the coefficient of variation (COV) among the macrowells of each HTS-CometChip to be less than 10% (Table 2-1, Fig. 2-4 and Supplementary Fig. 2-2). This result is consistent with those of Ge et al., who showed that the COV for well-to-well variation was about 5%. Furthermore, the COV among the three plates was also less than 10%, which is again consistent with the results of Weingeist et al[34]. Together, these results indicate that the HTS CometChip preserves the improvements in consistency achieved using the original CometChip, as compared to the traditional comet assay.

To demonstrate that the HTS CometChip can be used for larger-scale experiments using high throughput robotics, we performed a γIR dose-response experiment and combined this with a DNA repair time course experiment for each dose of γIR used. We chose to use γIR due to its reliability in inducing DNA DSBs in cells. We performed this experiment using M059J and M059K cell lines, which were derived from the same brain tumor biopsy[37]. The M059J cells do not express functional DNA-PKcs[38], a key enzyme in the NHEJ repair pathway[39], which is responsible for the repair of the

majority of radiation induced DNA DSBs. Therefore, we expected the M059J cells to repair DNA DSBs at a much slower rate compared to M059K cells that have wild type levels of DNAPKcs. Based on previous studies[34], we thus expected that the M059J cells would have increased persistence of DNA DSBs, which would lead to longer comet tails compared to M059K cells.

We loaded cells into three HTS CometChips using the robotic equipment and assigned one HTS CometChip for each dose of γIR at 25, 50 and 100 Gy. We divided the HTS CometChips into sections and lysed the sections assigned to be non-treated controls immediately after the HTS CometChips were prepared. All the other sections were irradiated with their assigned doses of γIR and placed in complete media in an incubator to allow cells to repair DNA damage for a predetermined amount of time, prior to overnight lysis. First, we observed that there was a radiation dose dependent increase in the comet tail lengths from M059K cells (Fig. 2-5A). Using images obtained from the HTS CometChip that was treated with 100 Gy of γIR, we observed that the comet tails from M059K cells were the longest immediately after radiation and became shorter when cells were allowed more time to repair DNA damage (Fig. 2-5B, top panels). In contrast, the comet tails from M059J cells remained longer than the M059K cells for the entire duration of the experiment, as expected (Fig. 2-5B, bottom panels). When pooled across all three HTS CometChips, we found that the negative controls with M059J and M059K cells had low COV of 8% and 4% respectively (Fig. 2-5C, first pair of bars in each panel), consistent with the COV values we had obtained in Table 2-1 and Figure 2-4. Immediately after radiation, we observed no significant differences between the M059K and M059J cell lines, as the cells did not have time to perform DNA

repair. We also observed a clear trend of decreasing comet tail lengths with increasing time, indicative of cells performing DNA repair and reducing the number of DNA DSBs in their genomes. We further observed that at 2 and 4 hours after exposure to γIR, the differences in comet tail lengths between M059K and M059J cells increased when the dose of γIR was increased from 25 Gy to 100 Gy. One possibility is that other DNA DSB repair pathways, such as alternative NHEJ[40,41], could compensate for the lack of NHEJ activity when 25 Gy of γIR was applied to M059J cells, but their activities were insufficient for repair DNA DSBs when the cells were exposed to 100 Gy of γIR.

To test the possibility that the HTS CometChip can detect changes in DNA DSB repair when specific genes were depleted, we subjected M059K cells to gene knockdown using lentiviral shRNA technology[42,43] and measured the extend of DNA DSBs after these cells had been exposed to γIR. We designed a custom-made 96-well plate of lentiviruses expressing shRNAs that are either anticipated to have no effect, or that knock down NHEJ genes (Fig. 2-6A). Each negative control gene and each NHEJ gene were targeted using two and three unique shRNAs, respectively. The top and bottom rows of the plate were used for untreated M059K and M059J cells, as cell-line controls. We first plated M059K cells on standard 96-well plates and treated the cells with lentiviruses from the custom-made lentiviral plate. We applied puromycin to select for successfully transduced cells and transferred the cells onto HTS CometChips. We placed the non-treated HTS CometChip into lysis buffer immediately after plating, to allow us to assay for the background levels of DNA DSBs in the cells. All the other HTS CometChips were irradiated with 100 Gy of γIR and placed in complete media in an incubator to allow cells to repair DNA DSBs for up to 4 hours, prior to cell lysis. We

observed that the un-transduced M059K and M059J cells behaved similarly to previous experiments, wherein M059K cells repaired most of the DNA DSBs within 4 hours, while M059J cells showed reduced repair (Fig. 2-6B, red and blue lines, Fig. 2-5A, rightmost panel). As expected, M059K cells that were transduced with negative control shRNAs behaved similarly to the M059K un-transduced cells (Fig. 2-6B, green circles). For some of the hairpins targeting NHEJ genes, we observed that DNA damage persisted relative to negative control samples (see top 5 purple circles, 4 hours after γIR in Fig. 2-6B). 4 hours after γIR, we observed that there appear to be two distinct groups of shRNAs, with 8 out of 21 shRNAs appearing to cause higher levels of unrepaired DNA damage after γIR exposure. Six out of the seven NHEJ genes selected in our custom-made lentiviral shRNA plate were represented by those 8 shRNAs. We performed the experiment in duplicates and compared the results for DNAPKcs shRNAs (Fig. 2-7A). We observed a high level of reproducibility for our un-transduced M059K and M059J cell lines as expected (blue and red lines respectively), since these cell lines have shown similar results in previous experiments (Fig. 2-4 and 2-5). Importantly, while one of the DNAPKcs shRNAs (shRNA #1) resulted in high levels of persistent DNA DSBs in both duplicate screens, shRNAs #2 and #3 did not appear to do so, likely due to inefficient knockdown efficiency. To test this possibility, we performed a western blot to probe of the levels of DNAPKcs from whole cell extracts harvested from M059K cells treated with DNAPKcs shRNAs from a separate lentiviral preparation. We found that shRNA #1 resulted in the most efficient knockdown of DNAPKcs (Fig. 2-7B), which is consistent with the observation that this hairpin resulted in high levels of persistent DNA DSBs. We noted that shRNA #3 showed normal levels of DSB repair in the pilot screen,

even though cells treated with shRNA #3 from a separate lentivirus preparation showed that shRNA #3 appeared to be as efficient in depleting DNAPKcs as shRNA #1. It is possible that shRNA#3 was a defective reagent due to technical reasons in the lentiviral preparation of the shRNA for the pilot screen, leading to ineffective knockdown. These results show that shRNAs have different levels of effectiveness in depleting expression of their target genes, such that inefficient knockdown correlates with WT levels of DNA repair as expected.

2.5   Discussion

In this study, we developed a method to perform large-scale comet assay based experiments utilizing high throughput screening robotic technology and demonstrate that it is able to detect genes that participate in DNA DSB repair, in an experiment that mimics a genome-wide shRNA screen. The original comet assay, although well accepted by the DNA repair community, is an assay that is rarely adopted when researchers intend to perform large-scale experiments. This is primarily due to two reasons: the cumbersome nature of the comet assay and the high variability in data produced by the assay. The CometChip alleviates the problems of the comet assay by maximizing the number of comets obtainable per unit area of the assay. This allows multiple samples to be tested together on the same assay. Testing multiple samples on the same assay reduces the amount of work needed to prepare each sample separately, therefore making the assay less cumbersome to perform. Testing multiple samples on the same assay also reduces noise between samples, therefore reducing

variability in the data produced. The HTS CometChip takes this a step further, enabling the assay to be performed with the assistance of high throughput screening robotics. The equipment typically found in a high throughput screening facility typically consists of robotic arms that can pick up and move assay plates between workstations, as well as liquid handlers that pipettes liquids between assay plates. The HTS CometChip is compatible with these equipment, since it mimics the dimensions of typical multiwell assay plates that are used in high throughput screens. Using robotic equipment relieves the researcher of manually pipetting samples onto the HTS CometChip, therefore avoiding pipetting fatigue when thousands of samples are to be tested. Pairing the HTS CometChip with high throughput screening robotics therefore enables the assay to be potentially used in genome wide screens, which is physically impossible with the traditional comet assay or the original comet chip.

Apart from relieving manual work to transfer cells from tissue culture plates onto the HTS CometChip, the HTS CometChip also greatly reduces the effort needed to collect images from the assay. For the traditional comet assay, each glass slide containing one sample has to be individually mounted onto the microscope and scanned for representative regions of acceptably dense comets. More images will have to be taken if the comets are sparse, and some images might have to be discarded if overly dense comets result in overlapping comets. Also, due to the non-uniformity of the cells within the depth of the agarose in the traditional comet assay, a small percentage of comets will be blurred, resulting in a lower yield of analyzable comets. The original CometChip eliminates both of these problems by placing cells in a uniformly dense array and in the same planar depth of field throughout the assay. Having 96 samples on

a single CometChip also eliminates the tremendous amount of time (estimated to be between 30 seconds to a minute per sample) needed to switch between slides and relocate the focal plane for every sample. Despite its advantages over the traditional comet assay, the original CometChip still requires the researcher to swap the assay after every 96 samples and control the microscope to obtain sharp images. With the HTS CometChip, the researcher no longer has to be physically present during the imaging process. The HTS CometChip enables us to employ automatic imaging microscopes to acquire images, leveraging software to programmatically control the image acquisition process. Multiple HTS CometChips can now be queued to be imaged automatically overnight, with minimal human intervention, which further increases the rate at which data can be collected with the HTS CometChip – an important factor in reducing overall screening time in high throughput screens.

Our study has focused on the application of HTS CometChip to detect DNA DSB repair defects using either existing cell lines with DNA DSB repair differences or using reagents that target genes known to participate in DNA DSB repair. Apart from measuring DNA DSBs, the comet assay can also be used to measure DNA single stranded breaks (SSBs) and alkali labile base lesions by employing alkaline conditions during electrophoresis. DNA damaging agents such as methyl methanesulfonate or hydrogen peroxide create base lesions and DNA SSBs, and are used to test a cell's ability to repair the resulting DNA damage via Base Excision Repair. Similarly, agents that create Mismatch Repair and Nucleotide Excision Repair lesions can be used to measure the activity of these repair pathways in a cell. This suggests that the HTS CometChip, with the same underlying principle of detecting DNA damage as the comet

assay, can be effective in discovering genes that modulate other DNA repair pathways. Similarly, the HTS CometChip can also be used as a screening tool to discover drugs that can potently damage DNA, as well as in population epidemiological studies whereby cells from many individuals within a population can be tested for their response to one or several DNA damaging agents.

In summary, the HTS CometChip dramatically increases the efficiency at which measurements of the levels of DNA damage in cells can be made while at the same time reducing the amount of manual work required. With these advantages over the traditional comet assay, the HTS CometChip can now be used in large-scale screens, as a tool to discovery genes and drugs that modulate various DNA repair pathways.

2.6   Conclusion

We have developed a platform with which large-scale comet assay based experiments can be performed by harnessing high throughput screening technologies. Capitalizing on the advantages the CometChip had over the traditional assay, the HTS CometChip fully realizes the potential of the assay to be utilized in large-scale drug discovery or genomic screens. We achieved this by designing the HTS CometChip, such that it mimics typical multiwell plates that are used in high throughput screens. In doing so, the HTS CometChip can now be prepared with the assistance of high throughput screening robotics, which greatly reduces the amount of manual work needed to perform the assay. This allows the researcher to execute the assay at a higher rate and over longer periods of time with less fatigue, enabling measurement of

DNA damage over thousands of samples. In this work, we have first shown that the HTS CometChip could produce consistent data. We then showed that the HTS CometChip could detect persistent DNA DSBs created by γIR and left unrepaired in repair deficient cells. Finally, we showed that with a panel of reagents that deplete known DNA DSB repair genes, we were able to detect a DNA DSB repair defect for six out of the seven genes targeted. Taken together, we have designed an apparatus that greatly reduces the amount of manual labor work required when performing typical comet assay experiments, opening doors to the discovery of new genes and molecules that affect DNA repair by enabling researchers to perform experiments that were not physically possible before the invention of HTS CometChip.

References

1.   Hoeijmakers, J. H. J. (2009). DNA damage, aging, and cancer. *The New England Journal of Medicine*, *361*(15), 1475–1485.

2.   Shimizu, I., Yoshida, Y., Suda, M., & Minamino, T. (2014). DNA damage response and metabolic disease. *Cell Metabolism*, *20*(6), 967–977.

3.   Hanahan, D., & Weinberg, R. A. (2011). Hallmarks of cancer: the next generation. *Cell*, *144*(5), 646–674.

4.   Hoeijmakers, J. H. (2001). Genome maintenance mechanisms for preventing cancer. *Nature*, *411*(6835), 366–374.

5.   Nickoloff, J. A., Jones, D., Lee, S.-H., Williamson, E. A., & Hromas, R. (2017). Drugging the Cancers Addicted to DNA Repair. *Journal of the National Cancer Institute*, *109*(11), 85.

6.   Lord, C. J., & Ashworth, A. (2012). The DNA damage response and cancer therapy. *Nature*, *481*(7381), 287–294.

7.   Goldstein, M., & Kastan, M. B. (2015). The DNA damage response: implications for tumor responses to radiation and chemotherapy. *Annual Review of Medicine*, *66*(1), 129–143.

8.   Kabir, Y., Seidel, R., Mcknight, B., & Moy, R. (2015). DNA repair enzymes: an important role in skin cancer prevention and reversal of photodamage--a review of the literature. *Journal of Drugs in Dermatology : JDD*, *14*(3), 297–303.

9.   Helleday, T., Petermann, E., Lundin, C., Hodgson, B., & Sharma, R. A. (2008). DNA repair pathways as targets for cancer therapy. *Nature Reviews. Cancer*, *8*(3), 193–204.

10.   Curtin, N. (2007). Therapeutic potential of drugs to modulate DNA repair in cancer. *Expert Opinion on Therapeutic Targets*, *11*(6), 783–799.

11.   Ding, J., Miao, Z.-H., Meng, L.-H., & Geng, M.-Y. (2006). Emerging cancer therapeutic opportunities target DNA-repair systems. *Trends in Pharmacological Sciences*, *27*(6), 338–344.

12.   Madhusudan, S., & Hickson, I. D. (2005). DNA repair inhibition: a selective tumour targeting strategy. *Trends in Molecular Medicine*, *11*(11), 503–511.

13.   Olive, P. L., & Banáth, J. P. (1993). Detection of DNA double-strand breaks through the cell cycle after exposure to X-rays, bleomycin, etoposide and 125IdUrd. *International Journal of Radiation Biology*, *64*(4), 349–358.

14.   Feuerhahn, S., & Egly, J.-M. (2008). Tools to study DNA repair: what's in the box? *Trends in Genetics : TIG*, *24*(9), 467–474.

15.   Valdiglesias, V., Pásaro, E., Méndez, J., & Laffon, B. (2011). Assays to determine DNA repair ability. *Journal of Toxicology and Environmental Health. Part A*, *74*(15-16), 1094–1109.

16.   Löbrich, M., Shibata, A., Beucher, A., Fisher, A., Ensminger, M., Goodarzi, A. A., et al. (2010). gammaH2AX foci analysis for monitoring DNA double-strand break repair: strengths, limitations and optimization. *Cell Cycle*, *9*(4), 662–669.

17.   Sharma, A., Singh, K., & Almasan, A. (2012). Histone H2AX phosphorylation: a marker for DNA damage. *Methods in Molecular Biology (Clifton, N.J.)*, *920*(Chapter 40), 613–626.

18.   Nakamura, A., Sedelnikova, O. A., Redon, C., Pilch, D. R., Sinogeeva, N. I., Shroff, R., et al. (2006). Techniques for gamma-H2AX detection. *Methods in Enzymology*, *409*, 236–250.

19.   Nagel, Z. D., Margulies, C. M., Chaim, I. A., McRee, S. K., Mazzucato, P., Ahmad, A., et al. (2014). Multiplexed DNA repair assays for multiple lesions and multiple doses via transcription inhibition and transcriptional mutagenesis. *Proceedings of the National Academy of Sciences of the United States of America*, *111*(18), E1823–32.

20.   Johnson, J. M., & Latimer, J. J. (2005). Analysis of DNA repair using transfection-based host cell reactivation. *Methods in Molecular Biology (Clifton, N.J.)*, *291*, 321–335.

21.   Mendez, P., Taron, M., Moran, T., Fernandez, M. A., Requena, G., & Rosell, R. (2011). A modified host-cell reactivation assay to quantify DNA repair capacity in cryopreserved peripheral lymphocytes. *DNA Repair*, *10*(6), 603–610.

22.   Latimer, J. J., & Kelly, C. M. (2014). Unscheduled DNA synthesis: the clinical and functional assay for global genomic DNA nucleotide excision repair. *Methods in Molecular Biology (Clifton, N.J.)*, *1105*(Chapter 36), 511–532.

23.   Celotti, L., Ferraro, P., & Biasin, M. R. (1992). Detection by fluorescence analysis of DNA unwinding and unscheduled DNA synthesis, of DNA damage and repair induced in vitro by direct-acting mutagens on human lymphocytes. *Mutation Research*, *281*(1), 17–23.

24.   Ostling, O., & Johanson, K. J. (1984). Microelectrophoretic study of radiation-induced DNA damages in individual mammalian cells. *Biochemical and Biophysical Research Communications*, *123*(1), 291–298.

25.   Collins, A. R. (2004). The comet assay for DNA damage and repair: principles, applications, and limitations. *Molecular Biotechnology*, *26*(3), 249–261.

26.   Olive, P. L., & Banáth, J. P. (2006). The comet assay: a method to measure DNA damage in individual cells. *Nature Protocols*, *1*(1), 23–29.

27.   Singh, N. P., McCoy, M. T., Tice, R. R., & Schneider, E. L. (1988). A simple technique for quantitation of low levels of DNA damage in individual cells. *Experimental Cell Research*, *175*(1), 184–191.

28.   Azqueta, A., Langie, S. A. S., Slyskova, J., & Collins, A. R. (2013). Measurement of DNA base and nucleotide excision repair activities in mammalian cells and tissues using the comet assay--a methodological overview. *DNA Repair*, *12*(11), 1007–1010.

29.   Fortini, P., Raspaglio, G., Falchi, M., & Dogliotti, E. (1996). Analysis of DNA alkylation damage and repair in mammalian cells by the comet assay. *Mutagenesis*, *11*(2), 169–175.

30.   Speit, G., & Rothfuss, A. (2012). The comet assay: a sensitive genotoxicity test for the detection of DNA damage and repair. *Methods in Molecular Biology (Clifton, N.J.)*, *920*(Chapter 6), 79–90.

31.   Hartmann, A., Schumacher, M., Plappert-Helbig, U., Lowe, P., Suter, W., & Mueller, L. (2004). Use of the alkaline in vivo Comet assay for mechanistic genotoxicity investigations. *Mutagenesis*, *19*(1), 51–59.

32.   Forchhammer, L., Johansson, C., Loft, S., Möller, L., Godschalk, R. W. L., Langie, S. A. S., et al. (2010). Variation in the measurement of DNA damage by comet assay measured by the ECVAG inter-laboratory validation trial. *Mutagenesis*, *25*(2), 113–123.

33.   Wood, D. K., Weingeist, D. M., Bhatia, S. N., & Engelward, B. P. (2010). Single cell trapping and DNA damage analysis using microwell arrays. *Proceedings of the National Academy of Sciences of the United States of America*, *107*(22), 10008–10013.

34.   Weingeist, D. M., Ge, J., Wood, D. K., Mutamba, J. T., Huang, Q., Rowland, E. A., et al. (2013). Single-cell microarray enables high-throughput evaluation of DNA double-strand breaks and DNA repair inhibitors. *Cell Cycle*, *12*(6), 907–915.

35.   Ge, J., Prasongtanakij, S., Wood, D. K., Weingeist, D. M., Fessler, J., Navasummrit, P., et al. (2014). CometChip: a high-throughput 96-well platform for measuring DNA damage in microarrayed human cells. *Journal of Visualized Experiments : JoVE*, (92), e50607–e50607.

36.   Sykora, P., Witt, K. L., Revanna, P., Smith-Roe, S. L., Dismukes, J., Lloyd, D. G., et al. (2018). Next generation high throughput DNA damage detection platform for genotoxic compound screening. *Scientific Reports*, *8*(1), 2771.

37.   Allalunis-Turner, M. J., Barron, G. M., Day, R. S., Dobler, K. D., & Mirzayans, R. (1993). Isolation of two cell lines from a human malignant glioma specimen differing in sensitivity to radiation and chemotherapeutic drugs. *Radiation Research*, *134*(3), 349–354.

38.   Lees-Miller, S. P., Godbout, R., Chan, D. W., Weinfeld, M., Day, R. S., Barron, G. M., & Allalunis-Turner, J. (1995). Absence of p350 subunit of DNA-activated protein kinase from a radiosensitive human cell line. *Science (New York, N.Y.)*, *267*(5201), 1183–1185.

39.   Lieber, M. R., Ma, Y., Pannicke, U., & Schwarz, K. (2003). Mechanism and regulation of human non-homologous DNA end-joining. *Nature Reviews. Molecular Cell Biology*, *4*(9), 712–720.

40.   Frit, P., Barboule, N., Yuan, Y., Gomez, D., & Calsou, P. (2014). Alternative end-joining pathway(s): bricolage at DNA breaks. *DNA Repair*, *17*, 81–97.

41.   Sallmyr, A., & Tomkinson, A. E. (2018). Repair of DNA double-strand breaks by mammalian alternative end-joining pathways. *The Journal of Biological Chemistry*, jbc.TM117.000375.

42.   Moffat, J., Grueneberg, D. A., Yang, X., Kim, S. Y., Kloepfer, A. M., Hinkle, G., et al. (2006). A lentiviral RNAi library for human and mouse genes applied to an arrayed viral high-content screen. *Cell*, *124*(6), 1283–1298.

43.   Manjunath, N., Wu, H., Subramanya, S., & Shankar, P. (2009). Lentiviral delivery of short hairpin RNAs. *Advanced Drug Delivery Reviews*, *61*(9), 732–745.

A

Molten agarose

Apply stamp with cell-sized posts

Agarose gelates

Remove stamp

Microwells

Agarose slab
(dimensions of a 96 well plate)

Glass plate for support

B

Macrowells

Bottomless 96 well plate

Binder clips

Agarose on a glass plate

Microwells

Load cell suspension

Cells settle by gravity

Remove bottomless plate and wash off excess cells
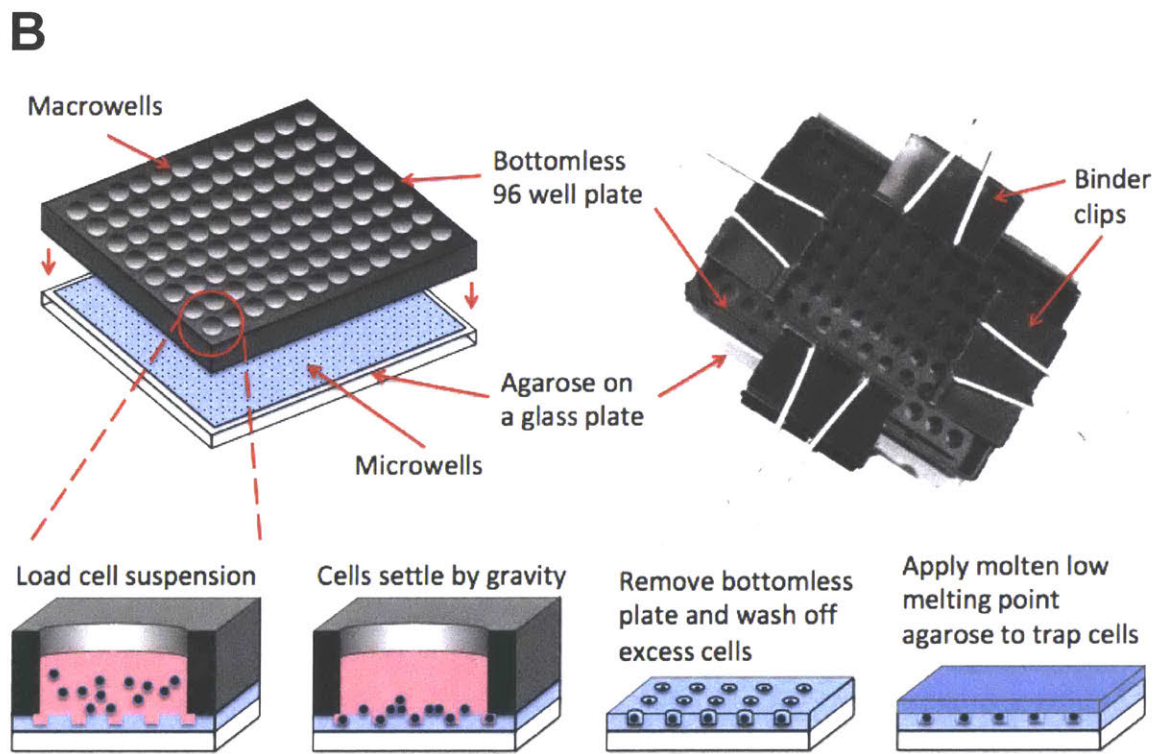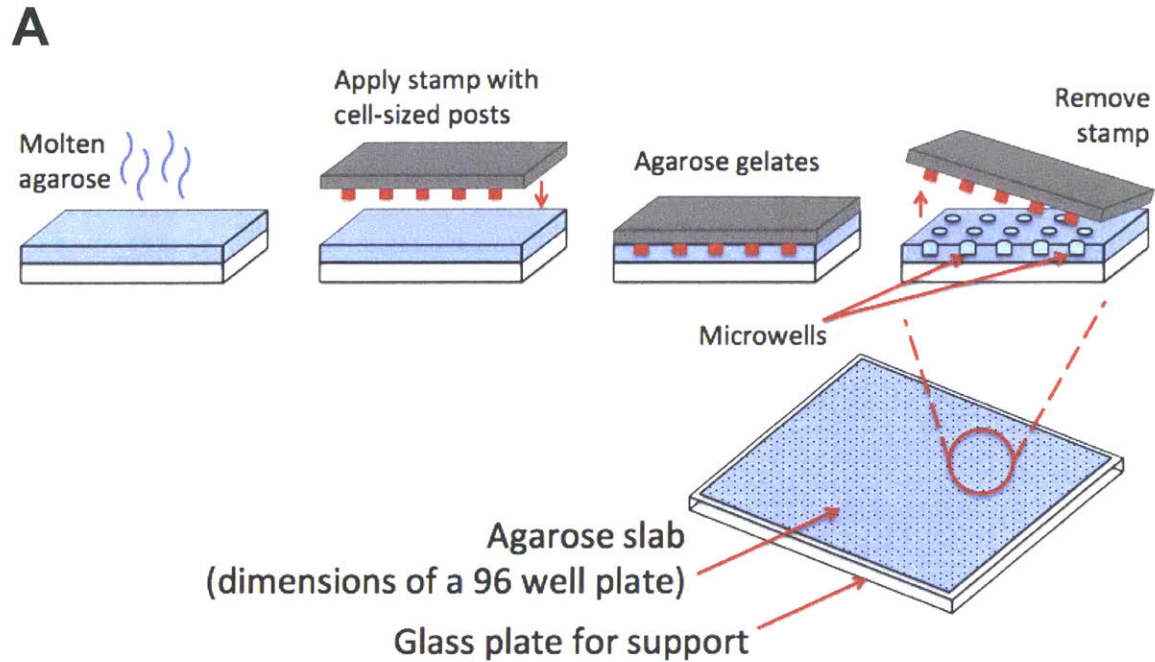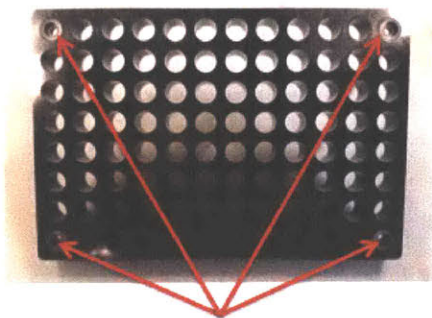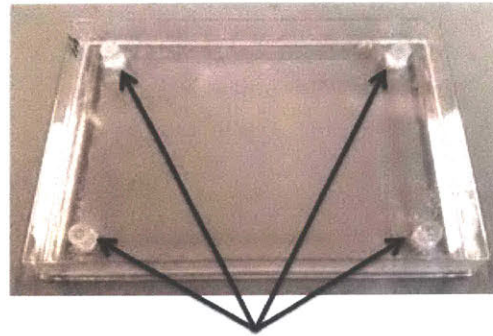
Apply molten low melting point agarose to trap cells

Figure 2-1. Casting, assembling and loading the CometChip. (A) Molten agarose is poured onto a Gel-Bond film and patterned with cell sized micro-wells using a custom-made stamp. (B) The CometChip is clamped with a bottomless 96-well plate and cells are loaded into the micro-wells.

A

Pegs glued onto bottomless 96-well plate   Threaded posts glued onto uni-well tray

B

Side view of fastening mechanism:

Cylindrical peg glued within a well

Center hole for screw to pass through

Internal screw threads at the center of the post

Post glued onto uni-well tray

Uni-well tray

Screw

Bottomless 96-well plate

Fastened apparatus

Microwell arrayed agarose sandwiched between bottomless 96-well plate and uni-well tray
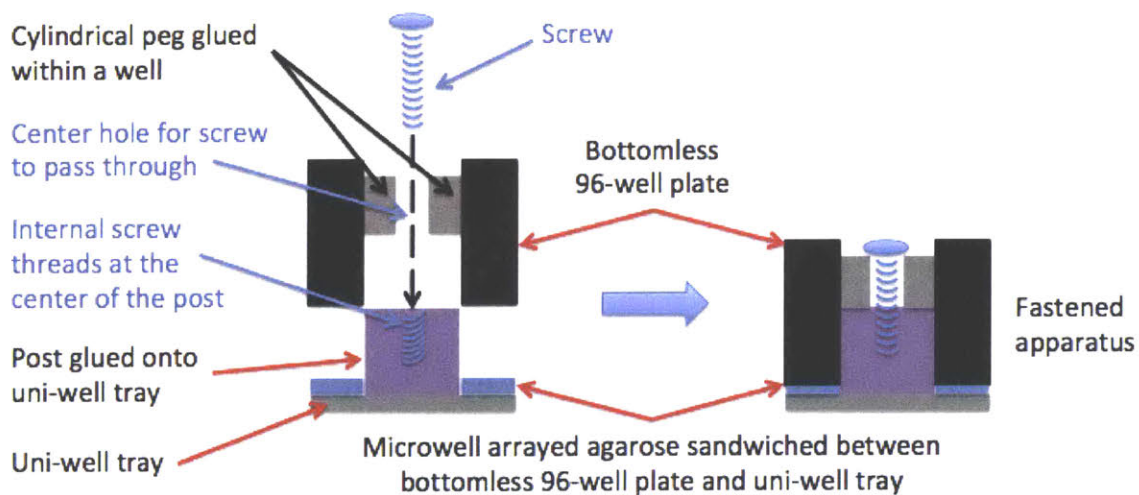
Figure 2-2.   First iteration of HTS CometChip. (A) Four polystyrene pegs each with a 2 mm diameter hole at the center were fused to wells A1, A12, H1 and H12 on a bottomless 96-well plate and four internally threaded polystyrene posts were fused onto a standard uni-well tray at positions corresponding to wells A1, A12, H1 and H12 on a 96-well plate. (B) Pictorial representation of the fastening mechanism. The uni-well tray and the bottomless 96-well plate were fastened together with the microwell arrayed agarose sandwiched in between by aligning the posts and the pegs and passing a screw through each of the post and peg pair.

A

B
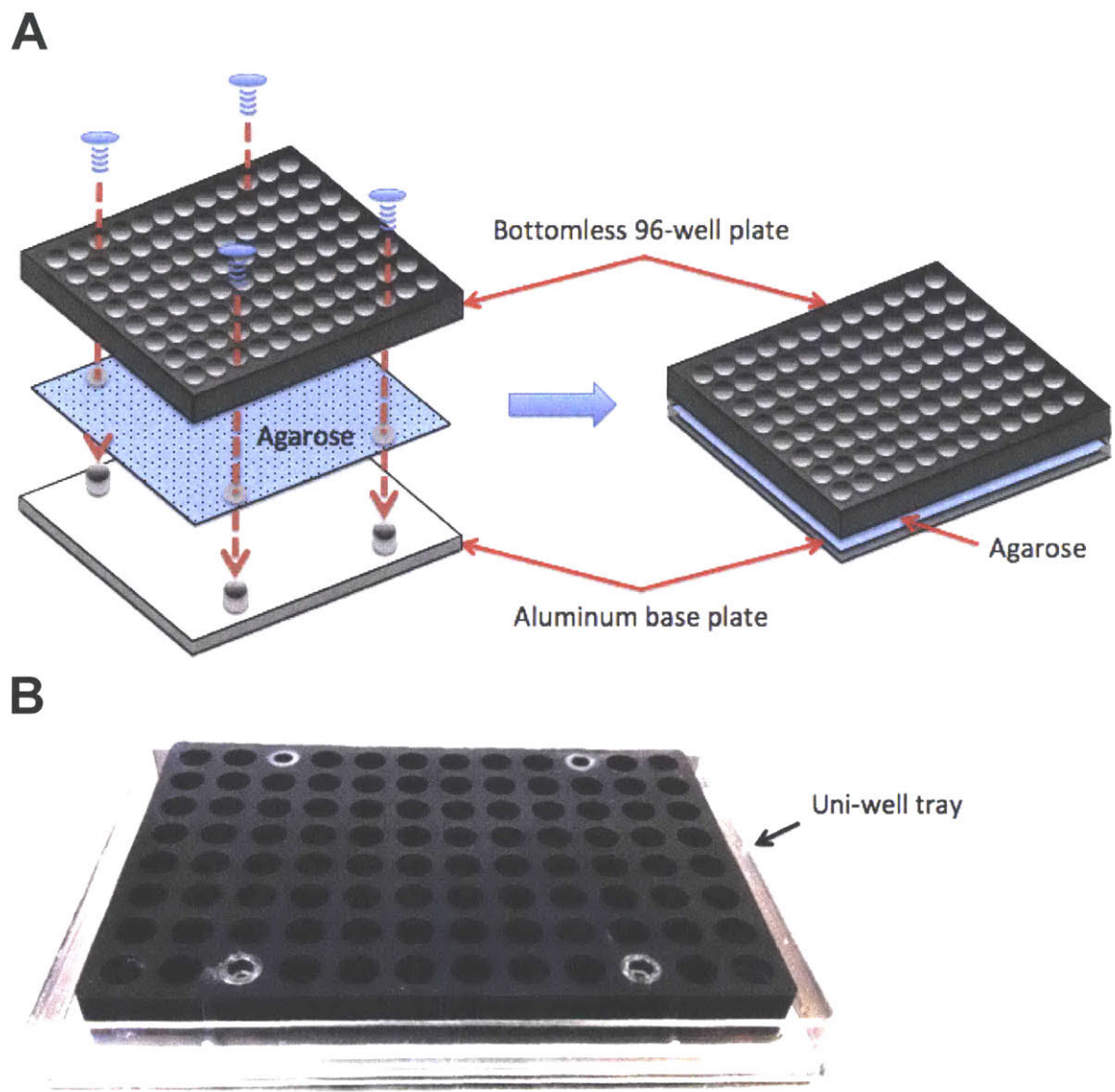
Figure 2-3.   Assembly of the HTS CometChip. (A) CometChip is cast over a gel-bond film and sandwiched between an aluminum base plate and a bottomless 96-well plate. Polystyrene posts in the first iteration were replaced by aluminum posts and attached to the aluminum base plate at positions corresponding to wells A3, A10, H3 and H10 on a 96-well plate. Pegs on the bottomless 96-well plate were shifted to wells A3, A10, H3 and H10. (B) Final assembly of HTS CometChip when placed within a uni-well tray.

Plate #	Average comet tail length ± Standard deviation	Coefficient of variation (COV)	COV for traditional comet assay
1	115 µm ± 6.9 µm	6.0 %	
2	107 µm ± 9.5 µm	8.8 %	~20 %
3	121 µm ± 7.0 µm	5.7 %	

Table 2-1. Average comet tail lengths and standard deviations obtained from 3 HTS CometChips loaded with M059K cells and treated with 50 Gy γ-rays. 92 wells were used in each HTS CometChip.
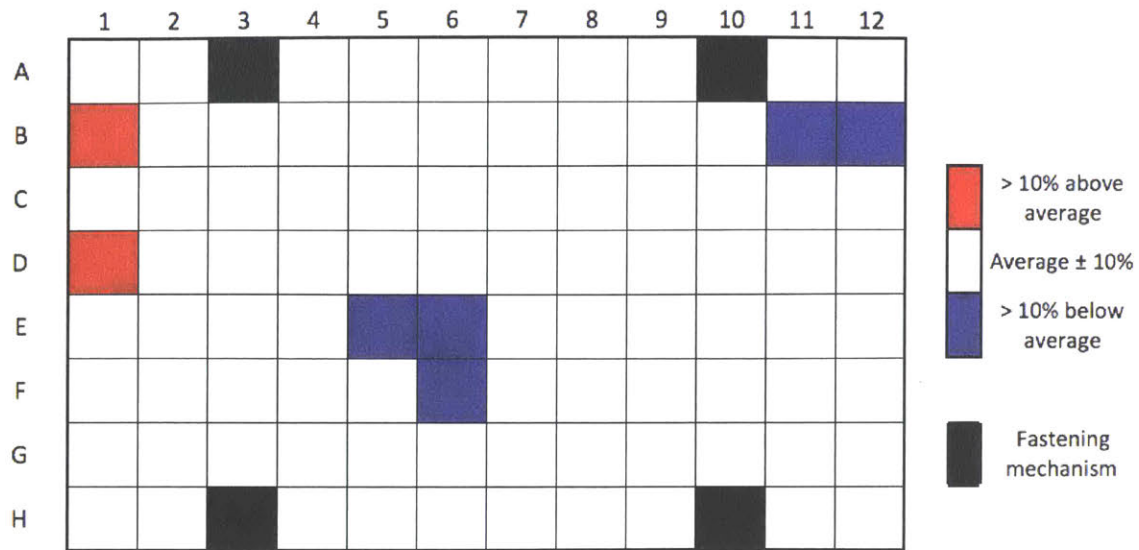
Figure 2-4. Variation between wells within a HTS CometChip. M059K cells were loaded into a HTS CometChip and treated with 50 Gy γ-rays. Variation between wells from plate #1 in Table 2-1 is shown here. Black boxes indicate the well positions of the posts in the HTS CometChip. Wells with an average comet tail length of more than 10% above the plate's average were highlighted red while wells with an average comet tail length of less than 10% below the plate's average were highlighted blue.
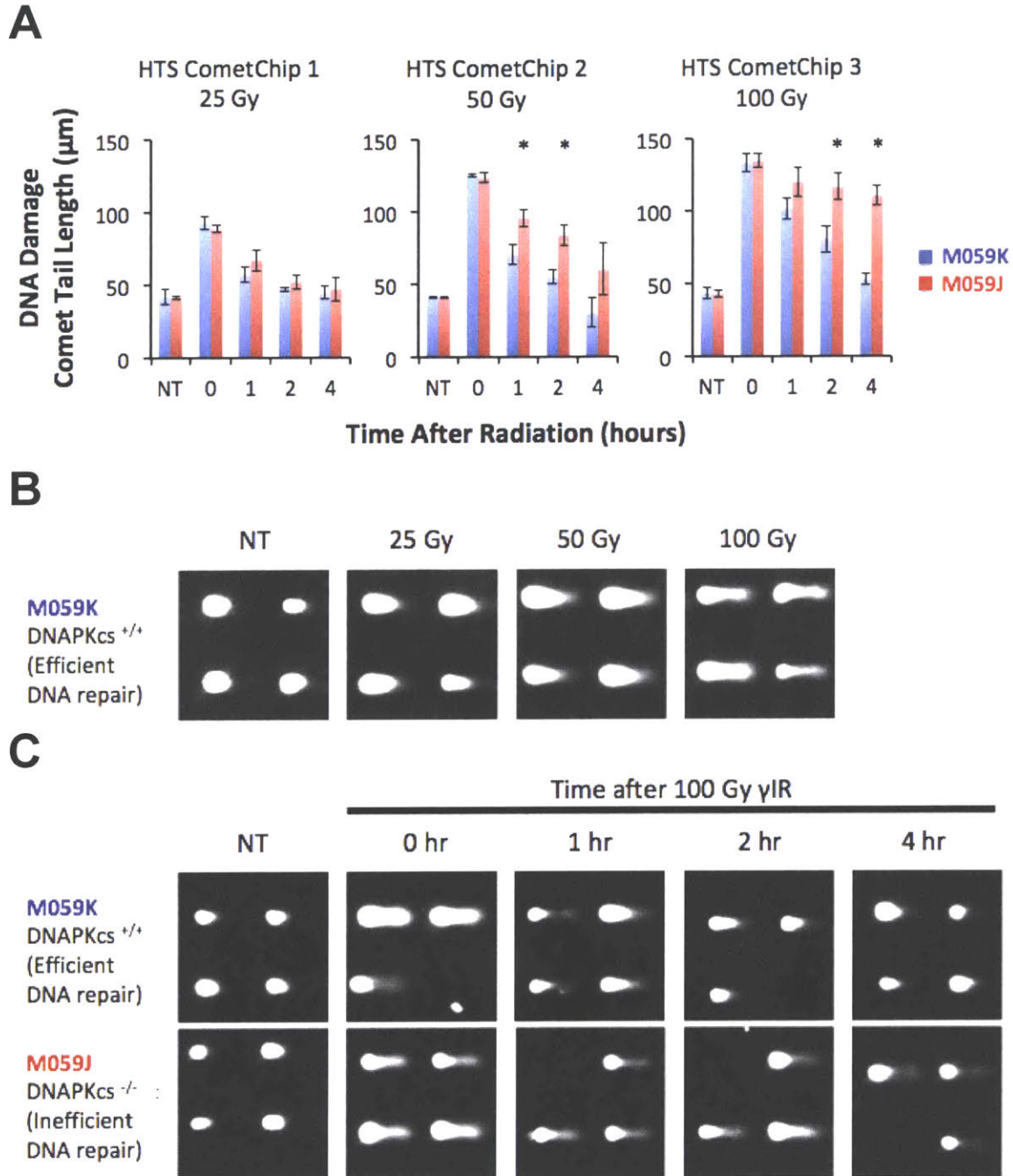
Figure 2-5. γ-irradiation dose response and DNA repair time course. (A) M059K and M059J cells were loaded into 3 HTS CometChip and treated with 25, 50 or 100 Gy γ-rays and allowed to repair the damage for 1, 2 or 4 hours. Bars show the average of 3 wells and error bars represent 1 SD. (B) Increasing doses of γ-rays applied to M059K cells result in increasing comet tail lengths. (C) M059K and M059J cells were treated with 100 Gy of γ-rays and allowed up to 4 hours to repair the resulting DNA damage.

A

Gene	Function
lacZ, RFP, GFP, LUC, Empty vector	Negative control
DNApkcs, Ku70, Ku80, XRCC4, Artemis, XLF, Ligase4	Core NHEJ genes

B
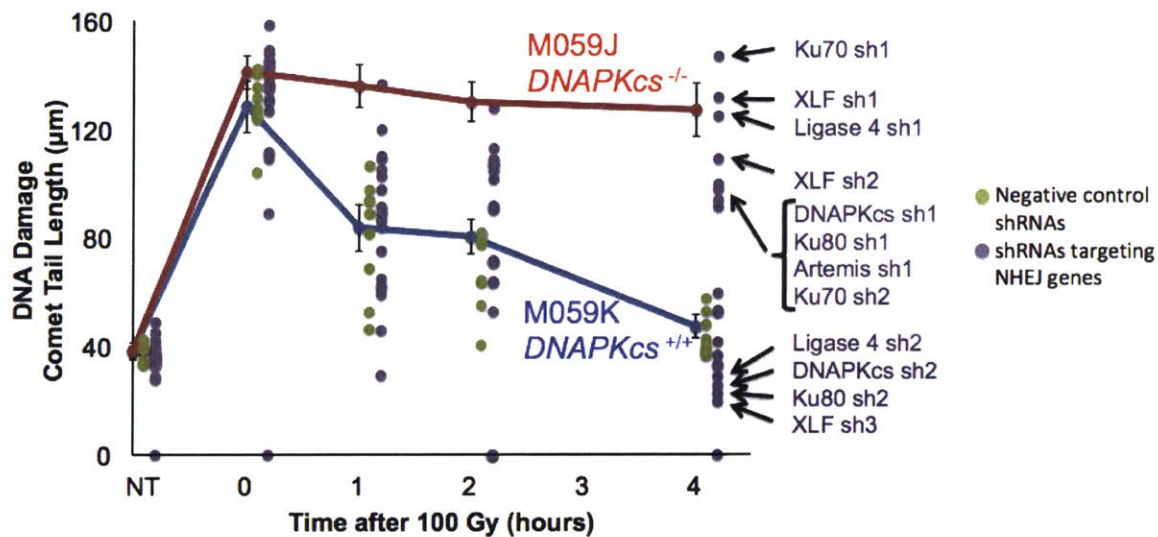
Figure 2-6.   Detection of DNA DSB repair with HTS CometChip, using M059K cells treated with a panel of shRNAs. (A) Table of genes selected for testing in (B). (B) Comparison between M059K cells treated with negative control shRNAs and shRNAs targeting NHEJ genes. Each dot represents data from 1 shRNA and are color-coded according to Fig. 2-6A. (Data points represent average comet tail length and error bars represent 1 SD)
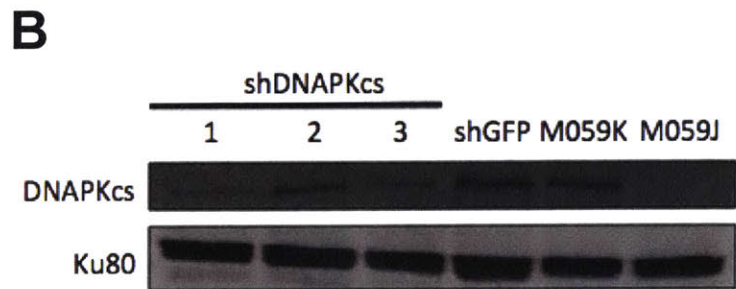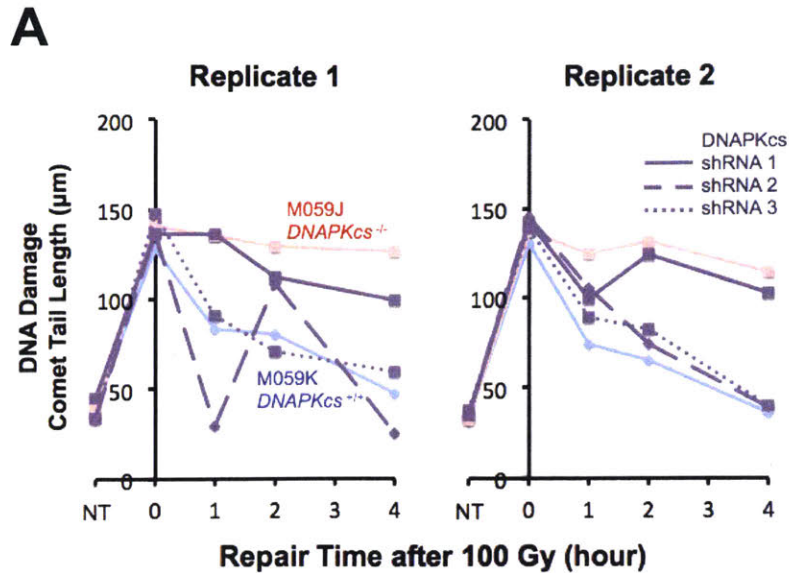
Figure 2-7. Knockdown of DNAPKcs resulting in DNA DSB repair defects. (A) Comparison between DNA DSB repair curves obtained from replicate 1 and 2 for shRNAs targeting DNAPKcs. (B) Western blot showing DNAPKcs protein levels after shRNA knockdown. M059K cells were transduced with lentiviral shRNA constructs (shRNA 1, 2, and 3 targeting DNAPKcs and shRNA targeting GFP) and whole cell extracts were prepared after selection for successfully transduced cells. M059K (DNAPKcs $^{+/+}$) and M059J cells (DNAPKcs $^{-/-}$) were used as DNAPKcs probing controls. Ku80 was used as a loading control.

Negative control shRNAs		
Target gene	TRC ID number	Target sequence
GFP	TRCN0000072194	CCACATGAAGCAGCACGACTT
GFP	TRCN0000072181	ACAACAGCCACAACGTCTATA
lacZ	TRCN0000072240	TCGTATTACAACGTCGTGACT
lacZ	TRCN0000072236	CCAACGTGACCTATCCCATTA
Luciferase	TRCN0000072250	AGAATCGTCGTATGCAGTGAA
Luciferase	TRCN0000072256	ACGCTGAGTACTTCGAAATGT
RFP	TRCN0000072209	CTCAGTTCCAGTACGGCTCCA
RFP	TRCN0000072212	CCGTAATGCAGAAGAAGACCA
Empty vector	TRCN0000208001	-

NHEJ targeting shRNAs		
Target gene	TRC ID number	Target sequence
Artemis	TRCN0000276608	ATTTGCCCAAAGGATACTTAC
Artemis	TRCN0000276612	TATGGATAAAGTTGTCGAAAT
Artemis	TRCN0000276609	ACGAGAGCATTTACAATATTT
DNAPKcs	TRCN0000194719	CCTGAAGTCTTTACAACATAT
DNAPKcs	TRCN0000194985	CCATCCCTTATAGGTTAATAT
DNAPKcs	TRCN0000197152	GAAACAGCTGTCTCCGTAAAT
Ku70	TRCN0000039609	GATGAGTCATAAGAGGATCAT
Ku70	TRCN0000009846	GAAGAGTCTACCCGACATAAG
Ku70	TRCN0000039611	CCCAAGGTTGAAGCAATGAAT
Ku80	TRCN0000010467	TGAAGATGGACCTACAGCTAA
Ku80	TRCN0000039842	CGTGGGCTTTACCATGAGTAA
Ku80	TRCN0000221592	GCAGCCCTTGTGATGTGATTA
LIG4	TRCN0000229989	TTGCTATGGTGATAGTTATTT
LIG4	TRCN0000257124	GCCTATCTCATGACCATATTG
LIG4	TRCN0000040005	GCTCGCATCTAAACACCTTTA
XLF	TRCN0000275700	CCAACATTTGATTCGTCCTCT
XLF	TRCN0000275631	ATGGGCATGAGTCTGGCATTA
XLF	TRCN0000275629	ATTCCTTCTTGGAACAATTTA
XRCC4	TRCN0000040116	CCAGCTGATGTATACACGTTT
XRCC4	TRCN0000421915	ATGATGTTCAAGGACGATTTG
XRCC4	TRCN0000040115	GCTGCTGTAAGTAAAGATGAT

Supplementary Figure 2-1. List of shRNAs with their target genes, ID numbers and target sequences obtained from MIT Broad Institute, the RNAi Consortium.
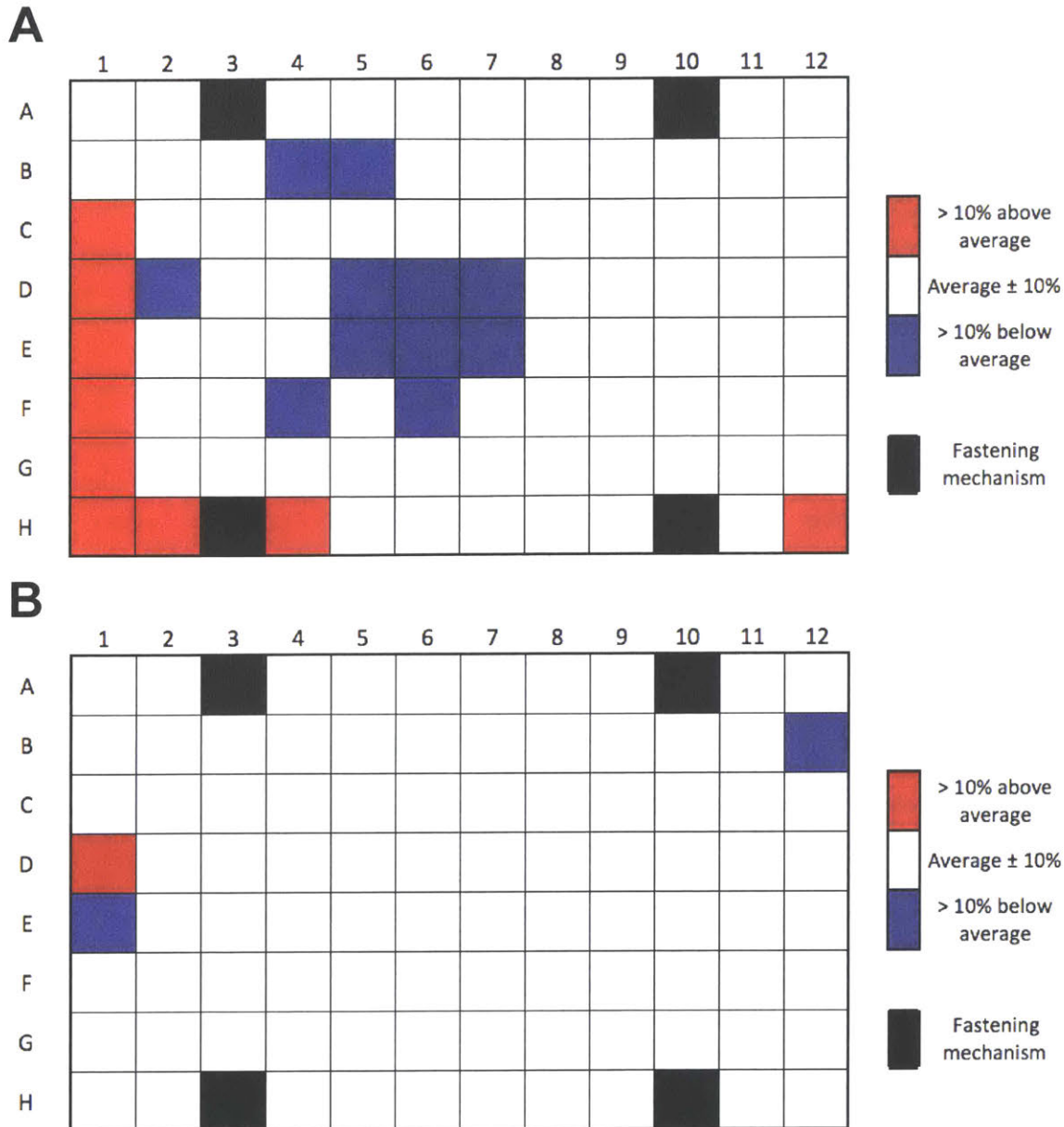
Supplementary Figure 2-2. Variation between wells within a HTS CometChip. M059K cells were loaded into a HTS CometChip and treated with 50 Gy γ-rays. Variation between wells from plate #2 and #3 in Table 2-1 is shown here in (A) and (B) respectively. Black boxes indicate the well positions of the posts in the HTS CometChip. Wells with an average comet tail length of more than 10% above the plate's average were highlighted red while wells with an average comet tail length of less than 10% below the plate's average were highlighted blue.

Chapter 3

High Throughput DNA Double Strand Break Screen Using a Cell Microarray Comet Assay

3.1   Abstract

The underlying basis for many cancer chemotherapeutic agents and radiation is that they damage DNA. Since tumor cells can mitigate the damage by repairing their DNA, and therefore survive therapy, inhibiting DNA repair during therapy could increase the efficacy of the therapy. In order to achieve this, DNA repair factors have to be identified and characterized for their roles in chemotherapy. Here, we have developed a screening method using the High Throughput Screening CometChip (HTS CometChip) in order to identify novel DNA repair genes by measuring repair of DNA double strand breaks (DSBs). This platform enables the use of high throughput screening robotics, which increases the throughput of the assay while at the same time greatly reducing the amount of manual work required. In this study, we utilized the HTS CometChip to screen an shRNA library that targets 2564 genes for factors that, when knocked down, results in a DSB repair impairment. Here, we identify LATS2 as a novel gene that impacts DNA repair capacity. Further investigation of LATS2 depleted cells revealed

that these cells were less likely than control cells to repair DNA DSBs by the homologous recombination repair pathway and were more sensitive to ionizing radiation, which was consistent with a DNA DSB repair defect detected in these cells. Thus, results show the utility of the HTS CometChip as a screening tool for measuring unrepaired DNA DSBs after exposing cells to γ-radiation. Since DSBs are created during apoptosis, the screen also enables detection of genes that when knocked down, lead to increased probability of cells undergoing apoptosis. Taken together, the HTS CometChip provides an effective approach for identifying novel DNA DSB repair factors and genes that modulate susceptibility to apoptosis.

3.2   Introduction

Tumor cells are often genomically unstable due to defects in DNA repair[1,2], and such defects can render tumor cells vulnerable to DNA damage[3-5]. This characteristic of tumor cells contributes to the efficacy of many cancer chemotherapeutics. However, tumor cells can have differential DNA repair capacities based on the expression levels of various DNA repair genes, and therefore will respond differently to treatment, resulting in variability in tumor responses[6-8]. Two examples of this observation include the fact that MethylGuanine DNA Methyl Transferase (MGMT) expressing cells are resistant to the chemotherapeutic agent Temozolomide[9,10] (TMZ), and cells deficient in the catalytic subunit (DNA-PKcs) deficient are sensitive to radiotherapy[11-13]. Therefore, it is critical to develop a better understanding of the network of genes that impact DNA repair capacity in order to maximize tumor cell killing during chemotherapy and

radiotherapy. The ability to identify novel genes that participate in DNA repair would enable the development of drugs that modulate the activity of those genes, which would be of great value for improving cancer therapy[15-21]. Here, we describe an approach to screen a lentiviral shRNA library for modulators of DNA DSB repair. In addition, since DSBs are created during apoptosis, the screen also enables discovery of genes that modulate susceptibility to apoptosis.

DNA DSBs are considered to be one of the most deleterious classes of DNA damage[22]. Unrepaired DNA DSBs can lead to activation of cell cycle checkpoints and apoptosis[23], which are favorable outcomes in the context of treating cancer. DNA DSBs are repaired via two major pathways in human cells, namely the Non Homologous End Joining (NHEJ) and Homologous Recombination (HR) pathways. Briefly, in the NHEJ repair pathway, broken ends of DNA strands are stabilized and brought together by Ku70, Ku80 and DNAPKcs, and they are ultimately re-ligated by XLF, XRCC4 and Lig4 to form a continuous DNA double helix[24-25]. In the HR pathway, the broken DNA is first end resected to create 3' overhangs. These overhangs are then bound by Rad51 proteins, forming a nucleoprotein filament that can invade homologous DNA. Genetic information is generally donated by the sister chromatid, which is used as a template to extend the broken DNA strands. For the synthesis dependent strand annealing subpathway of HR, following release of the newly synthesized DNA, the ends can anneal and be religated[26,27]. Apart from the known core proteins that participate in these repair pathways, recent research has revealed proteins that modulate the activity of DNA repair genes. This includes proteins that participate in determining whether a DNA

DSB will be repaired via NHEJ or HR[28,29], as well as proteins that can remodel chromatin surrounding a DNA DSB to activate or inhibit its repair[30].

Many DNA repair genes were discovered by exposing model organisms to known DNA damaging agents in large scale screening experiments. Early studies of DNA repair genes were conducted in *S. cerevisiae*[31,32], which subsequently led to the discovery of DNA repair gene homologs in human cells. Recently, the development of genome wide RNAi and CRISPR gene editing libraries as well as high throughput analytical tools such as mass spectrometry and automated imaging systems has led to an increase in screening activities performed on human cells. Prominent studies in this field include the work performed by Matsouka and coworkers in 2007, which revealed a vast phosphorylation network involving at least 700 proteins that is initiated by the ATM and ATR kinases as part of the DNA damage response after cells are exposed to γ-radiation (γIR)[33]. Network analysis of the phosphorylated proteins revealed gene clusters that were not previously known to participate in repairing radiation induced DNA damage. The study also uncovered previously unknown phosphorylation sites on known phosphorylated proteins. These newly found phosphorylation sites could be useful targets for improved therapy. In addition, Paulson and coworkers conducted a genome wide DNA damage response screen in human cells, where they measured changes in γH2AX, a histone that is phosphorylated at sites of DSBs. In their screen, unrepaired DNA damage after gene knockdown revealed a network of mRNA processing genes that could be involved in maintaining genomic stability[34]. More recently, Floyd and coworkers conducted a screen measuring γH2AX following γIR, leading to the identification of BRD4 as a modulator of DNA damage response signaling[35]. These, as

well as many other studies[36,37], allude to the possibility that there are many more DNA repair factors that are yet to be discovered.

There are several possible approaches for studying DNA damage and repair in human cells[38]. Immunofluorescence based assays are frequently used in screens to study DNA repair factors, due to the convenience of automated microscopes and the versatility of analyzing digital images. These assays can be conducted with the assistance of high throughput screening robotics for the steps that require liquid changes, such as the addition of antibodies for detection and washing steps. The completed assay can then be queued for imaging using modern automated microscopes, and the images collected can be analyzed digitally, require little manual work. This makes the assays ideal for large-scale genome wide screening, where thousands of genes are screened in a single experiment.

An alternative to immunofluorescence assay is the comet assay, a well established assay that can be used to measure multiple types of physical DNA damage[39-41], including DNA DSBs[42]. The principle of the comet assay is that damaged DNA, which has lost superhelical tension or is fragmented, has increased electrophoretic mobility in an agarose gel. Thus, when an electric field is applied to the DNA in the agarose, damaged DNA will travel further than intact DNA, with the distance of travel correlating with the extent of damage. Traditionally, the comet assay is performed by encapsulating cells in agarose, treating them with DNA damaging agents and then plating them on glass slides, before subjecting them to electrophoresis. Images obtained from this assay typically show circular areas of staining originating from the nucleoid of cells, as well as tails exiting from the nucleoids, resembling a

comet. Due to the requirement to plate every sample onto its own glass slide, the traditional comet assay has a very low throughput and is tedious to perform when multiple samples have to be processed simultaneously. It is therefore unsurprising that to date, there are no studies that utilize the comet assay to screen for DNA repair factors.

To address the limitations of the comet assay, Engelward and co-workers developed the CometChip[43-46], which exploits a micropatterned cell array on agarose to maximize the number of useful comets per unit area of agarose. This agarose can be made to the size of a standard multiwell plate, and can be partitioned into 96 compartments by using a bottomless 96-well plate, yielding up to 300 comets per well. Each compartment can be treated with DNA damaging agents and analyzed for levels of DNA damage using the same protocol as the standard comet assay. In doing so, each glass slide can now be substituted with a single well in a 96 well. We have recently improved upon the design of the CometChip, named High Throughput Screening CometChip (HTS CometChip)[47], specifically to enable it to be compatible with high throughput screening robotics, which requires that the outer dimensions of the hardware conform to standard dimensions. Rather than using binding clips, which render the hardware incompatible with HTS robotics, the HTS CometChip leverages a screw system to press a bottomless 96 well plate against the agarose microwells by sandwiching using an aluminum base plate. This apparatus is then placed within a commercially available uni-well tray, which conforms to the dimensions of a typical multilwell plate, allowing it to be used with high throughput screening equipment, such as automatic liquid pipetters and automated microscopes. Having previously developed

the HTS CometChip[47], we can now analyze hundreds of samples in parallel, using a fraction of the time and effort relative to the traditional comet assay, thus paving the way to screen for novel DNA repair factors or genes that modulate susceptibility to DSBs created during apoptosis.

Here, we harnessed the unique advantages of the HTS CometChip to perform a large-scale shRNA screen of 2564 genes in human cells, and identified DNA repair factors that influence DNA DSB repair following exposure to γIR. Network analysis of the top hits from our screen led to the discovery that LATS2, a member of the HIPPO signaling pathway, modulates DNA repair activity in cells. We also discovered that LATS2 modulates apoptosis when cells are grown in a three dimensional environment (rather than attached to a tissue culture plate). Discovery of LATS2 as a novel DNA repair modulator opens doors to the development of inhibitors that could potentially sensitize cells to DNA damage induced by chemotherapy and radiotherapy. Furthermore, since the comet assay can be modified to detect different types of DNA damage, the results of this screen point to the possibility of leveraging the HTS CometChip for additional high throughput screens that assay for repair of other classes of DNA damage.

3.3   Materials and Methods

Cell culture. M059K and M059J glioblastoma cells were cultured in 1:1 DMEM/F12 nutrient mix (Invitrogen) supplemented with 10% FBS (Atlanta Biologicals, Atlanta, GA), MEM Non-Essential Amino Acids (Invitrogen) and 100-units/ml penicillin-streptomycin

(Invitrogen). HeLa human cervical adenocarcinoma cells were cultured in DMEM (Invitrogen) supplemented with 10% FBS (Atlanta Biologicals, Atlanta, GA) and 100-units/ml penicillin-streptomycin (Invitrogen).

HTS CometChip apparatus fabrication. A 120 by 78 mm aluminum base plate was cut from a 3 mm thick aluminum sheet to fit tightly in a uni-well tray (VWR). Four aluminum posts (6 mm in diameter and 6.5 mm in height) were welded onto the base plate with their centers 28.5 mm and 7.5 mm from the short and long edges of the plate respectively. A 2 mm wide and 5 mm deep hole was drilled into each aluminum post and threaded on surface. The outer edges of a bottomless 96-well plate (VWR) were sawed off, leaving a 110 by 74 mm grid of 96 wells. Wells A3, A10, H3 and H10 were plugged with tight fitting polystyrene cylinders with a 2 mm wide hole drilled at their centers. HTS CometChip was assembled by sandwiching the microwell arrayed agarose between the aluminum base plate and the bottomless well plate, such that the posts on the aluminum plate meet the pegs on the bottomless plate, and fastened together by screws.

Neutral CometChip. The CometChip was prepared as described previously. Briefly, 12ml of 1% molten agarose in PBS was poured over a GelBond flim (Lonza) placed on a uni-well tray (VWR) before applying a reusable PDMS stamp arrayed with microposts. When the agarose was solidified, the PDMS stamp was removed to reveal microwells for cell loading. After the CometChip was loaded with cells, excess cells were washed off with PBS and a thin layer of 1% molten low melting point agarose in PBS was

applied. Cells were lysed at 43°C overnight after desired timepoints by submerging the CometChip into lysis buffer containing 2.5M NaCl, 100 mM Na_2EDTA, 10 mM Tris, 1% N-Lauroylsarcosine, pH 9.5 with 0.5% Triton X-100 and 10% DMSO. The CometChip was washed thrice with neutral electrophoresis buffer containing 90 mM Tris, 90 mM Boric Acid, 2 mM Na_2EDTA, pH 8.5. Electrophoresis was conducted using pre-chilled neutral electrophoresis buffer at 4°C for 1 hr at 0.6 V/cm and 6 mA.

High throughput screening robotics. Access to high throughput screening robotics and equipment was obtained via MIT's Koch Institute of Integrative Cancer Research, Swanson Biotechnology Center, High Throughput Screening Core Facility. Robotic manipulation of the HTS CometChip was performed using a Tecan Evo 100 liquid handler, equipped with a 96-well MultiChannel Arm (MCA96) and a Robotic Manipulator (RoMa) arm. The Evo 100 is also integrated with a Liconic STX110 incubator with temperature, humidity, CO_2 control. Imaging of the HTS CometChip was performed using Thermo Scientific Cellomics® ArrayScan® VTI HCS Reader using a 5X objective.

Pilot shRNA screen. shRNA lentiviral reagents were obtained from the Genetic Perturbation Platform of the Broad Institute of MIT and Harvard. The list of shRNA IDs and their target sequences used in the pilot screen are shown in Supplementary Fig. 3-1. M059K cells were plated on 5 tissue culture 96-well plates per experiment at a density of 600 cells per well, transduced with lentiviruses with an average MOI of 8, 24 hours after cell plating and selected with 1.5 µg/ml puromycin 48 hours after transduction. Puromycin was applied for 72 hours and cells were allowed to recover in

selection free media for 24 hours. All media changes were performed using a BioTek EL406 microplate washer under sterile conditions. Transfer of cells from tissue culture plates to HTS CometChips was performed using high throughput screening robotics equipment (see above). During the transfer, media was removed from the tissue culture plates before trypsin was added to dislodge the cells. Media was added to quench the trypsin and triturated to create single cell suspensions in each well. Cell suspensions from each tissue culture plate were transferred onto 1 HTS CometChip for a total of 5 HTS CometChips and allowed to incubate at 37°C for 20 minutes. Excess unloaded cells were washed off and a thin layer of low melting point agarose was applied to encapsulate cells trapped in microwells. The HTS CometChip assigned as non-treated control is lysed immediately while the 4 remaining HTS CometChips were submerged in media and treated with 100 Gy of γ-rays at 1 Gy/min using a ^{137}Cs source. Cells were allowed to repair DNA damage at 37°C for 0, 1, 2, or 4 hours in media before they were lysed. The neutral comet assay was performed to measure the extent of DNA DSBs.

HTS CometChip shRNA screen. shRNA lentiviral reagents were obtained from MIT's Koch Institute of Integrative Cancer Research, Swanson Biotechnology Center, High Throughput Screening Core Facility. This shRNA library was purchased from the MIT Broad Institute's The RNAi Consortium as a sub-genome library of 2564 genes, with three unique targeting shRNAs per gene. The genes targeted by this library are listed on this webpage: https://ki.mit.edu/files/ki/cfile/sbc/hts/Koch_shRNA_Gene_ Webpage_List_June2012-1.pdf. This library was formatted as an arrayed library, with lentivirus targeting one gene in each well of a 96 well plate, across 89 of plates. The

screening effort was divided into alternating screening days and imaging days. Prior to screening days, M059K cells were plated on tissue culture 96-well plates at a density of 600 cells per well, transduced with lentiviruses with an average MOI of 8 the next day after cell plating and selected with 1.5 µg/ml puromycin 48 hours after transduction. Puromycin was applied for 72 hours and cells were allowed to recover in selection free media for 24 hours. All media changes were performed using a BioTek EL406 microplate washer under sterile conditions. On screening days, media was removed from the tissue culture plates before trypsin was added to dislodge the cells. Media was added to quench the trypsin and triturated to create single cell suspensions in each well. Cell suspensions from each tissue culture plate were transferred onto one HTS CometChip and allowed to incubate at 37°C for 20 minutes. Excess unloaded cells were washed off and a thin layer of low melting point agarose was applied to encapsulate cells trapped in microwells. CometChips were submerged in media and treated with 100 Gy of γ-rays at 1 Gy/min using a ^{137}Cs source. Cells were allowed to repair DNA damage at 37°C for 4 hours in media before they were lysed. On imaging days, the HTS CometChips were washed thrice with neutral electrophoresis buffer and electrophoresis was conducted to measure the extent of DNA DSBs. HTS CometChips were stained with SyBR Gold and imaged with Thermo Scientific Cellomics® ArrayScan® VTI HCS Reader using a 5X objective.

Treatment with ionizing radiation. Cells that were encapsulated in the HTS CometChip were exposed to 100 Gy of γ-radiation at a dose rate of 1 Gy/min from a ^{137}Cs source (GammaCell 40 Exactor, Best Theratronics).

siRNA transfection. Negative control siRNA (Cat# 4390843) and siRNAs targeting LATS2 (Cat# 4392420, ID s25505) and DNAPKcs (Cat# 4390824, ID s774) were purchased from Ambion at the 5 nmole scale and dissolved in 500 ml of nuclease free water. 40,000 HeLa cells were plated on each well of a 6 well plate and transfected with siRNA reagents 24 hours later. During the transfection process, 2 tubes of 150 ul OptiMEM was prepared. 9.5 ul of Lipofectamine RNAimax (Invitrogen) was added to one of the tubes and 3.5 ul of dissolved siRNA was added to the other. The 2 tubes were mixed together and allowed to incubate at room temperature for 15 minutes, before adding 250 ul into each well. Media was changed 5 hours post transfection and transfected cells were allowed to grow for 3 days before they were used in further experiments.

qRT-PCR. Total RNA was extracted from approximately 500,000 HeLa cells treated with LATS2 or negative control siRNA using RNeasy kit (Qiagen). Complementary DNA was generated using random hexamers with M-MLV reverse transcriptase (Invitrogen) using manufacturer's instructions. Semi quantitative PCR was performed using an Applied Biosystems 7500 Fast Real Time PCR System machine, with Fast SYBR Green master mix (Applied Biosystems) using the following primers: Actin (forward) – AGA GCT ACG AGC TGC CTG AC, Actin (reverse) – AGC ACT GTG TTG GCG TAC AG, LATS2 (forward) – TCA GAC AGG ACA GCA TGG AG, LATS2 (reverse) – TAG TTT GGA GTC CCC ACC AG. Data from the experiment was analyzed using the $\Delta\Delta C_T$ method[48].

Western blotting. HeLa cells treated with LATS2 or negative control siRNA were treated with 10 Gy of ionizing radiation, and allowed to incubate at 37°C, 5% CO_2 for up to 1 hour. Whole cell lysates were collected using RIPA buffer (Pierce) supplemented with HALT protease inhibitor (ThermoFisher Scientific) and frozen at -20°C. Lysates were thawed on ice and spun down at max speed for 15 minutes. Lysates were mixed with Laemmli sample buffer (BIO-RAD) according to manufacturer's instructions and incubated at 95°C for 5 minutes and then chilled on ice. Samples were loaded onto precast TRIS-HCL 4-20% linear gradient gels (BIO-RAD), and electrophoresed at 200V for about 45 minutes with TRIS-glycine-SDS running buffer (BIO-RAD). Proteins were transferred onto nitrocellulose membranes (BIO-RAD) at 100V for 2 hours in TRIS-glycine-methanol transfer buffer (BIO-RAD). Membranes were blocked in Odyssey blocking buffer (LI-COR) for 2 hours at room temperature with gentle shaking. B-actin and γH2AX were probed with primary antibodies (Sigma cat# A5441 and Cell Signaling Technologies cat#2577) in blocking buffer overnight at 4°C with gentle shaking. Secondary antibodies (LI-COR) were applied to the membrane in blocking buffer for 2 hours at room temperature with gentle shaking. Bands were visualized using a LI-COR Odyssey scanner.

CellTitre-Glo assay. HeLa cells treated with LATS2 or negative control siRNA were treated with up to 20 Gy of ionizing radiation in 96-well plates and allowed to recover for 3 days before performing the CellTitre-Glo assay. 50 ul of reconstituted CellTitre-Glo reagent (Promega) was added to each well containing 50 ul of media and allowed to

incubate in room temperature for 10 minutes with gentle shaking. Analyte was transferred to a white 96-well plate (Evergreen Scientific) and analyzed with a Tecan M1000 plate reader, with an integration time of 1 second per well.

Annexin V staining. HeLa cells treated with LATS2 or negative control siRNA were transferred onto HTS CometChip and analyzed immediately or after 4 hours incubation at 37°C in media by annexin V staining (Life Technologies) using manufacturer's instructions. DNA was stained using Vybrant® DyeCycle™ Violet stain (Life Technologies).

DSB Spectrum. 293T cells stably expressing the DSB Spectrum cassette were plated on tissue culture 96 well plates at ~10 000 cells per well. 2 pmol of siRNAs (Negative control or LATS2) were mixed with 0.6 µl of Lipofectamine RNAimax (Invitrogen) in 10 µl of OptiMEM and added to each well. Media was changed 16 hours after siRNA transfection. After 48 hours, cells were transfected with PX459-Cas9-AAVS1 sgRNA or BFP sgRNA plasmids, using 0.1 µg of plasmid with 0.3 µl of Lipofectamine 2000 (Invitrogen) in 10 µl of OptiMEM. Cells were analyzed for fluorescence on a BD LSR Fortessa (BD Biosciences) 72 hours after sgRNA transfection.

3.4 Results

Here, we set out to perform a high-throughput screen for DSBs using the HTS CometChip. As such, the first step in this process is to create conditions where there is

clear differentiation between wild type cells and cells deficient in DNA repair. To this end, we used a pair of human glioblastoma cell lines, M059K and M059J derived from the same tumor[11]. These cell lines are normal and deficient in repair, respectively. Specifically, the M059J cell line was found to harbor a truncation mutation in the DNAPKcs gene, which results in acute sensitivity to agents that create DNA DSBs, such as γIR[12]. DNAPKcs is essential for canonical NHEJ. Consequently, M059J cells have been shown to be deficient in DSB repair.

By creating a cell microarray, the CometChip increases both throughput and sensitivity compared to the traditional comet assay[43-45]. We therefore set out to exploit this format in order to perform a screen of shRNAs against genes either known or suspected of being relevant to cancer. The first step was to optimize conditions that differentiate M059K and M059J with regard to DSB repair. To test for differential sensitivity to DSBs, we loaded these cell lines into the HTS CometChip and irradiated them using 100 Gy of γIR. It is noteworthy that this high level of γIR was selected for its ability to differentiate between M059K and M059J, as we have described previously[47]. Although this is a very high dose of radiation, it is common to exploit high-level exposure conditions in order to query early molecular processes that are conserved across a wide range of doses.

After exposing cells to γIR, cells were incubated in media for up to 4 hours before lysis and electrophoresis at neutral pH (the neutral comet assay is an established approach for DSB detection[42]). DNA was then stained and imaged using an epifluorescent microscope, and the tail length was used as a measure of DSBs. We observed that both cell lines show short comet tails when untreated, which is consistent

with low levels of spontaneous DSBs in untreated cells (Fig. 3-1B, first column). Cells that were exposed to γIR had much longer tails, consistent with high levels of DNA DSBs (Fig. 3-1B, second column). Over the course of 4 hours, the length of the comet tails for the M059K cells progressively shortened as a result of DSB repair (Fig. 3-1B, top row, third and fourth column). However, the length of the comet tails for M059J remained significantly longer (Fig. 3-1B, bottom row, third and fourth column), which is consistent with the severe DNA repair defect in these cells. Of note, the difference between M059K and M059J was greatest at 4 hours post exposure (Fig. 3-1C), conditions that were thus adopted for the shRNA screen. These results show that the HTS CometChip can be used effectively to detect a DNA DSB repair defect.

In order to test the efficacy of the selected dose and time conditions for identifying genes that impact DNA repair, we executed a series of small-scale pilot screens. We designed a 96-well plate of shRNA expressing lentiviruses containing negative control shRNA, shRNA targeting known NHEJ genes, as well as shRNA targeting chromatin-modifying genes (Fig. 3-2A). The chromatin modifiers used in this pilot were already known to influence the rate of DNA DSB repair, and several of these genes have been shown to participate in NHEJ or HR repair pathways[49-51]. Untransduced M059K and M059J cells were included in the pilot screen as controls.

In our pilot screen, we first plated M059K cells on five standard tissue culture 96-well plates and treated the cells with shRNAs from the lentiviral plate. We applied puromycin to select for successfully transduced cells and transferred the cells onto HTS CometChips. All liquid transfer steps in this experiment were conducted with the assistance of HTS robotics. The first HTS CometChip was left unirradiated to allow us to

query background DNA DSB levels in the shRNA transduced cells. All the other HTS CometChips were irradiated with 100 Gy of γIR and placed in complete media in an incubator for up to 4 hours to allow time for repair before lysis and electrophoresis at neutral pH.

We observed that the results for untransduced M059K and M059J cells were consistent with the results Figure 3-1C. Specifically, wherein M059K repaired most of the DNA DSBs within 4 hours, while M059J showed inefficient repair (Fig. 3-2B, blue and red lines, respectively). M059K cells that were transduced with negative control shRNAs should behave similarly to the M059K untransduced cell line. We indeed observed that hairpins for the negative control targets did not impinge on the ability of cells to rapidly repair their DNA, leading to disappearance of damage (Fig. 3-2B, green circles). However, for some of the hairpins targeting NHEJ genes (Fig. 3-2B, purple circles), we observed persistent DNA DSBs. Specifically, 4 hours after exposure of the cells to γIR, we observed that were shRNAs with different levels of DNA DSBs. For 8 out of 21 shRNAs tested, there was persistent unrepaired DNA damage. These 8 shRNAs target six out of the seven NHEJ genes chosen for testing in our pilot screen, showing that we can deplete DNA DSB repair factors using the shRNA library and that we can effectively assay cells for DNA DSB repair defects using the HTS CometChip. For the shRNAs that target chromatin-modifying genes (Fig. 3-2C, orange circles), we also observed that several of the shRNAs have higher levels of unrepaired DNA DSBs, indicating that those shRNAs were effective in depleting factors that were important for DSB repair, as expected. Note that not all of the shRNA against chromatin-modifying genes (known previously for impacting DNA repair) were effective in suppressing DNA

repair in our assay. This could be due to ineffective shRNAs that do not sufficiently knock down expression, as described below.

We performed the pilot screen in duplicates and compared the results for DNAPKcs shRNAs (Fig. 3-3A). We observed a high level of reproducibility for our un-transduced M059K and M059J cell lines (blue and red lines respectively), as expected given that these cell lines have shown similar results in previous experiments (Figs. 3-1C, 3-2B and C). Importantly, while one of the DNAPKcs shRNAs (shRNA #1) resulted in high levels of persistent DNA DSBs in both duplicate screens, shRNAs #2 and #3 did not appear to do so, likely due to inefficient knockdown efficiency. To test this possibility, we performed a western blot to probe of the levels of DNAPKcs from whole cell extracts harvested from M059K cells treated with DNAPKcs shRNAs from a separate lentiviral preparation. We found that shRNA #1 resulted in the most efficient knockdown of DNAPKcs (Fig. 3-3B), which is consistent with the observation that this hairpin resulted in high levels of persistent DNA DSBs. We noted that shRNA #3 showed normal levels of DSB repair in the pilot screen, even though cells treated with shRNA #3 from a separate lentivirus preparation showed that shRNA #3 appeared to be as efficient in depleting DNAPKcs as shRNA #1. It is possible that shRNA#3 was a defective reagent due to technical reasons in the lentiviral preparation of the shRNA for the pilot screen, leading to ineffective knockdown. These results show that shRNAs have different levels of effectiveness in depleting expression of their target genes, such that inefficient knockdown correlates with WT levels of DNA repair. For this reason, for the bigger screen, we used 3 separate hairpins to knockdown gene expression.

Having observed results that are consistent with efficacy in detecting genes that impact the levels of DSBs, we next expanded our screen. Through the Broad Institute, we have available to us an shRNA knockdown library that was made as a curated subset of The RNAi Consortium (TRC) genomic shRNA library. This 2564 gene sub-library was formatted as an arrayed library, and prepared on 89 tissue culture 96-well plates. Each gene was targeted with three unique lentiviral shRNA constructs with each well in the library containing one shRNA. Cells were plated on duplicate 96-well plates and transduced with lentiviruses from the shRNA library, with the exception of 4 wells on each plate to allow the inclusion of wild type M059K (wells H11 and H12), wild type M059J (well H9) and in-house prepared DNAPKcs shRNA lentiviral particles (well G12). Successfully transduced cells were trypsinized and transferred onto the HTS CometChip before they were irradiated with 100 Gy of γIR. The cells were then incubated for four hours in complete media before overnight lysis. A filter was applied to comet images to remove shRNAs that were represented by fewer than 20 comets on either replicate. An average value between replicates was then calculated for the remaining shRNAs. Each shRNA was normalized using the values obtained for M059J and M059K on its corresponding plate, and the top two shRNAs was averaged to obtain a score for each gene. The normalized data set was then rank-ordered, as shown in Figure 3-4A. The overall average comet tail lengths obtained for the M059K and M059J controls were 58 ± 13 and 120 ± 11 μm respectively. The averages of the luciferase and lacZ negative control shRNAs after normalization were 67 ± 12 and 66 ± 11 μm respectively. This was an expected result, since luciferase and lacZ were negative control targets and should not impinge on the ability of cells to rapidly repair their DNA.

On the other hand, the average of the DNAPKcs positive control shRNA was 85 ± 13 μm and was significantly higher than that of all the negative controls (adjusted p values = 2.6 x 10^{-10}, Tukey's multiple comparisons test). This result is consistent with the result obtained from DNAPKcs shRNA #1 in the pilot screen where partial knockdown of DNAPKcs resulted in an intermediate level of persistent DNA DSBs (Figs. 3-4A and 3-3A)

To survey for potentially significant pathways that were represented by the top genes in our list, we utilized Ingenuity Pathway Analysis (IPA) on the first 100 genes from our ranked list. We observed that several genes participate in many of the canonical pathways (Fig. 3-4B) identified by IPA, such as SFN, which is also represented in the 14-3-3 mediated signaling pathway. SFN, also known as 14-3-3σ, has been implicated in modulating other known DNA repair genes, and has been shown to affect cellular resistance to several cancer therapies, including radiotherapy[52-54]. 14-3-3 proteins are known to bind and modulate many DNA repair factors[55], therefore it was unsurprising that the 14-3-3 mediated signaling pathway was the top canonical pathway in our analysis.

The second pathway identified by IPA is the Hippo signaling pathway, known to control the rates of cell growth and organ sizes in an organism[56]. Several proteins in the Hippo signaling pathway have been shown to be activated when cells are exposed to DNA damage[57-59]. We selected LATS2 for further studies (ranked #62 in Fig. 3-4A) and showed that long comet tails 4 hours after γIR caused by LATS2 depletion could be recapitulated using siRNA knockdown (Fig. 3-5A and Supplementary Fig. 3-2). Indeed, when quantified, we observed that LATS2 depleted cells exhibited a relatively small but

statistically significant increase in persistent DNA DSBs after exposure to γIR (Fig. 3-5B). As an independent approach for evaluating the levels of DSBs, we also tested the effect of LATS2 depletion on the formation of γH2AX after exposure to γIR. We found that LATS2 depleted cells have a higher level of γH2AX (Fig. 3-5C), which is consistent with the presence of higher levels of DNA DSBs as compared to control cells.

Having observed that LATS2 knockdown cells had higher levels of persistent DNA DSBs, we asked if LATS2 knockdown cells had a DNA DSB repair defect. NHEJ and HR are the major pathways that cells repair DNA DSBs, therefore we further hypothesized that LATS2 knockdown resulted in reduced NHEJ or HR activity. We tested the activity of NHEJ or HR in cells using a stably integrated fluorescence-based cassette named DSB Spectrum (B. van de Kooij and M. Yaffe, unpublished). For this assay, the expression cassette expresses fluorescent proteins based on the type of repair pathway used to repair DNA DSBs. Briefly, the cassette consisted of a constitutively expressing BFP sequence and a GFP fragment. The BFP sequence and GFP fragment were homologous to one another, except for a single base pair substitution. Upon introduction of a DNA DSB at the BFP sequence using Cas9-gRNA site specific targeting, if the DNA DSB was repaired via error free NHEJ, the BFP sequence will be reconstituted and the cell will continue to express BFP. If the DNA DSB was repaired via NHEJ such that there are associated mutations or if alt-NHEJ repair pathway is responsible for repair, the BFP sequence will be disrupted and the cell will no longer express BFP. If the DNA DSB was repaired via HR using the GFP fragment as a template, the BFP sequence will undergo gene conversion and become a GFP sequence, resulting in the cell expressing GFP.

To test if LATS2 depletion resulted in reduced activity of NEHJ or HR, we treated cells that expressed DSB Spectrum with LATS2 siRNA. We assayed for changes in fluorescence protein expression via flow cytometry after the DNA DSB was introduced into the cells. We found that there was no significant change in the percentage of cells that became non-fluorescent between control and LATS2 depleted cells (Fig. 3-5D, left panel), indicating that LATS2 did not significantly affect the repair activity of mutagenic NHEJ pathway. However, we observed a significant decrease in the percentage of GFP positive cells after LATS2 depletion as compared to control (Fig. 3-5D, right panel), indicating that loss of LATS2 resulted in a small but significant decrease in HR activity. Given that LATS2 depletion resulted in a DNA DSB repair defect in cells, we next asked if LATS2 depleted cells are more sensitive to cytotoxicity induced by γIR exposure. We found that LATS2 depleted cells proliferated at a slower rate when exposed to γIR as compared to control cells (Fig. 3-5E), supporting the hypothesis that LATS2 knockdown resulted in diminished DNA DSB repair after exposure to γIR, leading to reduced growth or increased cell death in these cells. Taken together, analysis of the LATS2 knockdown cells shows that LATS2 contributes to DNA repair. Although the magnitude of the effect of LATS2 is relatively low, the results are nevertheless significant. Interestingly, CRISPR knockout of LATS2 did not lead to detectable differences in DNA damage, which may be the result of compensatory gene expression over time, when cells are knocked out for LATS2.

Interestingly, we also found that LATS2 depletion can lead to an apparent increase in DNA DSB levels even when LATS2 depleted cells were not exposed to γIR. Specifically, we loaded LATS2 depleted cells and control cells onto the HTS

CometChip, treated them with either 0 or 100 Gy γIR and lysed them immediately after radiation or allowed the cells to incubate in media for 4 hours. We observed that the unirradiated cells did not show signs of DNA damage immediately after the HTS CometChip was prepared (Fig. 3-6A, first column). In addition, both LATS2 depleted cells and control cells showed significant DNA damage immediately after exposure to 100 Gy γIR, as expected (Fig. 3-6A, second column). After allowing the cells to incubate in media for 4 hours, control cells did not have significant DNA damage, while LATS2 depleted cells showed high levels of DNA damage (Fig. 3-6A, third column). Unexpectedly, when the cells were incubated for 4 hours in the absence of γIR, we nevertheless observed the appearance of DNA damage in LATS2 depleted, but not control cells (Fig. 3-6A, fourth column). This result showed that DNA DSBs were generated in LATS2 depleted cells, when the cells were encapsulated in the HTS CometChip agarose and incubated in media for 4 hours. Upon closer inspection of the images obtained in Figure 3-6A, we found that there were two groups of comets with distinctively different shapes. The comets obtained from LATS2 depleted cells incubated for 4 hours in the HTS CometChip have a tear shaped tail and the pixels with maximum brightness intensity tend to be near the middle region of the tail (Fig. 3-6A, bottom row, third and fourth column). This is contrasted with the cone shaped comet tails obtained immediately after cells had been radiated, with the brightness intensity of the pixels in the tails tapering off as their distance from the comet head increases (Fig. 3-6A, second column).

It has been reported that tear shaped comets might be indicative of apoptotic cells and the resulting DNA fragmentation during apoptosis led to long comet tails (in

the literature, these are referred to as "hedghogs" because of their shape)[60]. To test if cells were indeed undergoing apoptosis when encapsulated in agarose for 4 hours, we analyzed cells using Annexin V staining. We found that most cells were negative for Annexin V staining when they were first placed in the HTS CometChip (Fig. 3-6B, third and fourth columns). However, when the cells were left in HTS CometChip for 4 hours, we saw that approximately 40% of the LATS2 siRNA treated cells or cell clusters were stained positively for Annexin V, compared with no significant staining for control siRNA treated cells (Fig. 3-6B, fifth and sixth columns). These results suggest that the comets we observed when LATS2 depleted cells were left in agarose for 4 hours were likely due to apoptosis. The observation that LATS2 depleted cells undergo apoptosis when cultured in agarose is consistent with the known role of the HIPPO pathway in maintaining cell-cell adhesion and contact inhibition, possibly inducing apoptosis when cell-cell contacts are lost.

3.5   Discussion

In this study, we developed a screening strategy to query a library of shRNAs targeting 2564 genes using the HTS CometChip[47], in order to identify genes that are potentially important for DNA DSB repair. We treated cells with the shRNA library to deplete specific gene targets, and assayed for persistent DNA DSBs after cells were exposed to γIR. We performed bioinformatics analysis on 100 genes with the highest levels of persistent DNA DSBs. We selected LATS2 for further studies, and found that LATS2 depleted cells had a DNA DSB repair defect, specifically in the HR pathway.

Additionally we also found that LATS2 depleted cells more readily undergo apoptosis when they were transferred from tissue culture plates onto agarose, inducing DSBs that were also assayed in our screen.

LATS2 is a member of the Hippo signaling pathway, which is known to control the rates of cell growth and organ sizes in an organism[56]. The members of the Hippo pathway were first identified in *Drosophila*, where mutant Hippo pathway genes led to massive overgrowth in the organs that harbored the mutated cells. The Hippo pathway consists of 4 kinases MST1, MST2, LATS1 and LATS2, which receive input signals such as cell adhesion and cell-to-cell contact. The end result of the kinase cascade activation in this pathway, is the phosphorylation of the YAP/TAZ transcriptional co-activators, leading to their degradation. When the kinases are inactive, YAP and TAZ can translocate into the cell nucleus, and promote the activity of TEADs and SMADs, which in-turn promotes cell growth and tumorigenesis. Several proteins in the core Hippo pathway have been shown to be activated when cells are exposed to DNA damage and could be modulating DNA repair[57-59].

From our data, we found that the loss of LATS2 in cells led to sustained levels of DNA DSBs after exposure to γIR. We also found that LATS2 depleted cells had lower HR activity, and the slower rate of DNA DSB repair led to increased levels of γH2AX signaling. We also observed that LATS2 depleted cells grow more slowly when exposed to γIR as compared to control cells, and this was likely due to the higher level of unrepaired DNA DSBs in LATS2 depleted cells, causing cell cycle arrest and apoptosis in those cells. We also observed that LATS2 depletion led to an increase in rate of cell death, when the cells were trypsinized and transferred from tissue culture plates to

agarose. This phenotype was observed even when cells were not exposed to γIR, suggesting that it was independent of DNA damage and repair pathways. Since the Hippo pathway responds to changes in cell-cell contacts and to changes in the extracellular matrix environment, we hypothesize that transferring the cells from a monolayer on a tissue culture plate, to a 3D environment encapsulated by agarose, may change the activity of the pathway, and loss of LATS2 in this context may lead to activation of cell death.

Importantly, HTS CometChip screen also has the ability to detect DNA damage caused by apoptotic cells, induced possibly by the action of transferring cells from tissue culture plates onto agarose (or induced by exposures). LATS2 is one example of a gene that when depleted, led to a DNA repair defect phenotype, as well as an apoptotic phenotype. Candidate genes from the HTS CometChip screen can be secondarily screened to ascertain if they participate in DNA repair or apoptotic pathways. An alternative approach for detecting a DNA repair defect, as opposed to increased apoptosis induced by growth on agarose, would be to allow cells to repair DNA damage when cultured on a 2D plate, prior to transferring them onto the HTS CometChip. The cells will be lysed immediately after the transfer, in order to avoid detecting apoptosis due to cells being on agarose for extended periods of time. Experiments can be conducted to investigate both processes simultaneously, or each of those pathways in isolation, making the HTS CometChip a versatile assay for studying DNA repair and apoptosis.

We have shown the utility of HTS CometChip as a screening tool for the specific discovery of DNA DSB repair factors in this study. The experimental procedures that we

have described here can be easily modified for screening efforts to discover genes that participate in other DNA repair pathways, or to discover small molecules that can modulate the activity of DNA repair pathways. To discover genes that are involved in DNA DSB repair, we treated cells with γIR as a source of DNA DSBs, and performed the neutral comet assay to measure them. The same workflow developed in this study can be adapted to discover genes that participate in other pathways, for example, base excision repair, by using agents such as methyl methanesulfonate or hydrogen peroxide to crease base lesions and performing the alkaline comet assay to measure the resulting alkali labile sites on DNA. Alternatively, the screening workflow can also be adapted such that the HTS CometChip becomes a drug discover tool. Instead of treating cells with RNAi reagents, cells can be treated with a small molecule library for a predetermined amount of time, before the cells are exposed to a source of DNA damage. Molecules that result in persistent DNA damage can potentially be used as adjuvant therapies to enhance the effectiveness of treatments that induce DNA damage as a mechanism of killing tumor cells. The small molecule library can also be directly applied onto cells and queried for their ability to induce DNA damage to potentially discover effective molecules that can be developed into drugs.

To our knowledge, this is the first high throughput screen that measures the repair of physical DNA DSBs in the genomes of cells, using the comet assay technique. In this screen, we queried 2564 genes to test if depleting each of those genes will result in persistent DNA DSBs after cells were exposed to γIR. Each of those genes was targeted by three shRNAs, and all the shRNAs were distributed across 89 96-well plates. We took nine images per shRNA, for a total of about 130,000 images, containing

over 750,000 comets. To put the sheer size of the screen in perspective, given a liberal estimate of being able to complete 50 traditional comet assay slides per week, it would take a typical researcher at least 300 weeks to collect the same amount of data as we did in about 10 weeks.

On top of the vast increase in throughput that was achieved with our screen, further improvements in the rate of data collection can be made. For our screen, we alternated between screening and imaging days. On screening days, we transferred cells onto eight HTS CometChips with the assistance of HTS robotics, irradiate the HTS CometChips and allow cells to repair the damage before lysis. Four HTS CometChips were loaded during each run of the HTS robotic scripts and two runs were conducted each day, with each run taking approximately 45 minutes to complete. It is possible to conduct up to six runs within typical working hours, which will yield data from about 2200 samples (6 runs x 4 HTS CometChips x 92 wells). We could also double our rate of screening by performing screening and imaging activities concurrently, since they require different robotic systems (i.e. screening activities require HTS liquid handlers and incubators, imaging activities require HTS automatic microscope). This will allow us to query 11,000 samples in a typical 5-day work week. Given that a typical genomic shRNA library targets approximately 20,000 genes using three distinct shRNAs per gene, a genome-wide HTS CometChip screen be completed in as little as 12 weeks to complete, with duplicate data for each shRNA. The possibility of performing a genome wide screen for DNA repair factors by measuring physical DNA damage can now be fully realized with the advent of HTS CometChip as an enabling innovation.

3.6   Conclusions

We have developed a novel strategy to query thousands of genes for their ability to modulate DNA repair, made possible by the invention of HTS CometChip previously. In this work, we have shown that the HTS CometChip is an effective tool for discovering genes that result in persistent DNA DSBs by performing a small-scale screen, using a panel of lentiviral shRNAs to perform gene knockdown and assaying cells for persistent DNA DSBs after exposure to γIR. We then expanded to screen a library of lentiviral shRNAs targeting 2564 genes for their effects on DNA DSB repair activity, with each gene being knocked down by three unique shRNAs. We performed bioinformatics analysis on the top 100 genes rank ordered by the extent of DNA DSB repair defect caused by the shRNAs that targeted them and selected LATS2 for further investigation. We showed that LATS2 depletion led to a DNA DSB repair defect, as well as apoptosis when cells were transferred onto a 3D agarose environment for an extended period of time. Both phenotypes resulted in the accumulation of DNA DSBs in LATS2 depleted cell. We showed further that LATS2 depleted cells were less likely to repair DNA DSBs by the HR pathway. We also showed that LATS2 depleted cells are more sensitive to ionizing radiation, which was consistent with their inability to repair DNA DSBs as efficiently as wild type cells. Finally, we showed that LATS2 depleted cells undergo apoptosis when placed in the HTS CometChip agarose for an extended period of time, showing that the screen can also reveal genes that impact susceptibility to apoptosis. Taken together, the HTS CometChip is an effective tool for performing large-scale studies for genes that impact DNA DSBs.

References

1.   Thibodeau, S. N., French, A. J., Roche, P. C., Cunningham, J. M., Tester, D. J., Lindor, N. M., et al. (1996). Altered expression of hMSH2 and hMLH1 in tumors with microsatellite instability and genetic alterations in mismatch repair genes. *Cancer Research*, *56*(21), 4836–4840.

2.   King, M.-C., Marks, J. H., Mandell, J. B., New York Breast Cancer Study Group. (2003). Breast and ovarian cancer risks due to inherited mutations in BRCA1 and BRCA2. *Science (New York, N.Y.)*, *302*(5645), 643–646.

3.   Nickoloff, J. A., Jones, D., Lee, S.-H., Williamson, E. A., & Hromas, R. (2017). Drugging the Cancers Addicted to DNA Repair. *Journal of the National Cancer Institute*, *109*(11), 85.

4.   Lord, C. J., & Ashworth, A. (2012). The DNA damage response and cancer therapy. *Nature*, *481*(7381), 287–294.

5.   Goldstein, M., & Kastan, M. B. (2015). The DNA damage response: implications for tumor responses to radiation and chemotherapy. *Annual Review of Medicine*, *66*(1), 129–143.

6.   Hanahan, D., & Weinberg, R. A. (2011). Hallmarks of cancer: the next generation. *Cell*, *144*(5), 646–674.

7.   Hoeijmakers, J. H. (2001). Genome maintenance mechanisms for preventing cancer. *Nature*, *411*(6835), 366–374.

8.   Frosina, G. (2009). DNA Repair and Resistance of Gliomas to Chemotherapy and Radiotherapy. *Molecular Cancer Research : MCR*, *7*(7), 989–999.

9.   Hegi, M. E., Diserens, A.-C., Gorlia, T., Hamou, M.-F., de Tribolet, N., Weller, M., et al. (2005). MGMT gene silencing and benefit from temozolomide in glioblastoma. *The New England Journal of Medicine*, *352*(10), 997–1003.

10.   Gerson, S. L. (2004). MGMT: its role in cancer aetiology and cancer therapeutics. *Nature Reviews. Cancer*, *4*(4), 296–307.

11.   Allalunis-Turner, M. J., Barron, G. M., Day, R. S., Dobler, K. D., & Mirzayans, R. (1993). Isolation of two cell lines from a human malignant glioma specimen differing in sensitivity to radiation and chemotherapeutic drugs. *Radiation Research*, *134*(3), 349–354.

12.   Lees-Miller, S. P., Godbout, R., Chan, D. W., Weinfeld, M., Day, R. S., Barron, G. M., & Allalunis-Turner, J. (1995). Absence of p350 subunit of DNA-activated protein kinase from a radiosensitive human cell line. *Science (New York, N.Y.)*, *267*(5201), 1183–1185.

13.   Priestley, A., Beamish, H. J., Gell, D., Amatucci, A. G., Muhlmann-Diaz, M. C., Singleton, B. K., et al. (1998). Molecular and biochemical characterisation of DNA-dependent protein kinase-defective rodent mutant irs-20. *Nucleic Acids Research*, *26*(8), 1965–1973.

14.   Happold, C., Roth, P., Wick, W., Schmidt, N., Florea, A.-M., Silginer, M., et al. (2012). Distinct molecular mechanisms of acquired resistance to temozolomide in glioblastoma cells. *Journal of Neurochemistry*, *122*(2), 444–455.

15.   Jiang, G., Wei, Z.-P., Pei, D.-S., Xin, Y., Liu, Y.-Q., & Zheng, J.-N. (2011). A novel approach to overcome temozolomide resistance in glioma and melanoma: Inactivation of MGMT by gene therapy. *Biochemical and Biophysical Research Communications*, *406*(3), 311–314.

16.   Wedge, S. R., Porteous, J. K., & Newlands, E. S. (1997). Effect of single and multiple administration of an O6-benzylguanine/temozolomide combination: an evaluation in a human melanoma xenograft model. *Cancer Chemotherapy and Pharmacology*, *40*(3), 266–272.

17.   Schaue, D., & McBride, W. H. (2005). Counteracting tumor radioresistance by targeting DNA repair. *Molecular Cancer Therapeutics*, *4*(10), 1548–1550.

18.   Helleday, T., Petermann, E., Lundin, C., Hodgson, B., & Sharma, R. A. (2008). DNA repair pathways as targets for cancer therapy. *Nature Reviews. Cancer*, *8*(3), 193–204.

19.   Curtin, N. (2007). Therapeutic potential of drugs to modulate DNA repair in cancer. *Expert Opinion on Therapeutic Targets*, *11*(6), 783–799.

20.   Ding, J., Miao, Z.-H., Meng, L.-H., & Geng, M.-Y. (2006). Emerging cancer therapeutic opportunities target DNA-repair systems. *Trends in Pharmacological Sciences*, *27*(6), 338–344.

21.   Madhusudan, S., & Hickson, I. D. (2005). DNA repair inhibition: a selective tumour targeting strategy. *Trends in Molecular Medicine*, *11*(11), 503–511.

22.   Khanna, K. K., & Jackson, S. P. (2001). DNA double-strand breaks: signaling, repair and the cancer connection. *Nature Genetics*, *27*(3), 247–254.

23.   Petrini, J. H. J., & Stracker, T. H. (2003). The cellular response to DNA double-strand breaks: defining the sensors and mediators. *Trends in Cell Biology*, *13*(9), 458–462.

24.   Lees-Miller, S. P., & Meek, K. (2003). Repair of DNA double strand breaks by non-homologous end joining. *Biochimie*, *85*(11), 1161–1173.

25.   Burma, S., Chen, B. P. C., & Chen, D. J. (2006). Role of non-homologous end joining (NHEJ) in maintaining genomic integrity. *DNA Repair*, *5*(9-10), 1042–1048.

26.   West, S. C. (2003). Molecular views of recombination proteins and their control. *Nature Reviews. Molecular Cell Biology*, *4*(6), 435–445.

27. Li, X., & Heyer, W.-D. (2008). Homologous recombination in DNA repair and DNA damage tolerance. *Cell Research*, *18*(1), 99–113.

28. Shrivastav, M., De Haro, L. P., & Nickoloff, J. A. (2008). Regulation of DNA double-strand break repair pathway choice. *Cell Research*, *18*(1), 134–147.

29. Takata, M., Sasaki, M. S., Sonoda, E., Morrison, C., Hashimoto, M., Utsumi, H., et al. (1998). Homologous recombination and non-homologous end-joining pathways of DNA double-strand break repair have overlapping roles in the maintenance of chromosomal integrity in vertebrate cells. *The EMBO Journal*, *17*(18), 5497–5508.

30. Price, B. D., & D'Andrea, A. D. (2013). Chromatin remodeling at DNA double-strand breaks. *Cell*, *152*(6), 1344–1354.

31. Falk, M., Lukasova, E., Gabrielova, B., Ondrej, V., & Kozubek, S. (2007). Chromatin dynamics during DSB repair. *Biochimica Et Biophysica Acta*, *1773*(10), 1534–1545.

32. Begley, T. J., Rosenbach, A. S., Ideker, T., & Samson, L. D. (2002). Damage recovery pathways in Saccharomyces cerevisiae revealed by genomic phenotyping and interactome mapping. *Molecular Cancer Research : MCR*, *1*(2), 103–112.

33. Matsuoka, S., Ballif, B. A., Smogorzewska, A., McDonald, E. R., Hurov, K. E., Luo, J., et al. (2007). ATM and ATR substrate analysis reveals extensive protein networks responsive to DNA damage. *Science (New York, N.Y.)*, *316*(5828), 1160–1166.

34. Paulsen, R. D., Soni, D. V., Wollman, R., Hahn, A. T., Yee, M.-C., Guan, A., et al. (2009). A Genome-wide siRNA Screen Reveals Diverse Cellular Processes and Pathways that Mediate Genome Stability. *Molecular Cell*, *35*(2), 228–239.

35. Floyd, S. R., Pacold, M. E., Huang, Q., Clarke, S. M., Lam, F. C., Cannell, I. G., et al. (2013). The bromodomain protein Brd4 insulates chromatin from DNA damage signalling. *Nature*, *498*(7453), 246–250.

36. Gong, F., Chiu, L.-Y., Cox, B., Aymard, F., Clouaire, T., Leung, J. W., et al. (2015). Screen identifies bromodomain protein ZMYND8 in chromatin recognition of transcription-associated DNA damage that promotes homologous recombination. *Genes & Development*, *29*(2), 197–211.

37. Berns, K., Hijmans, E. M., Mullenders, J., Brummelkamp, T. R., Velds, A., Heimerikx, M., et al. (2004). A large-scale RNAi screen in human cells identifies new components of the p53 pathway. *Nature*, *428*(6981), 431–437.

38. Valdiglesias, V., Pásaro, E., Méndez, J., & Laffon, B. (2011). Assays to determine DNA repair ability. *Journal of Toxicology and Environmental Health. Part A*, *74*(15-16), 1094–1109.

39. Ostling, O., & Johanson, K. J. (1984). Microelectrophoretic study of radiation-induced DNA damages in individual mammalian cells. *Biochemical and Biophysical Research Communications*, *123*(1), 291–298.

40.   Singh, N. P., McCoy, M. T., Tice, R. R., & Schneider, E. L. (1988). A simple technique for quantitation of low levels of DNA damage in individual cells. *Experimental Cell Research, 175*(1), 184–191.

41.   Collins, A. R. (2004). The comet assay for DNA damage and repair: principles, applications, and limitations. *Molecular Biotechnology, 26*(3), 249–261.

42.   Olive, P. L., & Banáth, J. P. (1993). Detection of DNA double-strand breaks through the cell cycle after exposure to X-rays, bleomycin, etoposide and 125IdUrd. *International Journal of Radiation Biology, 64*(4), 349–358.

43.   Wood, D. K., Weingeist, D. M., Bhatia, S. N., & Engelward, B. P. (2010). Single cell trapping and DNA damage analysis using microwell arrays. *Proceedings of the National Academy of Sciences of the United States of America, 107*(22), 10008–10013.

44.   Weingeist, D. M., Ge, J., Wood, D. K., Mutamba, J. T., Huang, Q., Rowland, E. A., et al. (2013). Single-cell microarray enables high-throughput evaluation of DNA double-strand breaks and DNA repair inhibitors. *Cell Cycle, 12*(6), 907–915.

45.   Ge, J., Prasongtanakij, S., Wood, D. K., Weingeist, D. M., Fessler, J., Navasummrit, P., et al. (2014). CometChip: a high-throughput 96-well platform for measuring DNA damage in microarrayed human cells. *Journal of Visualized Experiments : JoVE*, (92), e50607–e50607.

46.   Sykora, P., Witt, K. L., Revanna, P., Smith-Roe, S. L., Dismukes, J., Lloyd, D. G., et al. (2018). Next generation high throughput DNA damage detection platform for genotoxic compound screening. *Scientific Reports, 8*(1), 2771.

47.   Tay, I. J., Floyd, S. R., Engelward, B. P. (2018). Novel Apparatus for the CometChip Cell Microarray Enables High Throughput Screening for DNA Double Strand Breaks. *Manuscript in preparation*.

48.   Livak, K. J., & Schmittgen, T. D. (2001). Analysis of relative gene expression data using real-time quantitative PCR and the 2(-Delta Delta C(T)) Method. *Methods (San Diego, Calif.), 25*(4), 402–408.

49.   Ogiwara, H., Ui, A., Otsuka, A., Satoh, H., Yokomi, I., Nakajima, S., et al. (2011). Histone acetylation by CBP and p300 at double-strand break sites facilitates SWI/SNF chromatin remodeling and the recruitment of non-homologous end joining factors. *Oncogene, 30*(18), 2135–2146.

50.   Murr, R., Loizou, J. I., Yang, Y.-G., Cuenin, C., Li, H., Wang, Z.-Q., & Herceg, Z. (2006). Histone acetylation by Trrap-Tip60 modulates loading of repair proteins and repair of DNA double-strand breaks. *Nature Cell Biology, 8*(1), 91–99.

51.   Polo, S. E., Kaidi, A., Baskcomb, L., Galanty, Y., & Jackson, S. P. (2010). Regulation of DNA-damage responses and cell-cycle progression by the chromatin remodelling factor CHD4. *The EMBO Journal, 29*(18), 3130–3139.

52.   Chen, Y., Li, Z., Dong, Z., Beebe, J., Yang, K., Fu, L., & Zhang, J.-T. (2017). 14-3-3σ Contributes to Radioresistance By Regulating DNA Repair and Cell Cycle via PARP1 and CHK2. *Molecular Cancer Research : MCR*, *15*(4), 418–428.

53.   Lai, K. K. Y., Chan, K. T., Choi, M. Y., Wang, H. K., Fung, E. Y. M., Lam, H. Y., et al. (2016). 14-3-3σ confers cisplatin resistance in esophageal squamous cell carcinoma cells via regulating DNA repair molecules. *Tumour Biology : the Journal of the International Society for Oncodevelopmental Biology and Medicine*, *37*(2), 2127–2136.

54.   Chan, T. A., Hermeking, H., Lengauer, C., Kinzler, K. W., & Vogelstein, B. (1999). 14-3-3Sigma is required to prevent mitotic catastrophe after DNA damage. *Nature*, *401*(6753), 616–620.

55.   Mohammad, D. H., & Yaffe, M. B. (2009). 14-3-3 proteins, FHA domains and BRCT domains in the DNA damage response. *DNA Repair*, *8*(9), 1009–1017.

56.   Harvey, K. F., Zhang, X., & Thomas, D. M. (2013). The Hippo pathway and human cancer. *Nature Reviews. Cancer*, *13*(4), 246–257.

57.   Aylon, Y., Ofir-Rosenfeld, Y., Yabuta, N., Lapi, E., Nojima, H., Lu, X., & Oren, M. (2010). The Lats2 tumor suppressor augments p53-mediated apoptosis by promoting the nuclear proapoptotic function of ASPP1. *Genes & Development*, *24*(21), 2420–2429.

58.   Okada, N., Yabuta, N., Suzuki, H., Aylon, Y., Oren, M., & Nojima, H. (2011). A novel Chk1/2-Lats2-14-3-3 signaling pathway regulates P-body formation in response to UV damage. *Journal of Cell Science*, *124*(Pt 1), 57–67.

59.   Matallanas, D., Romano, D., Yee, K., Meissl, K., Kucerova, L., Piazzolla, D., et al. (2007). RASSF1A elicits apoptosis through an MST2 pathway directing proapoptotic transcription by the p73 tumor suppressor protein. *Molecular Cell*, *27*(6), 962–975.

60.   Olive, P. L., Frazer, G., & Banáth, J. P. (1993). Radiation-induced apoptosis measured in TK6 human B lymphoblast cells using the comet assay. *Radiation Research*, *136*(1), 130–136.
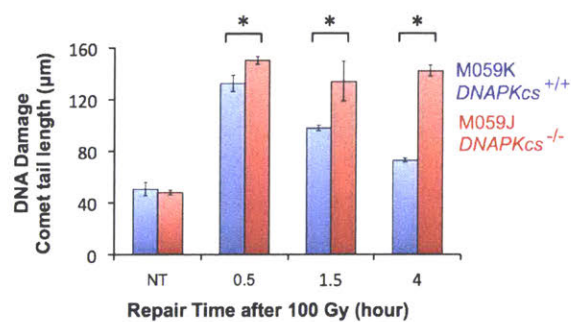
A
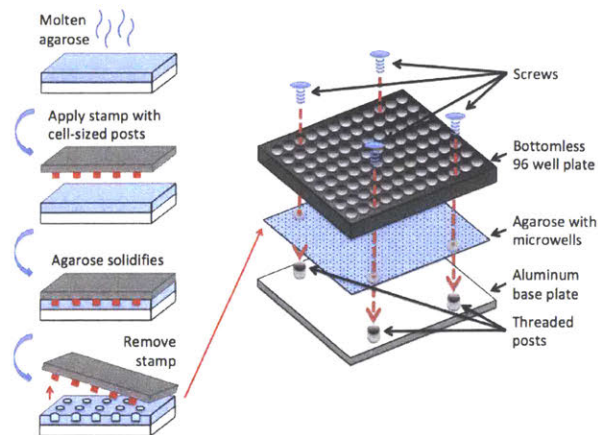
B
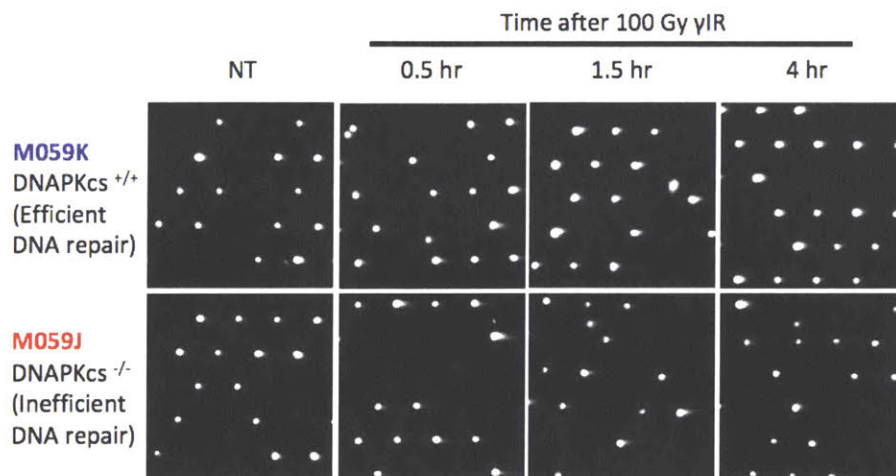
C

Figure 3-1.   Detecting DNA DSBs with the HTS CometChip. (A) Molten agarose was plated on a Gel-Bond film, patterned with cell-sized micro-wells and assembled into the HTS CometChip. (B) M059K and M059J cells (top and bottom row) were loaded into the HTS CometChip, treated with 100 Gy γIR and incubated in media for up to 4 hours. Representative images after DNA staining were shown. (C) Comet tail lengths from (B) were quantified (n=3, data points represent mean ± 1SD, * $p < 0.05$ for paired Student's T test).

Figure 3-2. Detection of DNA DSB repair with HTS CometChip, using M059K cells treated with a panel of shRNAs as a pilot screen. (A) Table of genes selected for pilot screening. Genes were color-grouped according to their functions. (B,C) Comparison between M059K cells treated with negative control shRNAs and shRNAs targeting NHEJ genes (B) or chromatin modifying genes (C). Each circle represents data from 1 shRNA and was color-coded according to Fig. 3-2A. (Data points represent average comet tail length and error bars represent 1SD)

A

Replicate 1   Replicate 2

DNAPKcs
— shRNA 1
– – shRNA 2
······ shRNA 3

M059J
DNAPKcs⁻ᐟ⁻

M059K
DNAPKcs ⁺ᐟ⁺

DNA Damage
Comet Tail Length (μm)

Repair Time after 100 Gy (hour)

B

shDNAPKcs

1   2   3   shGFP M059K M059J

DNAPKcs

Ku80
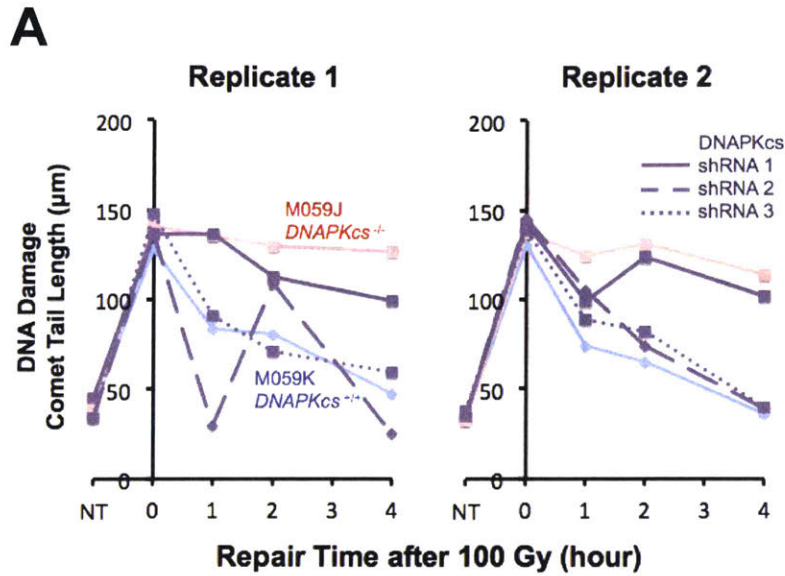
Figure 3-3. Knockdown of DNAPKcs resulting in DNA DSB repair defects. (A) Comparison between DNA DSB repair curves obtained from replicate 1 and 2 for shRNAs targeting DNAPKcs. (B) Western blot showing DNAPKcs protein levels after shRNA knockdown. M059K cells were transduced with lentiviral shRNA constructs (shRNA 1, 2, and 3 targeting DNAPKcs and shRNA targeting GFP) and whole cell extracts were prepared after selection for successfully transduced cells. M059K (DNAPKcs ⁺ᐟ⁺) and M059J cells (DNAPKcs ⁻ᐟ⁻) were used as DNAPKcs probing controls. Ku80 was used as a loading control.

A

B

Canonical pathways	p value	Associated genes
14-3-3 mediated signaling	7.22×10^{-8}	MAP3K5, PIK3C3, PIK3R5, SFN, SRPK2, TSC2, VIM, YWHAQ
Hippo signaling	1.43×10^{-7}	AJUBA, LATS2, PPP1R3A, PPP2R2C, PPP2R5E, SFN, YWHAQ
ERK/MAPK signaling	2.28×10^{-7}	PIK3C3, PIK3R5, PPP1R3A, PPP2R2C, PPP2R5E, PRKAR1B, PTK2B, YWHAQ
IGF-1 signaling	3.48×10^{-7}	PIK3C3, PIK3R5, PRKACG, PRKAR1B, SFN, SOCS1, YWHAQ
p70S6K signaling	1.69×10^{-6}	LYN, PIK3C3, PIK3R5, PPP2R2C, PPP2R5E, SFN, YWHAQ

Figure 3-4.   HTS CometChip shRNA screen. (A) Genes from the screen, rank-ordered according to the averaged normalized comet tail lengths of the top two shRNAs for each gene. shRNAs represented by fewer than 20 comets on either replicate were removed from analysis. (B) Highly significant pathways represented within the top 100 genes obtained from (A), as analyzed by Ingenuity Pathway Analysis software.
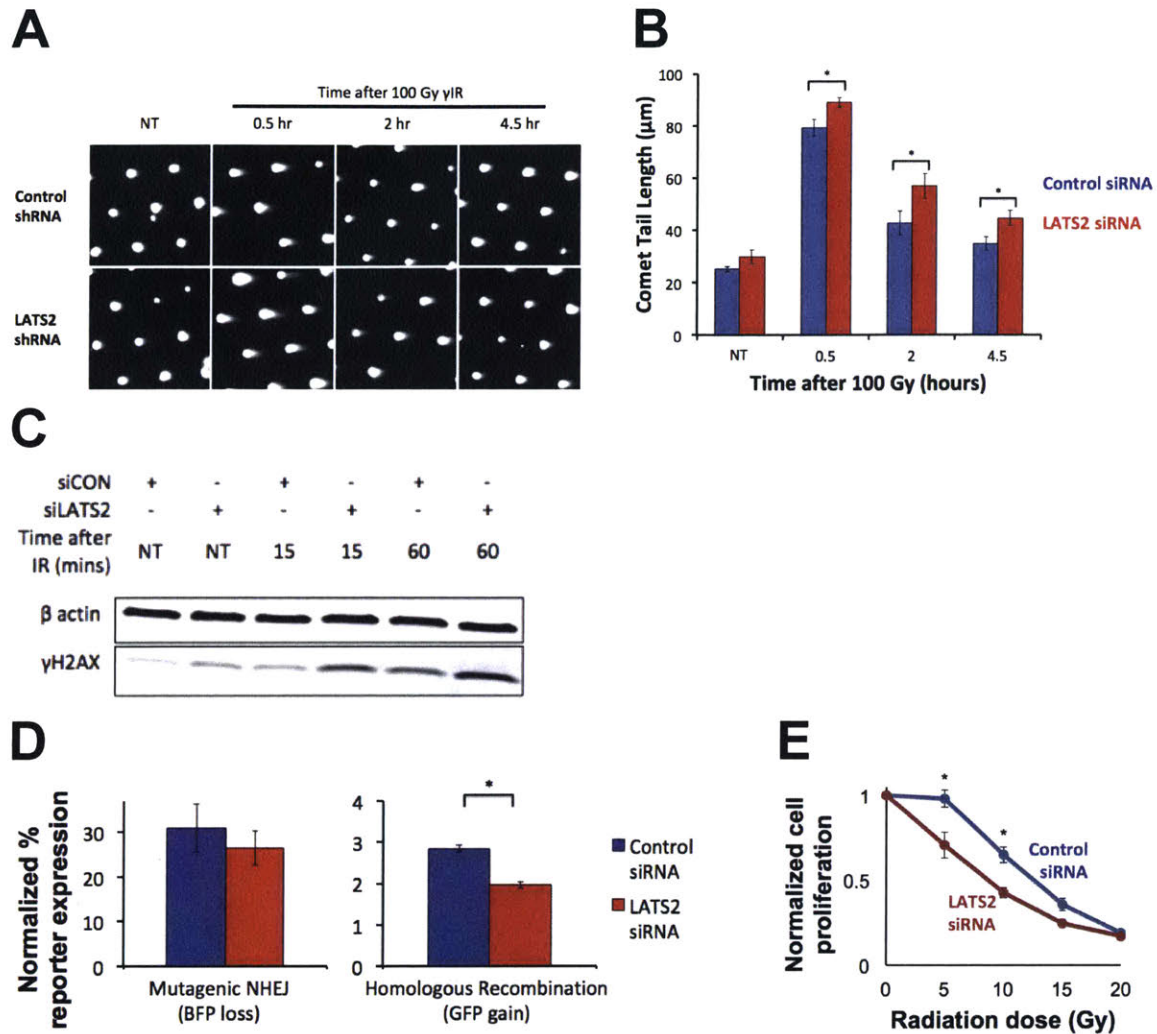
Figure 3-5.   LATS2 knockdown led to DNA DSB repair defects. (A) HeLa cells treated with control siRNA (top row) and LATS2 siRNA (bottom row) were treated with 100 Gy γIR and incubated in media before the cells were trypsinized and loaded onto the HTS CometChip. Representative images were shown. (B) Comet tail lengths from (A) were quantified (n=3, data points represent mean ± 1SD, * $p < 0.05$ for paired Student's T test) (C) Representative western blot showing HeLa cells transfected with control or LATS2 siRNA that were treated with 10 Gy γ-radiation, and probed for γH2AX levels at various timepoints. Cells depleted for LATS2 showed increased γH2AX levels over time as compared to control. (D) 293T cells transfected with control or LATS2 siRNA were tested for their ability to repair DNA DSBs via mutagenic NHEJ or HR pathways using DSB spectrum. Cells depleted for LATS2 showed a decrease in the relative percentage of DNA DSBs repaired via HR. (n=3, data points represent mean ± 1SD, * $p < 0.05$ for paired Student's T test) (E) Relative cell proliferation of HeLa cells transfected with control or LATS2 siRNA measured by Cell TitreGlo, 72 hours after γIR treatment. (n=3, data points represent mean ± 1SD, * $p < 0.05$ for paired Student's T test)

127
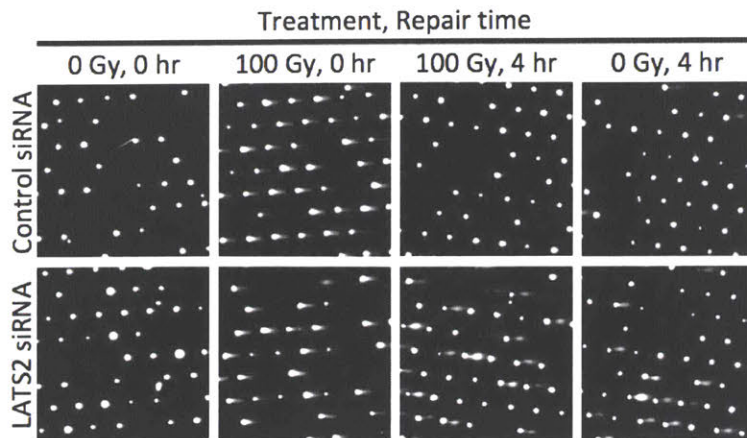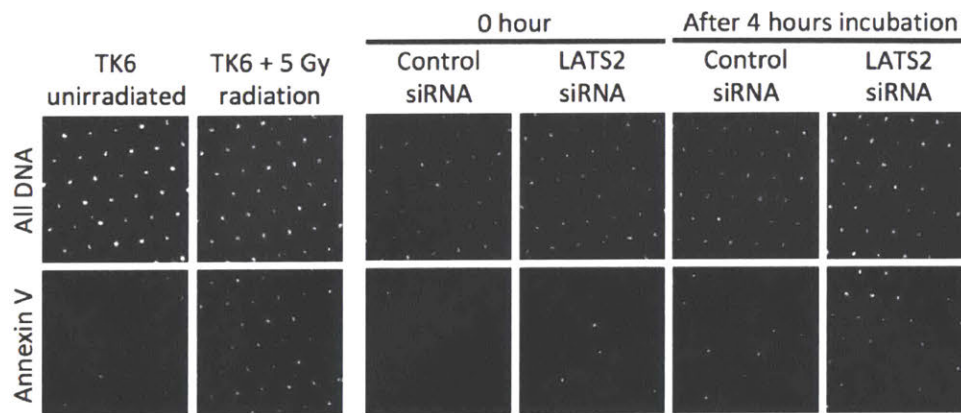
Figure 3-6.   Apoptotic comets observed in LATS2 knockdown cells. (A) HeLa cells treated with LATS2 or control siRNA were exposed to 0 or 100 Gy γIR and allowed to recover in media for 0 or 4 hr before lysis. LATS2 siRNA treated cells showed an increase in percentage of long tailed comets as compared to control after 4-hour recovery, regardless of radiation status. (B) HeLa cells treated with LATS2 or control siRNA were stained with a DNA stain and Annexin V immediately or 4 hours after they were transferred to HTS CometChip agarose. TK6 cells treated with 0 or 5 Gy of radiation and incubated for 24 hours were used as negative and positive controls for Annexin V staining.

Negative control shRNAs		
Target gene	**TRC ID number**	**Target sequence**
GFP	TRCN0000072194	CCACATGAAGCAGCACGACTT
GFP	TRCN0000072181	ACAACAGCCACAACGTCTATA
lacZ	TRCN0000072240	TCGTATTACAACGTCGTGACT
lacZ	TRCN0000072236	CCAACGTGACCTATCCCATTA
Luciferase	TRCN0000072250	AGAATCGTCGTATGCAGTGAA
Luciferase	TRCN0000072256	ACGCTGAGTACTTCGAAATGT
RFP	TRCN0000072209	CTCAGTTCCAGTACGGCTCCA
RFP	TRCN0000072212	CCGTAATGCAGAAGAAGACCA
Empty vector	TRCN0000208001	-

NHEJ targeting shRNAs		
Target gene	**TRC ID number**	**Target sequence**
Artemis	TRCN0000276608	ATTTGCCCAAAGGATACTTAC
Artemis	TRCN0000276612	TATGGATAAAGTTGTCGAAAT
Artemis	TRCN0000276609	ACGAGAGCATTTACAATATTT
DNAPKcs	TRCN0000194719	CCTGAAGTCTTTACAACATAT
DNAPKcs	TRCN0000194985	CCATCCCTTATAGGTTAATAT
DNAPKcs	TRCN0000197152	GAAACAGCTGTCTCCGTAAAT
Ku70	TRCN0000039609	GATGAGTCATAAGAGGATCAT
Ku70	TRCN0000009846	GAAGAGTCTACCCGACATAAG
Ku70	TRCN0000039611	CCCAAGGTTGAAGCAATGAAT
Ku80	TRCN0000010467	TGAAGATGGACCTACAGCTAA
Ku80	TRCN0000039842	CGTGGGCTTTACCATGAGTAA
Ku80	TRCN0000221592	GCAGCCCTTGTGATGTGATTA
LIG4	TRCN0000229989	TTGCTATGGTGATAGTTATTT
LIG4	TRCN0000257124	GCCTATCTCATGACCATATTG
LIG4	TRCN0000040005	GCTCGCATCTAAACACCTTTA
XLF	TRCN0000275700	CCAACATTTGATTCGTCCTCT
XLF	TRCN0000275631	ATGGGCATGAGTCTGGCATTA
XLF	TRCN0000275629	ATTCCTTCTTGGAACAATTTA
XRCC4	TRCN0000040116	CCAGCTGATGTATACACGTTT
XRCC4	TRCN0000421915	ATGATGTTCAAGGACGATTTG
XRCC4	TRCN0000040115	GCTGCTGTAAGTAAAGATGAT

shRNAs targeting chromatin modifiers		
Gene name	TRC ID number	Target sequence
ATRX	TRCN0000342811	GATAATCCTAAGCCTAATAAA
ATRX	TRCN0000342812	TCAACCTCTTGAGGATATAAT
ATRX	TRCN0000342874	CTTCGAAACATTGACTATTAC
BAZ1A	TRCN0000359204	CAAGGTTACAGATCGACATAT
BAZ1A	TRCN0000229784	TGCAATTGATCCCTTACTATT
BAZ1A	TRCN0000229786	CGTAGCGTGATATGGTCTAAA
CHD4	TRCN0000021363	GCGGGAGTTCAGTACCAATAA
CHD4	TRCN0000319288	GCGGGAGTTCAGTACCAATAA
CHD4	TRCN0000349610	CGAAGGTTTAAGCTCTTAGAA
CREBBP	TRCN0000356081	ATCGCCACGTCCCTTAGTAAC
CREBBP	TRCN0000356082	CGTTTACCATGAGATCCTTAT
CREBBP	TRCN0000367481	TAACTCTGGCCATAGCTTAAT
EP300	TRCN0000231134	ATACTCAGCCGGAGGATATTT
EP300	TRCN0000231136	ACCTCGTGATGCCACTTATTA
EP300	TRCN0000231133	TAACCAATGGTGGTGATATTA
KAT5	TRCN0000293417	CAAGTGTCTTCAGCGTCATTT
KAT5	TRCN0000020317	CCTCCTATCCTATCGAAGCTA
KAT5	TRCN0000293476	GGACGTAAGAACAAGAGTTAT
KDM2B	TRCN0000234590	GAGGGTGGACTTCGGAGAAAT
KDM2B	TRCN0000234589	CTGAACCACTGCAAGTCTATC
KDM2B	TRCN0000234587	ATGAGCGTGAAAGGTTGTTTC
MCPH1	TRCN0000426642	GAAGTTGGAAGGATCCATTAA
MCPH1	TRCN0000423827	ACACTTATCAAGCCTAATTAA
MCPH1	TRCN0000083785	GCCAACAAGAACATTAGTCAT
SIRT6	TRCN0000358693	CAAGTTCGACACCACCTTTGA
SIRT6	TRCN0000232531	ACCCGGATCAACGGCTCTATC
SIRT6	TRCN0000232530	GCTACGTTGACGAGGTCATGA
SMARCA4	TRCN0000379829	TGGAGCACAAACGCATCAATG
SMARCA4	TRCN0000231101	CTTTGCGTATCGCGGCTTTAA
SMARCA4	TRCN0000380532	CGTACGAGTACATCATCAAAG
SMARCA5	TRCN0000329918	GAATGGTATACTCGGATATTA
SMARCA5	TRCN0000013217	CGACTGCTGATGTAGTAATTT
SMARCA5	TRCN0000358498	ATTCCTCCTTCGTCGAATTAA
TRRAP	TRCN0000231912	TTTACGAATTGCGGCATTAAA
TRRAP	TRCN0000005365	GCTACGATTCTGGTGGAATAT
TRRAP	TRCN0000257346	GGCGCACATTATCGCCAAATT

Supplementary Figure 3-1. List of shRNAs with their target genes, ID numbers and target sequences obtained from MIT Broad Institute, the RNAi Consortium.
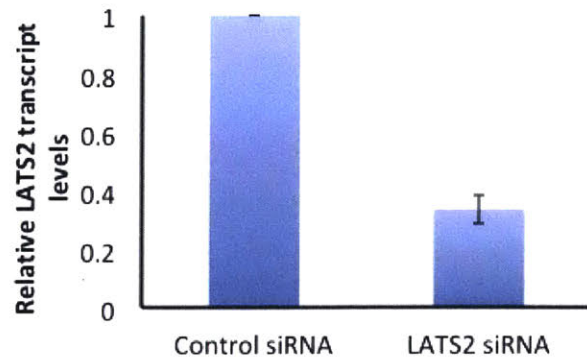
Supplementary Figure 3-2. Relative transcript levels of LATS2 as measured by semi quantitative qRT-PCR after siRNA knockdown. (N = 3)

Chapter 4

Integration of High Throughput DNA Strand Break Screen with DNA Strand Break Binding Assay to Identify Novel DNA Repair Factors

4.1   Abstract

DNA repair is critical for reversing DNA damage, maintaining genomic integrity and preventing cells from turning cancerous. While the core DNA repair factors have been identified and characterized, there are still gaps in the knowledge of how these proteins are coordinated and regulated in DNA repair networks. Recent research has provided evidence that the core DNA repair factors only make up a small fraction of the total number of proteins that respond to DNA damage, hinting at the possibility of a large number of novel DNA repair factors yet to be discovered. We have previously developed the High Throughput Screening CometChip, which allowed us to measure levels of DNA damage in hundreds of samples simultaneously. We used our assay in an RNAi screen, to identify potential DNA double stranded break (DSB) repair factors. Here, we designed an algorithm to further increase the accuracy of identifying potential DNA DSB repair factors from our screen, and combined our data with that from a novel

screen for proteins that bind to DSBs. Results show effective identification of known DNA DSB repair factors from the intersection of the two datasets, and pinpoint at least two novel factors for further investigation.

4.2   Introduction

DNA is the blueprint of life, and the transmission of information in DNA with high fidelity from parent to progeny cells is essential for an organism's viability. However, the genomes in our cells are constantly being assaulted by highly reactive molecules, which are generated from the cell's metabolic processes or introduced into the cell from its surroundings. The resulting damage can alter the information in DNA, and therefore interfere with the accurate transmission of genetic information when cells divide[1]. The accumulation of cells with highly damaged or mutated DNA in an organism can cause diseases, such as growth defects, aging and cancer[2,3]. To suppress the deleterious effects of DNA damage, cells possess the capability to repair DNA, which can restore the DNA structure[4,5]. Since DNA repair can reverse the deleterious effects of DNA damage, it is also an important susceptibility factor for diseases. On the other hand, DNA damaging agents are intentionally used to treat cancer, in part because tumor cells often have malfunctioning DNA repair pathways[6-8]. Expanding our understanding of DNA repair genes and pathways can thus contribute to advancements in the prevention of diseases resulting from DNA damage and to new targets for cancer treatment[9-15]. Here, we describe a strategy to identify novel DNA repair modulating genes by

combining two orthogonal DNA repair assays, one that senses repair of DSBs and one that identifies proteins that bind to DSBs.

DNA repair is a complex process that requires the coordination of many proteins to respond to specific classes of DNA damage. The major classes of DNA damage include base damage, crosslinks, single stranded breaks, double stranded breaks (DSBs) and others. Among these, DNA DSBs are one of the most deleterious to the cell, because they lead to cell death if left unrepaired and at the same time present opportunities for large-scale chromosomal rearrangements[16]. In human cells, DNA DSBs are repaired mainly via the Non-Homologous End Joining[17,18] (NHEJ) or Homologous Recombination[19,20] (HR) repair pathways. The proteins that directly participate in these pathways have been studied for decades and are well characterized.

Recent research has called attention that vast networks of proteins coordinate to promote DNA repair. By surveying the phosphoproteomic landscape in cells that were treated with γ ionizing radiation (γIR, which creates DNA DSBs), Matsuoka and co workers identified more than 700 proteins that were phosphorylated after the treatment[21]. Many known DNA repair factors were identified in their approach, but more interestingly, networks of genes not previously known to participate in DNA DSB repair were also identified, suggesting that these networks might play a role in DNA DSB repair. Other researchers have identified a class of proteins known as 'chromatin modifiers' that play major roles in modulating DNA DSB repair[22]. These proteins change the structure of chromatin near the DNA DSB, such as by phosphorylating or acetylating[23,24] histone tails, in order to create binding sites for DNA DSB repair factors

or to allow DNA DSB repair factors to gain access to the break. These studies showed that DNA repair is modulated by a large number of factors and it is possible that many more DNA repair factors are yet to be discovered.

Here, we combine two independent screens for genes that modulate DNA repair. One of the screens exploits RNAi technology to identify genes that cause a reduction in DNA repair capacity. Specifically, we measured the levels of DNA DSBs at fixed times after exposure to γIR. If the RNAi targeted a protein that was important for DNA DSB repair, we would expect to detect high levels of DNA DSBs, even after the cells were allowed time to repair the damage. To survey thousands of unique RNAi reagents targeting their respective genes for their ability to modulate DNA DSB repair, we recently developed the High Throughput Screening CometChip (HTS CometChip)[25], which enabled us to exploit high throughput robotic equipment to measure DNA DSBs in a parallel fashion.

The HTS CometChip technology exploits the same principle as the traditional comet assay to measure DNA DSBs – damaged DNA is more electrophoretically mobile in agarose than unbroken DNA[26]. This principle has been used in the traditional comet assay to study DNA damage since the 1980s. After encapsulating cells in agarose and subjecting their DNA to electrophoresis, researchers can measure the levels of DNA DSBs in those cells by staining DNA and collecting images. Images obtained from this assay typically show circular areas of staining originating from the nucleoid of cells, as well as tails exiting from the nucleoids, resembling a comet. The extent of DNA damage in the cell directly correlates with the length of the tail region of the comet. The traditional comet assay is easy to perform, but its usage in large scale DNA repair gene

discovery experiments have been limited, due to low throughput and poor reproducibility drawbacks.

The HTS CometChip exploits a micropatterned cell array on agarose to maximize the number of useful comets per unit area of agarose[27-30], such that dozens of samples can now be tested together on an agarose slab with the area of a typical multiwell plate. This is in contrast with the traditional comet assay, which requires one glass slide per sample. By accommodating many more samples into each assay, the throughput of conducting comet assays with the HTS CometChip is vastly increased, enabling large-scale measurements of DNA damage. We designed the HTS CometChip to be compatible with high throughput screening robotics, so as to minimize the amount of manual labor required to assay thousands of samples.

We previously exploited our HTS CometChip to assay physical DNA DSBs at an unparalleled rate, enabling a screen of an shRNA library targeting 2564 oncology associated genes[31]. We used a pair of human glioblastoma cell lines, M059K and M059J, which are normal and deficient in DNA DSB repair respectively[32]. The distinction between these cell lines stems from a truncation mutation in the *DNAPKcs* gene (essential for NHEJ) in the M059J cell line, impairing its ability to repair DNA DSBs efficiently[33]. In our screen, we plated M059K cells and treated them with the shRNAs from the library. After applying a selection pressure for cells that were successfully transduced, we transferred them onto HTS CometChips, irradiated them with 100 Gy γIR to induce DNA DSBs, and incubated the cells in media for 4 hours. We compared the levels of DNA DSBs across all shRNAs in our screen, and selected candidate genes with high levels of DNA DSBs for further investigation. Importantly, since DSBs are also

created during apoptosis[34]. We designed image segregation software to distinguish apoptotic comets from comets reflecting DNA damage from γIR based on their shapes. We excluded apoptotic comets in order to focus on DNA repair.

To increase the accuracy of our screen, we combined results from the HTS CometChip with results from a second independent screen that detects proteins bound to DNA DSBs. Specifically, proteins bound to DSBs were isolated based on their affinity for linearized DNA plasmids. This technique was previously developed by Isogawa and co workers to study protein complexes that bind to DNA (Fig. 4-1)[35]. Briefly, a plasmid was engineered to contain a DNA triple helix binding motif[36] (green bar on plasmids). An oligonucleotide was then designed to bind to the triple helix binding motif via Hoogsteen base pairing[37,38]. The resulting complex was then exposed to xenopus egg extracts to allow proteins to bind the DNA. This oligonucleotide was biotinylated at one of its ends, so that it could be retrieved using streptavidin beads, together with the proteins that were bound to the plasmid. The bound proteins were eluted from the complexes and analyzed using mass spectrometric techniques. The plasmids can be engineered to contain specific DNA structures. Since DNA DSB repair factors are likely to bind to DNA DSBs, we utilized linearized plasmids as a means to create DNA DSBs in the chromatin pull-down technique. The array of proteins that bind to the linearized plasmids were then compared to that of circular plasmids, to identify DNA DSB binding factors. The list of DNA DSB binding factors was then cross-referenced with the list of proteins generated by the HTS CometChip screen to isolate DNA DSB repair factors. Remarkably, we observed known DNA DSB repair factors among the top 10 hits using this method. At the same time, we were able to identify factors that were not yet known

to be DNA DSB repair factors, but had been shown to cause cellular phenotypes consistent with DNA repair defects when depleted. These findings show the utility of combining datasets from multiple assays querying for different aspects of DNA DSB repair, leading to the discovery of novel DNA DSB repair factors.

4.3   Materials and Methods

Cell culture. M059K and M059J glioblastoma cells were cultured in 1:1 DMEM/F12 nutrient mix (Invitrogen) supplemented with 10% FBS (Atlanta Biologicals, Atlanta, GA), MEM Non-Essential Amino Acids (Invitrogen) and 100-units/ml penicillin-streptomycin (Invitrogen).

HTS CometChip apparatus fabrication. A 120 by 78 mm aluminum base plate was cut from a 3 mm thick aluminum sheet to fit tightly in a uni-well tray (VWR). Four aluminum posts (6 mm in diameter and 6.5 mm in height) were welded onto the base plate with their centers 28.5 mm and 7.5 mm from the short and long edges of the plate respectively. A 2 mm wide and 5 mm deep hole was drilled into each aluminum post and threaded on surface. The outer edges of a bottomless 96-well plate (VWR) were sawed off, leaving a 110 by 74 mm grid of 96 wells. Wells A3, A10, H3 and H10 were plugged with tight fitting polystyrene cylinders with a 2 mm wide hole drilled at their centers. HTS CometChip was assembled by sandwiching the microwell arrayed agarose between the aluminum base plate and the bottomless well plate, such that the

posts on the aluminum plate meet the pegs on the bottomless plate, and fastened together by screws.

Neutral CometChip. The CometChip was prepared as described previously. Briefly, 12ml of 1% molten agarose in PBS was poured over a GelBond flim (Lonza) placed on a uni-well tray (VWR) before applying a reusable PDMS stamp arrayed with microposts. When the agarose was solidified, the PDMS stamp was removed to reveal microwells for cell loading. After the CometChip was loaded with cells, excess cells were washed off with PBS and a thin layer of 1% molten low melting point agarose in PBS was applied. Cells were lysed at 43°C overnight after desired timepoints by submerging the CometChip into lysis buffer containing 2.5M NaCl, 100 mM Na_2EDTA, 10 mM Tris, 1% N-Lauroylsarcosine, pH 9.5 with 0.5% Triton X-100 and 10% DMSO. The CometChip was washed thrice with neutral electrophoresis buffer containing 90 mM Tris, 90 mM Boric Acid, 2 mM Na_2EDTA, pH 8.5. Electrophoresis was conducted using pre-chilled neutral electrophoresis buffer at 4°C for 1 hr at 0.6 V/cm and 6 mA.

High throughput screening robotics. Access to high throughput screening robotics and equipment was obtained via MIT's Koch Institute of Integrative Cancer Research, Swanson Biotechnology Center, High Throughput Screening Core Facility. Robotic manipulation of the HTS CometChip was performed using a Tecan Evo 100 liquid handler, equipped with a 96-well MultiChannel Arm (MCA96) and a Robotic Manipulator (RoMa) arm. The Evo 100 is also integrated with a Liconic STX110 incubator with

temperature, humidity, CO_2 control. Imaging of the HTS CometChip was performed using Thermo Scientific Cellomics® ArrayScan® VTI HCS Reader using a 5X objective.

HTS CometChip shRNA screen. shRNA lentiviral reagents were obtained from MIT's Koch Institute of Integrative Cancer Research, Swanson Biotechnology Center, High Throughput Screening Core Facility. This shRNA library was purchased from the MIT Broad Institute's The RNAi Consortium as a sub-genome library of 2564 genes, with three unique targeting shRNAs per gene. The genes targeted by this library are listed on this webpage: https://ki.mit.edu/files/ki/cfile/sbc/hts/Koch_shRNA_Gene_ Webpage_List_June2012-1.pdf. This library was formatted as an arrayed library, with lentivirus targeting one gene in each well of a 96 well plate, across 89 of plates. The screening effort was divided into alternating screening days and imaging days. Prior to screening days, M059K cells were plated on tissue culture 96-well plates at a density of 600 cells per well, transduced with lentiviruses with an average MOI of 8 the next day after cell plating and selected with 1.5 μg/ml puromycin 48 hours after transduction. Puromycin was applied for 72 hours and cells were allowed to recover in selection free media for 24 hours. All media changes were performed using a BioTek EL406 microplate washer under sterile conditions. On screening days, media was removed from the tissue culture plates before trypsin was added to dislodge the cells. Media was added to quench the trypsin and triturated to create single cell suspensions in each well. Cell suspensions from each tissue culture plate were transferred onto one HTS CometChip and allowed to incubate at 37°C for 20 minutes. Excess unloaded cells were washed off and a thin layer of low melting point agarose was applied to encapsulate

cells trapped in microwells. CometChips were submerged in media and treated with 100 Gy of γ-rays at 1 Gy/min using a ^{137}Cs source. Cells were allowed to repair DNA damage at 37°C for 4 hours in media before they were lysed. On imaging days, the HTS CometChips were washed thrice with neutral electrophoresis buffer and electrophoresis was conducted to measure the extent of DNA DSBs. HTS CometChips were stained with SyBR Gold and imaged with Thermo Scientific Cellomics® ArrayScan® VTI HCS Reader using a 5X objective.

Chromatin pull-down via DNA triple helix formation. Triple helix (triplex) forming oligonucleotide-1 (TFO-1) probes are composed of a psoralen residue, a 22-mer LNA/DNA mixed oligonucleotide (5'-tTtTcTtTtCtCCtCtTCtCct), a spacer arm composed of tandemly oriented hexaethylene glycol, and a desthiobiotin residue. LNA and DNA residues are shown in small and capital letters, respectively. Capital C represents 5-methyl dC residue. A TFT cassette is 61 bp dsDNA and contains two different TFO-target sites (TFT-1 and TFT-2). TFT-1 is 5'-AAAAGAAAAGAGGAGAAGAGGA and TFT-2 is 5'- AGGAGAAGAGGAGAAAGAAAA. pAS03 is derived from pcDNA3.1(+)CAT (Invitrogen). pAS03.1 is derived from pAS03 by inserting a TFT cassette at a BstBI site. pAS03.2 is derived from pAS03.1 by inserting an additional TFT cassette at a BglII site. pAS04 is derived from pAS03.2 by inserting a third TFT cassette at an XbaI site. Linearized pAS04 is prepared by treating pAS04 with EcoRV and NotI restriction enzymes. Circular or linearized pAS04 was first mixed with TFO-1 probe to form the triplex followed by UVA irradiation to introduce a covalent crosslink between the plasmid and the psoralen moiety of TFO-1 (triple helix forming oligonucleotide). The

pAS04-conjugated TFO or pAS04 (in the absence of added TFO) is incubated with Dynabeads M-280 Streptavidin beads. After washing of the beads to remove unbound plasmids, the pAS04-immobilized plasmid was linearized to create DNA DSBs. The plasmid was then mixed and incubated at room temperature for 10 min with xenopus egg extracts[39]. Following washes of the beads, protein/DNA complexes are eluted from the beads and analyzed by 'label-free' mass spectrometry using an Orbitrap machine; both xenbase and Uniprot databases were used to assign peptide sequences to protein candidates.

4.4   Results

The objective of the work presented here is to merge the dataset obtained from our high throughput screening for DNA DSBs together with orthogonal datasets that measures DNA DSB binding, in order to identify novel DNA DSB repair factors. As such, we first utilized a dataset that identifies DNA DSB binding factors, since DNA DSB repair factors are likely to bind to DNA DSBs. Previously, Isogawa and co workers developed a chromatin pull-down technique based on DNA triple helix formation to isolate protein complexes that bind to DNA[35]. By using linearized plasmids to present DNA DSB ends and circular plasmids to control for proteins that bind DNA but not specifically to DSBs, we were able to specifically identify proteins that directly bind to DNA DSBs. Table 4-1 lists the gene names for proteins shown to be enriched under conditions where there was a DSB. The observation that many proteins known to directly participate in the NHEJ and HR repair pathways scored highly in the assay

showed that the approach was effective. For example, the XRCC5, XRCC6 and PRKDC proteins (also known as Ku80, Ku70 and DNAPKcs respectively) directly bind to DNA DSBs and initiate repair of the DSB via the NHEJ pathway[17]. The MRN complex, made up of MRE11, Rad50 and NBS, is known to be a DNA DSB sensor and activates downstream factors such as the ATM kinase upon binding to a DNA DSB[40]. Additionally, genes that are not known to be related to DSB repair were identified too, presenting opportunities for further investigation into possible roles in DNA repair.

The HTS CometChip[25] is well suited to measure DNA damage from thousands of samples simultaneously, as a means to identify DNA DSB repair factors. Briefly, an agarose slab filled with cell-sized microwells on its surface was cast and sandwiched between a base metal plate and a bottomless 96-well plate. The sandwich was securely fastened together by a set of four screw systems and the apparatus was placed in a uniwell tray, which serves as an interface for robotic equipment to engage with. We loaded cell suspensions into the apparatus and allowed the cells to settle into microwells in the agarose. We then sealed the microwells with a thin layer of agarose, creating a neatly arranged array of micropatterned cells on agarose. With this apparatus, we were able to assay multiple samples simultaneously with the assistance of robotic equipment to perform liquid transfers, as compared to one sample at a time without the HTS CometChip, greatly increasing our throughput and efficiency of conducting the assay.

We have previously utilized the HTS CometChip in a lentiviral shRNA screen targeting 2564 genes, in order to identify candidate genes that are potentially important for DNA DSB repair[31]. Briefly, we plated cells on tissue culture 96 well plates, and

transduced them with shRNA expressing lentiviruses. After selection for successful transductions, we transferred the cells onto the HTS CometChip. We irradiated cells on the HTS CometChip to 100 Gy γIR and allowed the cells to incubate in media for 4 hours, prior to analysis of DNA DSBs.

We observed that there were comets with different morphologies in the images collected from the screen (Fig. 4-2A). We found that for the M059K cells, which were able to efficiently repair DNA DSBs, the comet tails were consistently short and were approximately the length of one comet head diameter (Fig. 4-2A first panel). For the M059J cells, which do not repair DNA DSBs efficiently, the comet tails were consistently longer than that of the M059K comets and were approximately the length of three comet head diameters (Fig. 4-2A second panel). For both the M059K and M059J comets, the morphology of the comets tails were such that they were cone shaped, with the brightness intensity of the pixels in the tails decreasing as their distance from the comet head increases. We observed that in a subset of the images that were collected from shRNA treated M059K cells, the majority of the comets have the abovementioned morphology (Fig. 4-2A, third panel, boxed in blue). We also observed comets with a different morphology (Fig. 4-2A, fourth panel, boxed in red). These comets have a tear shaped tail and the pixels with maximum brightness intensity tend to be near the middle region of the tail. Previous experiments showed that these comets were likely formed due to DNA fragmentation during cellular apoptosis[32], and therefore were not indicative of the cell's ability to repair DNA.

In order to refine our analysis for detecting γIR induced DNA damage, we designed an image analysis program to exclude tear shaped comets and to only

144

measure the tail lengths of cone shaped comets. To achieve this, we designed and implemented an image analysis software program in MATLAB. The requirements of the program were that it needed to be able to identify all comets in an image, before classifying each comet as a cone shaped or tear shaped comet. To identify comets, a representative image was first used to measure the microwell size and the distance between microwells in pixels. Microwells with cells form the 'head' region of each comet, and were almost always saturated (pixel value = 256) in the images (Fig. 4-2B, left panel). A minimum pixel threshold value of 200 was used to identify the comet heads (Fig, 4-2B, top right panel). To minimize the occurrence of analyzing comets that were not in the microwell array, we filtered comet heads based on their area (microwells had a fixed diameter) and distance between one another (microwells were regularly spaced). The accompanying comet tail for each comet head was identified by setting a minimum pixel threshold intensity of 20. An area threshold filter was also applied, to avoid analyzing large artifacts originating from debris within the agarose.

We analyzed the tail brightness profile for each comet and created two filters to distinguish cone shaped comets from tear shaped comets (Fig, 4-2B, right panels). In the first filter, we calculated the positions of the centroid (C), weighted centroid (WC), and major axis length (MAL) for each comet. The WCs of tear shaped comets were frequently on the right of the comet centroid, due to the presence of high intensity pixels in the tails of the comets. We classified comets as cone shaped, if the WC lies to the left of C and classified comets as tear shaped, if WC lies to the right of C. In the second filter, we summed the vertical width of each comet along its major axis to generate a

cross section profile. Cone shaped comets have a consistently decreasing profile while tear shaped comets have a local minimum and maximum width.

We analyzed the distribution of comet tail lengths obtained from cone shaped comets and found two subpopulations of comets (Fig. 4-3A). For each the conditions examined, there was a population of comets with an average comet tail length of approximately 50 μm. For the M059J cells, which are known to have a DNA DSB repair defect, we detected a subpopulation of comets with an average comet tail length of approximately 110 μm. Analysis of several image sets obtained from M059K cells treated with shRNAs also showed two subpopulations of comets with tail length averages of about 50 and 110 μm. To maximize the difference between our M059K and M059J controls, we rank ordered the comets according to their tail lengths for each condition, and calculated the average of the top dectile of comets (Fig. 4-3B).

To compare the level of unrepaired DNA DSBs between cells that have been treated with different shRNAs, we normalized the values obtained for each shRNA against the values obtained for M059K and M059J cells on their corresponding plates, and averaged the values from duplicate plates. The normalized data set is rank-ordered as shown in Figure 4. As expected, the M059J cell line had high levels of unrepaired DNA DSBs and ranked 18 out of 2569, while the M059K cell line had low levels of unrepaired DNA DSBs and ranked 2175 out of 2569. This difference in ranking of the cell line controls is attributable to the expression status of DNAPKcs in these cells. Due to its repair defect, M059J cells accumulate DNA DSBs after exposure to γIR, which led to a high comet tail length signal in our screen, relative to the M059K cell line with functional DNA repair. We observed a spectrum of DNA DSB repair capacities in the

cells treated with the shRNA library with the M059J and M059K cells at the opposite ends of the spectrum and predicted that genes that were closer to M059J on the spectrum would be more likely to be DNA DSB repair factors.

To refine our screen, we merged our rank ordered gene list together with the list of genes obtained from chromatin pull down via DNA triple helix formation (Table 4-1). The positions of the genes present in the pull down list were indicated with blue arrows (Fig. 4-4). We observed that there were nine genes, which ranked within the top 1000 genes in the HTS CometChip screen list that were also identified in the chromatin pull down assay. These genes were listed in Table 4-2. Five of the top seven genes listed are known to be activated when cells were exposed to γIR. ATR and ATM belong to a class of kinases known as PI3KKs, which also includes DNAPKcs. These kinases bind to sites of DNA damage and become activated, triggering a phosphorylation signaling cascade that is part of DNA damage response signaling[41,42]. NBN is part of the MRN complex and is known to be a DNA DSB sensor and recruits ATM to the DSB[40]. PNKP functions in the NHEJ pathway, where it catalyzes 5' phosphorylation and 3' dephosphorylation at DNA ends in order to form compatible ends for DNA ligation[43]. Finally, BRIP1, also known as BACH1 or FANCJ, binds directly to BRCA1 and has been shown to impair γIR induced DNA DSB repair if mutated[44]. These results showed that genes that scored highly in both screens likely to be true DNA DSB repair genes.

Apart from known DNA DSB repair genes that were identified from the intersection of our data sets, the top two hits were RFC5 and CBX1. These genes have not been shown previously to directly impact DSB repair, and therefore represent opportunities for further investigation. For CBX1, it is known to be associated with the

histone acetyltransferase TIP60, which has been shown to participate in DNA DSB repair. It is therefore likely that CBX1 is a bona fide DNA DSB repair factor.

We inspected the images obtained from the HTS CometChip screen and found that the shRNAs that targeted RFC5 and CBX1 resulted in longer comet tails after the cells were allowed to perform DNA repair for 4 hours after exposure to γIR (Fig. 4-5). This showed that RFC5 and CBX1 depleted cells indeed have persistent DNA DSBs. Further investigations will be needed to determine the mechanisms by which these genes participate in DNA repair.

4.5   Discussion

In this study, we developed a strategy to identify novel DNA DSB repair factors by combining data from two orthogonal DNA repair assays, one that senses repair of DSBs and one that identifies proteins that bind to DSBs. We refined the analysis of images from our HTS CometChip screen, to exclude comets with shapes consistent with apoptosis and focused on comets that were reflective of the DNA DSB repair status of the cell. We merged the improved data set with that of an orthogonal data set to more confidently identify genes that are direct participants in DNA DSB repair. We found nine genes that scored highly in both datasets, out of which five of them were known DNA repair genes. Furthermore, we identified two genes that are not yet shown to impact DSB repair and therefore could be novel DNA DSB repair genes.

Previous research has shown that cells undergoing apoptosis led to long comet tails in our assay, due to DNA fragmentation. Here, we extended upon this work by

refining our analysis parameters for unrepaired DSBs. We previously observed that the shape of the comet tails from cells undergoing apoptosis were distinctively different from cells that are still viable. Specifically, cells that were exposed to γIR had cone shaped comet tails whereas cells that were undergoing apoptosis had tear shaped comets. We designed an algorithm that was able to differentiate comets based on their shape. Using this algorithm, we focused on studying the comets that reflect the DNA repair status of the cells.

We merged our refined HTS CometChip dataset with DNA DSB binding data, obtained from the chromatin pull-down methodology. The chromatin pull-down methodology, based on DNA triple helix formation, allows researchers to isolate proteins that bind to pre-designed DNA structures. Plasmids with specific DNA structures were used as bait for proteins to bind onto, and can be retrieved using an oligonucleotide that binds to a triple helix forming motif on the plasmid. To discover DNA DSB binding proteins, we mixed linearized plasmids with xenopus egg extracts and compared the abundance of proteins bound on linear plasmids compared to circular plasmids (to control for proteins that bind non specifically to DNA). Several known DNA DSB repair factors were identified from the chromatin pull-down methodology that also scored high in the HTS CometChip screen. The observation that that majority of the proteins that score high in both datasets shows that our strategy of combining data from orthogonal assays can greatly increase the probability of finding direct DNA DSB repair factors.

Our goal in this study is to identify novel DNA DSB repair factors for further investigation. By utilizing both datasets that query different aspects of proteins that

respond to DNA DSBs (modulating DSB levels and binding to DSBs), we found four genes that have not yet been directly shown to be involved in DNA DSB repair following cells' exposure to γIR. These genes are RFC5, CBX1, SKP1, and RBMS. In particular, there is evidence that RFC5 and CBX1 are associated with other factors that participate in DNA DSB repair. Since they also rank highly in the HTS CometChip screen, they are highly likely to be novel DNA DSB repair factors.

RFC5 is part of a complex known as Replication Factor C, and this complex is made up of five subunits, RFC1 – 5. During DNA replication, the RFC complex functions as a clamp loader and loads PCNA onto DNA, allowing it to bind to the DNA polymerases to increase their processivity[45]. The RFC complex is also recruited onto DNA at sites of damage, and loads the Rad9 – Rad1 – Hus1 checkpoint signaling complex onto DNA, indicating that it plays an active role when DNA is damaged[46]. Matsuda and coworkers recently reported that TRIM29, a histone binding protein that regulates the DNA damage response signaling pathway, also binds to the RFC complex[47], providing further evidence of RFC5's involvement in modulating DNA repair. *S. cerevisiae* RFC5 mutants were also found to be more sensitive to DNA damaging agents such as UV and MMS[48,49]. MMS is a radiomimetic agent; many yeast mutants that were sensitive to MMS were also sensitive to γIR[50], indicating that RFC5 is likely to play a role in modulating DNA DSB damage after γIR exposure.

CBX1, also known as heterochromatin protein 1 beta (HP1-β), is a chromatin associated protein that binds histone H3 methylated at the K9 residue (H3K9me)[51]. In the presence of DNA DSBs, CBX1 becomes phosphorylated and leaves the chromatin, allowing the histone acetyltransferase TIP60 to bind on H3K9me3 and activate DNA

DSB repair pathways[52,53]. Interestingly, data from our chromatin pull-down methodology showed that CBX1 was a DNA DSB binder, suggesting that it might be possible for CBX1 to participate in DNA DSB repair via a different mechanism from its interaction with H3K9me and TIP60.

4.6   Conclusion

We have developed a strategy to combine data from two orthogonal DNA repair assays, one that senses repair of DSBs and one that identifies proteins that bind to DSBs, leading to the identification of novel DNA DSB repair factors. In this work, we have shown that we were able to identify DNA DSB binding proteins. We also refined our analysis strategy for the images obtained from our HTS CometChip screen, in order to increase the probability of identifying true DNA repair genes. We overlaid the two datasets together, and shortlisted a group of nine genes that score highly in both assays. Five out of the nine genes identified were known DNA DSB repair factors, showing that we were able to reliably identify DNA DSB repair factors using this method. There is evidence that the top two hits in our shortlist (RFC5 and CBX1) associate closely with other known DNA DSB repair factors and deficiencies in the expression of these genes led to increase sensitivity to agents that cause DNA damage. The observation that the comet tails obtained from the HTS CometChip screen are longer in cells depleted for these genes is consistent with a direct impact on DNA DSB repair. Taken together, we have combined data from orthogonal assays to identify RFC5 and CBX1 as bona fide DNA repair genes.

References

1.   Aguilera, A., & Gómez-González, B. (2008). Genome instability: a mechanistic view of its causes and consequences. *Nature Reviews. Genetics, 9*(3), 204–217.

2.   Hoeijmakers, J. H. J. (2009). DNA damage, aging, and cancer. *The New England Journal of Medicine, 361*(15), 1475–1485.

3.   Shimizu, I., Yoshida, Y., Suda, M., & Minamino, T. (2014). DNA damage response and metabolic disease. *Cell Metabolism, 20*(6), 967–977.

4.   Hanahan, D., & Weinberg, R. A. (2011). Hallmarks of cancer: the next generation. *Cell, 144*(5), 646–674.

5.   Hoeijmakers, J. H. (2001). Genome maintenance mechanisms for preventing cancer. *Nature, 411*(6835), 366–374.

6.   Thibodeau, S. N., French, A. J., Roche, P. C., Cunningham, J. M., Tester, D. J., Lindor, N. M., et al. (1996). Altered expression of hMSH2 and hMLH1 in tumors with microsatellite instability and genetic alterations in mismatch repair genes. *Cancer Research, 56*(21), 4836–4840.

7.   Nickoloff, J. A., Jones, D., Lee, S.-H., Williamson, E. A., & Hromas, R. (2017). Drugging the Cancers Addicted to DNA Repair. *Journal of the National Cancer Institute, 109*(11), 85.

8.   Lord, C. J., & Ashworth, A. (2012). The DNA damage response and cancer therapy. *Nature, 481*(7381), 287–294.

9.   Jiang, G., Wei, Z.-P., Pei, D.-S., Xin, Y., Liu, Y.-Q., & Zheng, J.-N. (2011). A novel approach to overcome temozolomide resistance in glioma and melanoma: Inactivation of MGMT by gene therapy. *Biochemical and Biophysical Research Communications, 406*(3), 311–314.

10.   Wedge, S. R., Porteous, J. K., & Newlands, E. S. (1997). Effect of single and multiple administration of an O6-benzylguanine/temozolomide combination: an evaluation in a human melanoma xenograft model. *Cancer Chemotherapy and Pharmacology, 40*(3), 266–272.

11.   Schaue, D., & McBride, W. H. (2005). Counteracting tumor radioresistance by targeting DNA repair. *Molecular Cancer Therapeutics, 4*(10), 1548–1550.

12.   Helleday, T., Petermann, E., Lundin, C., Hodgson, B., & Sharma, R. A. (2008). DNA repair pathways as targets for cancer therapy. *Nature Reviews. Cancer, 8*(3), 193–204.

13.   Curtin, N. (2007). Therapeutic potential of drugs to modulate DNA repair in cancer. *Expert Opinion on Therapeutic Targets, 11*(6), 783–799.

14.   Ding, J., Miao, Z.-H., Meng, L.-H., & Geng, M.-Y. (2006). Emerging cancer therapeutic opportunities target DNA-repair systems. *Trends in Pharmacological Sciences*, *27*(6), 338–344.

15.   Madhusudan, S., & Hickson, I. D. (2005). DNA repair inhibition: a selective tumour targeting strategy. *Trends in Molecular Medicine*, *11*(11), 503–511.

16.   Aplan, P. D. (2006). Causes of oncogenic chromosomal translocation. *Trends in Genetics : TIG*, *22*(1), 46–55.

17.   Lees-Miller, S. P., & Meek, K. (2003). Repair of DNA double strand breaks by non-homologous end joining. *Biochimie*, *85*(11), 1161–1173.

18.   Burma, S., Chen, B. P. C., & Chen, D. J. (2006). Role of non-homologous end joining (NHEJ) in maintaining genomic integrity. *DNA Repair*, *5*(9-10), 1042–1048.

19.   West, S. C. (2003). Molecular views of recombination proteins and their control. *Nature Reviews. Molecular Cell Biology*, *4*(6), 435–445.

20.   Li, X., & Heyer, W.-D. (2008). Homologous recombination in DNA repair and DNA damage tolerance. *Cell Research*, *18*(1), 99–113.

21.   Matsuoka, S., Ballif, B. A., Smogorzewska, A., McDonald, E. R., Hurov, K. E., Luo, J., et al. (2007). ATM and ATR substrate analysis reveals extensive protein networks responsive to DNA damage. *Science (New York, N.Y.)*, *316*(5828), 1160–1166.

22.   Price, B. D., & D'Andrea, A. D. (2013). Chromatin remodeling at DNA double-strand breaks. *Cell*, *152*(6), 1344–1354.

23.   Ogiwara, H., Ui, A., Otsuka, A., Satoh, H., Yokomi, I., Nakajima, S., et al. (2011). Histone acetylation by CBP and p300 at double-strand break sites facilitates SWI/SNF chromatin remodeling and the recruitment of non-homologous end joining factors. *Oncogene*, *30*(18), 2135–2146.

24.   Murr, R., Loizou, J. I., Yang, Y.-G., Cuenin, C., Li, H., Wang, Z.-Q., & Herceg, Z. (2006). Histone acetylation by Trrap-Tip60 modulates loading of repair proteins and repair of DNA double-strand breaks. *Nature Cell Biology*, *8*(1), 91–99.

25.   Tay, I. J., Floyd, S. R., Engelward, B. P. (2018). Novel Apparatus for the CometChip Cell Microarray Enables High Throughput Screening for DNA Double Strand Breaks. *Manuscript in preparation*.

26.   Olive, P. L., & Banáth, J. P. (1993). Detection of DNA double-strand breaks through the cell cycle after exposure to X-rays, bleomycin, etoposide and 125IdUrd. *International Journal of Radiation Biology*, *64*(4), 349–358.

27.   Wood, D. K., Weingeist, D. M., Bhatia, S. N., & Engelward, B. P. (2010). Single cell trapping and DNA damage analysis using microwell arrays. *Proceedings of the National Academy of Sciences of the United States of America*, *107*(22), 10008–10013.

28. Weingeist, D. M., Ge, J., Wood, D. K., Mutamba, J. T., Huang, Q., Rowland, E. A., et al. (2013). Single-cell microarray enables high-throughput evaluation of DNA double-strand breaks and DNA repair inhibitors. *Cell Cycle*, *12*(6), 907–915.

29. Ge, J., Prasongtanakij, S., Wood, D. K., Weingeist, D. M., Fessler, J., Navasummrit, P., et al. (2014). CometChip: a high-throughput 96-well platform for measuring DNA damage in microarrayed human cells. *Journal of Visualized Experiments : JoVE*, (92), e50607–e50607.

30. Sykora, P., Witt, K. L., Revanna, P., Smith-Roe, S. L., Dismukes, J., Lloyd, D. G., et al. (2018). Next generation high throughput DNA damage detection platform for genotoxic compound screening. *Scientific Reports*, *8*(1), 2771.

31. Tay, I. J., Floyd, S. R., Engelward, B. P. (2018). High Throughput DNA Double Strand Break Screen Using a Cell Microarray Comet Assay. *Manuscript in preparation*.

32. Allalunis-Turner, M. J., Barron, G. M., Day, R. S., Dobler, K. D., & Mirzayans, R. (1993). Isolation of two cell lines from a human malignant glioma specimen differing in sensitivity to radiation and chemotherapeutic drugs. *Radiation Research*, *134*(3), 349–354.

33. Lees-Miller, S. P., Godbout, R., Chan, D. W., Weinfeld, M., Day, R. S., Barron, G. M., & Allalunis-Turner, J. (1995). Absence of p350 subunit of DNA-activated protein kinase from a radiosensitive human cell line. *Science (New York, N.Y.)*, *267*(5201), 1183–1185.

34. Olive, P. L., Frazer, G., & Banáth, J. P. (1993). Radiation-induced apoptosis measured in TK6 human B lymphoblast cells using the comet assay. *Radiation Research*, *136*(1), 130–136.

35. Isogawa, A., Fuchs, R. P., Fujii, S., (2018). Versatile and efficient chromatin pull-down methodology based on DNA triple helix formation. *Manuscript in preparation*.

36. Duca, M., Vekhoff, P., Oussedik, K., Halby, L., & Arimondo, P. B. (2008). The triple helix: 50 years later, the outcome. *Nucleic Acids Research*, *36*(16), 5123–5138.

37. Ito, T., Smith, C. L., & Cantor, C. R. (1992). Sequence-specific DNA purification by triplex affinity capture. *Proceedings of the National Academy of Sciences of the United States of America*, *89*(2), 495–498.

38. Takasugi, M., Guendouz, A., Chassignol, M., Decout, J. L., Lhomme, J., Thuong, N. T., & Hélène, C. (1991). Sequence-specific photo-induced cross-linking of the two strands of double-helical DNA by a psoralen covalently linked to a triple helix-forming oligonucleotide. *Proceedings of the National Academy of Sciences of the United States of America*, *88*(13), 5602–5606.

39. Arias, E. E., & Walter, J. C. (2004). Initiation of DNA replication in Xenopus egg extracts. *Frontiers in Bioscience : a Journal and Virtual Library*, *9*, 3029–3045.

40.   Lamarche, B. J., Orazio, N. I., & Weitzman, M. D. (2010). The MRN complex in double-strand break repair and telomere maintenance. *FEBS Letters*, *584*(17), 3682–3695.

41.   Myers, J. S., & Cortez, D. (2006). Rapid activation of ATR by ionizing radiation requires ATM and Mre11. *The Journal of Biological Chemistry*, *281*(14), 9346–9350.

42.   Lee, J.-H., & Paull, T. T. (2007). Activation and regulation of ATM kinase activity in response to DNA double-strand breaks. *Oncogene*, *26*(56), 7741–7748.

43.   Aceytuno, R. D., Piett, C. G., Havali-Shahriari, Z., Edwards, R. A., Rey, M., Ye, R., et al. (2017). Structural and functional characterization of the PNKP-XRCC4-LigIV DNA repair complex. *Nucleic Acids Research*, *45*(10), 6238–6251.

44.   Cantor, S. B., Bell, D. W., Ganesan, S., Kass, E. M., Drapkin, R., Grossman, S., et al. (2001). BACH1, a novel helicase-like protein, interacts directly with BRCA1 and contributes to its DNA repair function. *Cell*, *105*(1), 149–160.

45.   Mossi, R., & Hübscher, U. (1998). Clamping down on clamps and clamp loaders--the eukaryotic replication factor C. *European Journal of Biochemistry*, *254*(2), 209–216.

46.   Burtelow, M. A., Kaufmann, S. H., & Karnitz, L. M. (2000). Retention of the human Rad9 checkpoint complex in extraction-resistant nuclear complexes after DNA damage. *The Journal of Biological Chemistry*, *275*(34), 26343–26348.

47.   Masuda, Y., Takahashi, H., Sato, S., Tomomori-Sato, C., Saraf, A., Washburn, M. P., et al. (2015). TRIM29 regulates the assembly of DNA repair proteins into damaged chromatin. *Nature Communications*, *6*(1), 7299.

48.   Sugimoto, K., Ando, S., Shimomura, T., & Matsumoto, K. (1997). Rfc5, a replication factor C component, is required for regulation of Rad53 protein kinase in the yeast checkpoint pathway. *Molecular and Cellular Biology*, *17*(10), 5905–5914.

49.   Naiki, T., Shimomura, T., Kondo, T., Matsumoto, K., & Sugimoto, K. (2000). Rfc5, in cooperation with rad24, controls DNA damage checkpoints throughout the cell cycle in Saccharomyces cerevisiae. *Molecular and Cellular Biology*, *20*(16), 5888–5896.

50.   Xiao, W., Chow, B. L., & Rathgeber, L. (1996). The repair of DNA methylation damage in Saccharomyces cerevisiae. *Current Genetics*, *30*(6), 461–468.

51.   Ayoub, N., Jeyasekharan, A. D., Bernal, J. A., & Venkitaraman, A. R. (2008). HP1-beta mobilization promotes chromatin changes that initiate the DNA damage response. *Nature*, *453*(7195), 682–686.

52.   Ikura, T., Ogryzko, V. V., Grigoriev, M., Groisman, R., Wang, J., Horikoshi, M., et al. (2000). Involvement of the TIP60 histone acetylase complex in DNA repair and apoptosis. *Cell*, *102*(4), 463–473.

53.   Sun, Y., Jiang, X., Xu, Y., Ayrapetov, M. K., Moreau, L. A., Whetstine, J. R., & Price, B. D. (2009). Histone H3 methylation links DNA damage detection to activation of the tumour suppressor Tip60. *Nature Cell Biology*, *11*(11), 1376–1382.
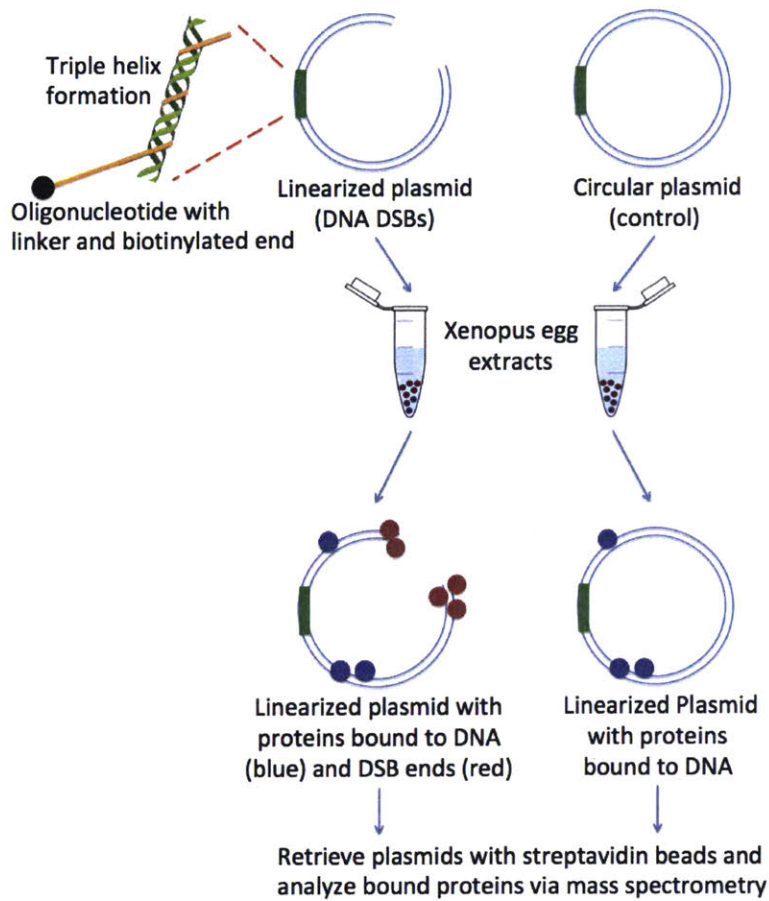
Figure 4-1.   Methodology for isolating proteins that bind to DNA DSB ends. Circular or linearized plasmids with a triple helix binding motif (green bars) pre-bound with the oligonucleotide probe were added to xenopus cell extracts for proteins (blue and red circles) to bind to the plasmid. Red circles represent proteins that specifically bind to DNA ends. Proteins bound to DSBs are enriched for the linearized plasmid. Plasmids were then incubated with streptavidin beads, and the proteins were eluted for analysis by mass spectrometry.

Gene symbols					
ABCF1	DNTTIP1	MKL1	PLAA	**RAD50**	TOPBP1
ATM	EIF2S1	MLF2	**PNKP**	RBPMS	TRAFD1
ATR	FANCI	**MRE11**	PPP3CB	RBPMS2	UFD1L
BANP	HMG20A	**NBN**	PRDX1	RFC3	**WRN**
BRIC7A	KIF2C	NPAT	PRDX2	RFC5	**XLF**
BRIP1	KIF4	ORC5	**PRKDC**	SKP1	**XRCC4**
CBX1	KPNA2	**PCNA**	PSMC2	SMARCAL1	**XRCC5**
CHUK	KPNB1	PCMT1	PSMD6	SOX3A	**XRCC6**
CUL1	**LIG4**	PDCD6IP	RAD26	THOC5A	

Table 4-1. List of genes with >4-fold enrichment for linearized plasmids as compared to circular plasmids. Genes that are directly involved in the NHEJ and HR pathways are listed in red.
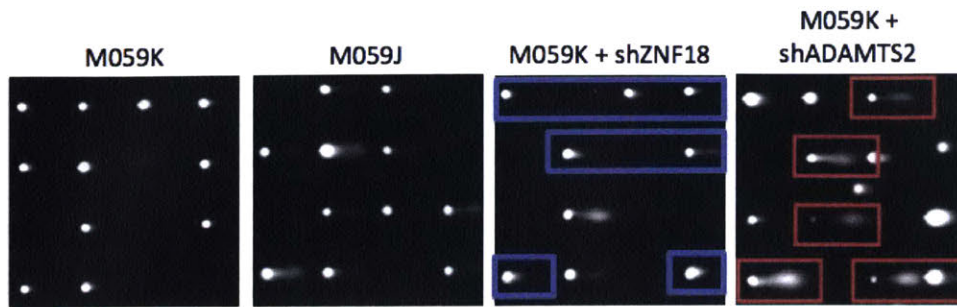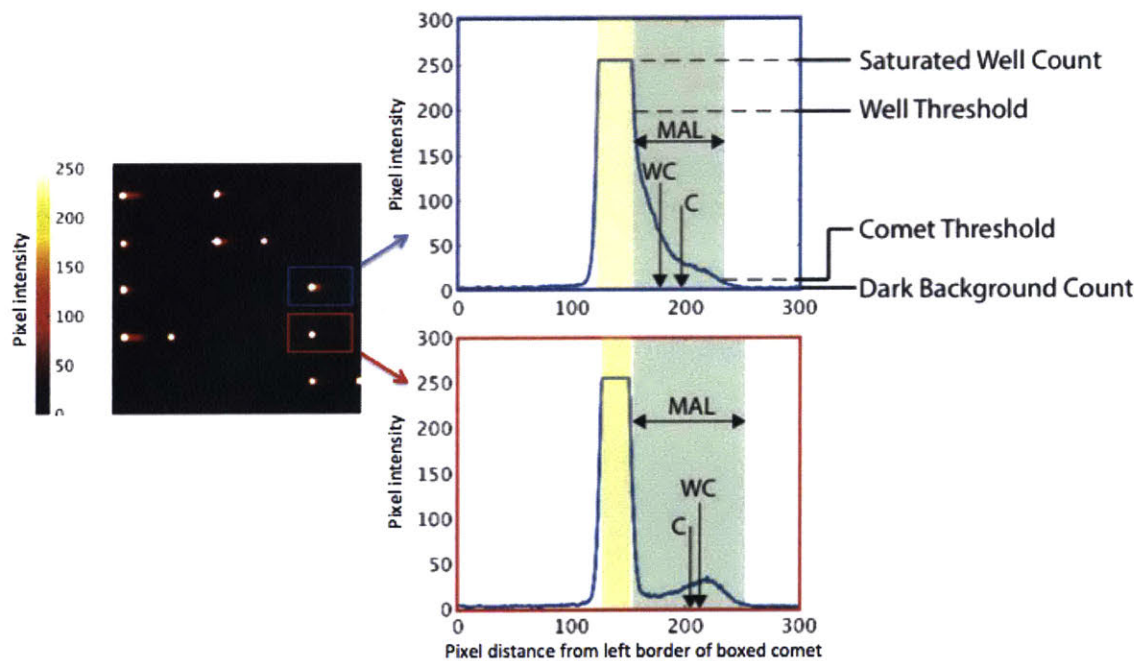
A

M059K   M059J   M059K + shZNF18   M059K + shADAMTS2

B

Figure 4-2. Identification of comets with different morphologies from the HTS CometChip screen. (A) Images obtained from untransduced M059K and M059J comets were juxtaposed with images obtained from M059K transduced with shRNAs that resulted in a majority of cone shaped comets (middle right panel, blue boxes) or tear shaped comets (far right panel, red boxes). (B) A representative image from the HTS CometChip Screen (left panel). Note that the wells were saturated with 256-pixel intensities (white circles). The top right panel shows the cross section of the cone-shaped comet. The well region shaded in yellow was intensity-saturated and the comet region shaded in green had significantly higher intensity count compared to the background. 'C', 'WC', and 'MAL' are the centroid, weighted centroid and the major-axis-length of the comet respectively. The bottom right panel shows the cross section of a tear-shaped comet. Note that 'WC' lies close to and right of 'C' in tear shaped comets in comparison to the cone shaped comet. Also note that the tear shaped comet had an intensity profile that had a local minimum and maximum in pixel intensities.
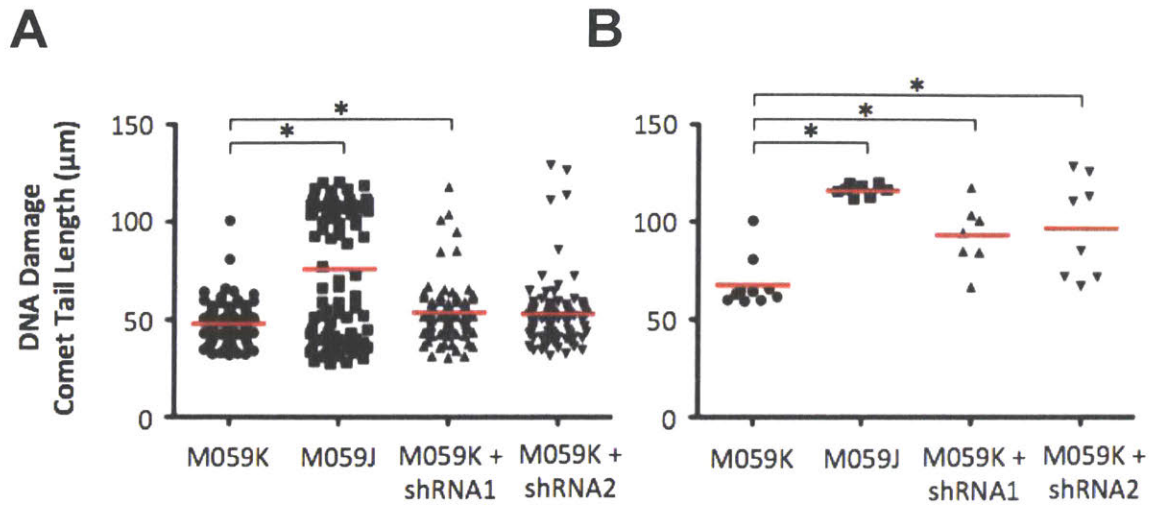
158

Figure 4-3.   Bimodal distribution of comet tail lengths. (A) Distribution of cone shaped comet tail lengths for each condition, (M059K and M059J untransduced, M059K transduced with two different shRNAs in the screen). (B) Distribution of the top decile of comet tail lengths for the same conditions as (A). Each dot represents data from one comet, and all dots in the same treatment condition were from the same well. Red bars represent average tail length of the comets plotted for each condition. * $p < 0.05$ for Mann Whitney test.
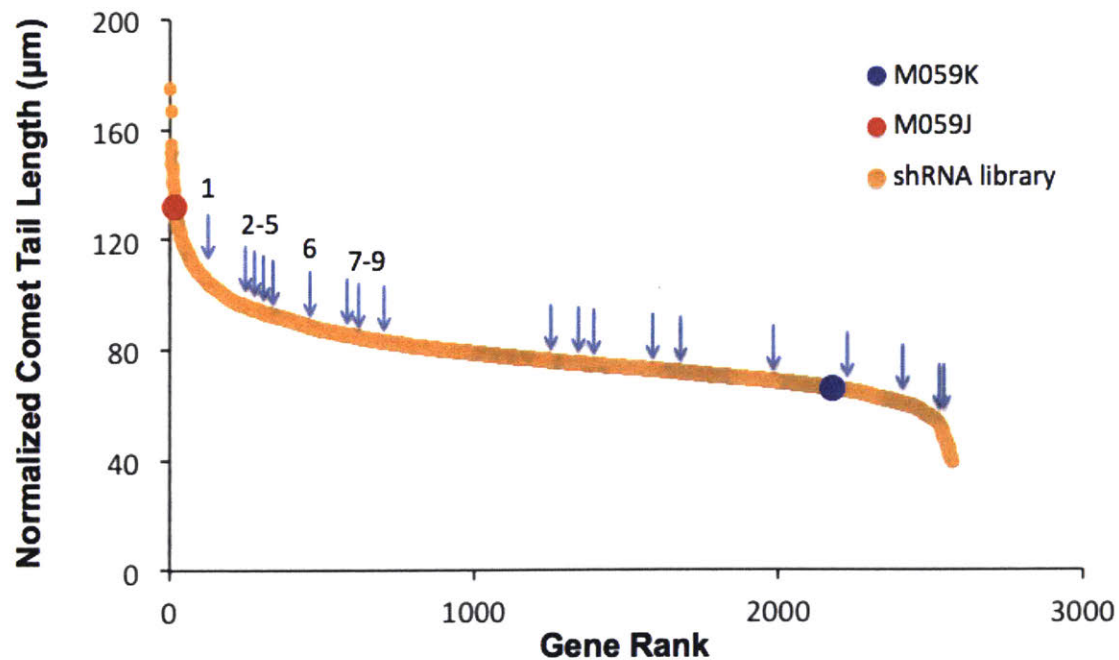
Figure 4-4. Overlay of HTS CometChip shRNA screen data with data from DNA-protein pull down via triple helix formation. Genes from the HTS CometChip screen was rank-ordered according to the top performing shRNA for each gene. The positions of genes that overlap with the gene list in Table 1 were indicated with an arrow.

Label number	Gene Symbol	Rank	Gene Name
1	RFC5	111	Replication Factor C subunit 5
2	CBX1	284	Chromobox 1
3	ATR	308	Ataxia Telangiectasia And Rad3-Related Protein
4	NBN	338	Nibrin
5	PNKP	352	Polynucleotide Kinase 3'-Phosphatase
6	ATM	463	Ataxia Telangiectasia Mutated
7	BRIP1	624	BRCA1 Interacting Protein C-Terminal Helicase 1
8	SKP1	657	S-Phase Kinase Associated Protein 1
9	RBPMS	723	RNA Binding Protein With Multiple Splicing

Table 4-2. Table of top ranking genes that overlap between the HTS CometChip screen and the DNA-protein pull down via triple helix formation assay. Genes that are directly involved in the NHEJ and HR pathways were listed in red.

A

M059K   M059K + RFC5 shRNA

B

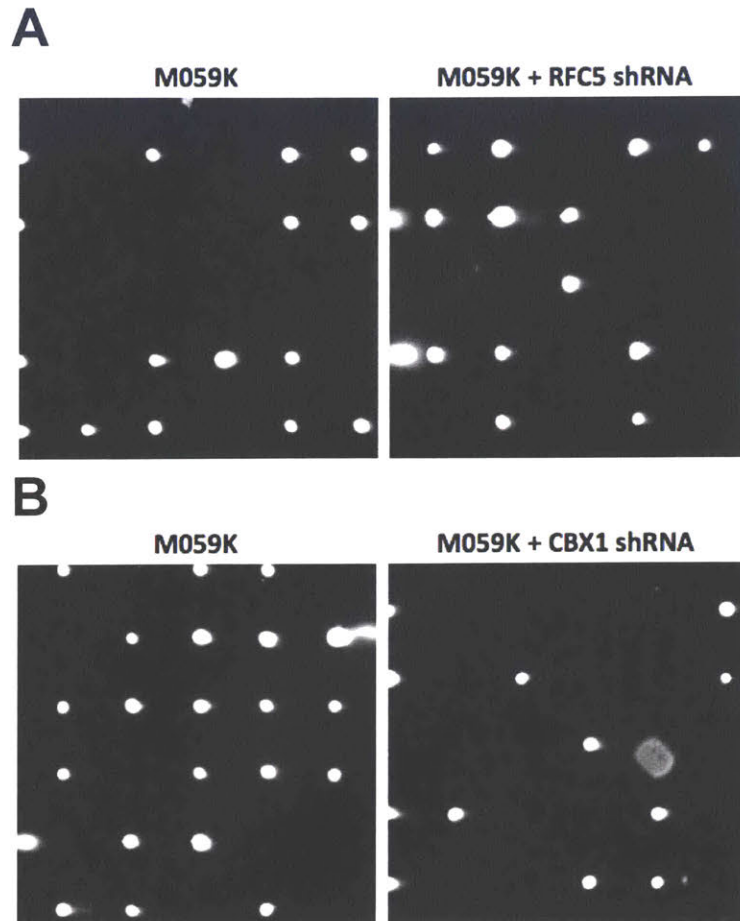M059K   M059K + CBX1 shRNA

Figure 4-5.   Images obtained from HTS CometChip screen for cells treated with (A) RFC5 shRNA or (B) CBX1 shRNA. Left panels show images from the untransduced M059K cell line that were from the same screening plate as the respective shRNAs. All cells were treated with 100 Gy γIR and allowed to incubate in media for 4 hours.

Chapter 5

Conclusions and Future Work

Our genome is constantly challenged by the presence of endogenous and exogenous DNA damaging agents. The ability of our cells to maintain genomic integrity and avoid disease depends on the capacity of DNA repair pathways to repair DNA damage and prevent their accumulation in cells. On the other hand, in cases such as cancer, the efficacy of various treatment strategies to eliminate diseased cells correlates with the inability of the target cells to repair DNA damage inflicted upon them. Therefore, a more comprehensive understanding of DNA repair pathways will lead to better strategies for disease prevention and improved outcomes in cancer therapy.

In this thesis, advances in the CometChip technology are described, as well as its application as a discovery tool to reveal novel genes that participate in DNA repair. Building upon the improvements in throughput and precision in measuring DNA damage that were afforded by the original CometChip, an HTS CometChip was developed that includes hardware to enable robotic manipulation and reduce manual labor required for the assay. Enabling automation in measuring DNA damage with HTS CometChip allowed us to develop a method to query thousands of genes for their modulatory effects in DNA damage and repair. Using this approach, we discovered a gene that was previously not known to participate in DNA repair. We characterized the gene using

other DNA repair assays and discovered that it modulates homologous recombination activity. We took a step further and combined our screen dataset with that from a novel screen for proteins that binds to DNA DSBs. We identified known DNA DSB repair factors using this approach. More excitingly, we isolated at least one other novel candidate gene that scored highly in both assays, making it an excellent target for further investigation. In this section, we review the findings from our results and discuss potential future directions.

5.1   Fabrication of HTS CometChip

The CometChip has been previously developed as a high-throughput replacement for the traditional comet assay to measure DNA damage in cells. Throughput and reliability issues have plagued the traditional comet assay since its inception in the 1980s, limiting its usage to small-scale experiments that test a small number of conditions each time. With the advent of the CometChip, researchers can now perform DNA damage measurements at least 100 times more efficiently than before. The CometChip thus opened the door to the possibility of assaying DNA damage in thousands of samples within a reasonable amount of time, making it ideal as a discovery tool for factors that impact DNA damage. To realize this potential of the CometChip, we embarked on integrating robotic tools with the assay, with the goal of reducing manual labor required to perform large-scale screens. We achieved this by designing the HTS CometChip, such that it reassembles typical multiwell plates that are used in high throughput screens.

The HTS CometChip is a technological advancement from its predecessor. Instead of manually pipetting individual samples onto the CometChip, we can now use 96-channel liquid handling robotics with the HTS CometChip for the sample transfer and washing steps. This vastly speeds up the process of preparing samples for DNA damage measurements and significantly reduces researcher fatigue. The HTS CometChip can also be imaged using an automated microscope, which allows multiple assays to be queued and imaged remotely without human intervention. Harnessing the advantages of HTS CometChip, we conducted proof-of-concept experiments that demonstrated the usage of HTS CometChip with high throughput screening robotics to test multiple conditions of inducing DNA damage. In a single experiment with a total assay time of less than 8 hours, we were able to apply four doses of γIR onto a pair of cell lines and measure DNA damage in triplicates at four different times to track repair of the damage. It would be extremely tedious to perform this experiment using nearly a hundred glass slides, and furthermore that the sample-to-sample variation would preclude the option of using the traditional comet assay.

More can be done to further increase the efficiency of HTS CometChip. In the current HTS CometChip workflow, the HTS CometChip is first assembled and loaded onto an automated liquid handling machine. This machine is also used to process cell samples grown separately on tissue culture multiwell plates. Media from the plates is removed and trypsin is added. When the cells detach from the plates, all samples on the plate is triturated in parallel and pipetted onto the HTS CometChip. After the cells enter the HTS CometChip microwells, the HTS CometChip apparatus is then manually disassembled and washed to remove excess cells. At the last step, a thin layer of

molten low melting point agarose is manually added across the agarose slab to encapsulate cells. If the washing and encapsulation steps can be performed by the liquid handling machines, significant amounts of time will be freed to allow researchers to perform other tasks.

A challenge that currently prevents automated washing of the HTS CometChip is that excess cells must be sufficiently washed away, to prevent comets that were not in microwells from overlapping with comets in the microwell array. At the same time, washes must be performed gently enough to avoid removing cells from their microwells and resulting in low density of comets obtained after imaging. We have initiated pilot experiments to test the possibility of performing washes on agarose without disassembling the apparatus. Further optimization of the forces applied during the wash step will be needed to maximize the number of cells remaining in the agarose microwell array. If the washing step can be performed without disassembling the apparatus, it will also be possible to perform the encapsulation step by utilizing robotic liquid handlers to apply a fixed volume of molten low melting point agarose in each macrowell.

The efficiency of HTS CometChip can also be improved by increasing the number of macrowells in the assay. Currently, the HTS CometChip agarose is cast to the size of a standard multiwell plate, and partitioned using a bottomless 96-well plate. Each 96-well macrowell encompasses about 300-500 microwells on the agarose. The current throughput can be increased four-fold, by using a bottomless 384-well plate instead. The well dimension of a typical 384-well plate is approximately 2 mm in diameter for each macrowell. Since the microwells are spaced between 0.25 to 0.3 mm apart, each 384 well can encircle about 25 to 50 microwells. Previous research has

shown that with the CometChip, robust data can be collected by analyzing as little as 20 comets per condition, which can be obtain in a single image from each well on a 384-well plate. The ability to measure DNA damage in a 384-well format will enable the assay to be used for primary drug screening for potential chemotherapeutics, since small molecule libraries can contain hundred thousands of chemical entities and are often presented in a 384-well format. These chemicals are also often produced in minuscule quantities, therefore performing DNA damage measurements in a 384-well format will enable the execution of such screens with minimal usage of the precious reagents.

5.2   Discovery of Novel DNA DSB Repair Factors

To discover novel DNA DSB repair factors, we utilized the HTS CometChip to screen a library of shRNA reagents targeting 2564 oncology-associated genes. We tested cells that were treated with the shRNA reagents for persistent DNA DSB levels after exposure to γIR. We rank ordered our results from highest to lowest levels of persistent DSBs and performed gene network analysis on the highly scoring genes. We subsequently selected LATS2, a member of the HIPPO pathway, as our candidate gene for further investigation, since several other genes in the same pathway have been associated with DNA repair.

To analyze LATS2's effects on DNA DSB repair, we depleted LATS2 using siRNA reagents and found that LATS2 depletion again led to persistent DSBs after exposure to γIR. This result was supported by the observation that LATS2 depleted cells

also had a higher level of γH2AX after γIR exposure as compared to control cells, due to persistent DSBs. We further demonstrated that LATS2 depleted cells were deficient in the HR repair pathway, which could explain why DSBs persisted in those cells. Consistent with a DSB repair defect, we found that LATS2 depleted cells were more sensitive to γIR as compared to control cells. Interestingly, we also found that LATS2 depletion can lead to an apparent increase in DNA DSB levels in cells that were not exposed to γIR. Subsequent experiments showed that LATS2 depleted cells were more susceptible to apoptosis when they were transferred from tissue culture plates to the HTS CometChip than control cells. These results suggest that the comets we observed when LATS2 depleted cells were left in agarose for 4 hours were likely due to apoptosis. In summary, our results signified that the HTS CometChip screen also has the ability to detect DNA damage caused by apoptotic cells, as well as from exposure to DNA damaging agents. LATS2 is one example of a gene that when depleted, led to a DNA repair defect phenotype, as well as an apoptotic phenotype. Further studies that determine the mechanism of action that LATS2 affects DNA DSB repair will be critical in determining LATS2's role in modulating cancer therapy outcomes. Additionally, our results also showed that the HTS CometChip platform can be used to assay for modulators of apoptosis, since cells undergo apoptosis also generate DSBs, which can be detected by our assay.

We also tested an alternative method to identify other novel DNA repair factors. We merged our data from the HTS CometChip screen with another dataset from a novel screen, which identifies proteins that bind to DNA DSBs. In the subset of genes that scored highly in both screens, we were able to identify several known DNA DSB repair

genes. More remarkably, we were also able to identify genes that were not directly shown to impact DNA DSB repair. RFC5 was a candidate gene identified this way, and past studies on RFC5 homologs in yeast have shown that RFC5 mutants are more sensitive to MMS, which is a radiomimetic. Taken together, our results showed the utility of comparing orthogonal screening datasets for gene scoring, culminating with the identification of RFC5 as a novel DNA DSB repair factor for future investigation.

5.3   Conclusion

In summary, we have presented a technological advancement in measuring DNA damage. Leveraging on the improvements in throughput and precision brought about by the CometChip, we designed an apparatus that enables its compatibility with high throughput screening robotics. We screen 2564 genes for modulatory effects on DNA DSB repair, and found two candidate genes for further investigation. We envision that the HTS CometChip can be further improved to enable primary drug screening for molecules that can target DNA repair genes, leading to novel therapeutics against diseases such as cancer.